DIPLOMARBEIT

Titel der Diplomarbeit
Differentiation Potential of Cardiovascular Progenitor Cell Line and Somatic Stem Cell Line Isolated from the Mouse

Verfasserin
Diana Walder

angestrebter akademischer Grad

Magistra der Naturwissenschaften (Mag.rer.nat.)

Wien, 2011

Contents

1 INTRODUCTION

1.1 CARDIOVASCULAR DISEASE

Cardiovascular diseases comprise especially the major disorders of the heart and the arterial circulation supplying the heart, brain and peripheral tissues. Cardiovascular disease is a term and includes following diseases (public health agency of Canada, phac):

- ischemic heart disease, describes defects in the transport of blood to the heart,

- cerebrovascular disease, describes the malfunction of blood vessels to transport sufficient blood to the brain and can lead to thrombosis or even stroke,

- peripheral vascular diseases, refers to an impairment of the blood supply to the extremities,

- heart failure, describes an insufficient blood supply to the body and is often a result of a myocardial infarct or a cardiomyopathy (heart muscle disease),

- rheumatic heart disease, starts with a bacterial infection in children and leads to inflammation. This further can results in dysfunctions of the heart in adults,

- congenital heart disease, is an anatomic structural defect of the heart and can vary in complexity.

Cardiovascular diseases have a common occurrence in most populations and a great attendant mortality. Such diseases go along with loss of independence and impaired quality of life as well as social and economic costs. Cardiovascular diseases are the main cause of death in Austria (Statistik Austria, 2010). In 2009 43% of all deaths were results of cardiovascular problems. This reflects a number of four out of ten deaths caused mainly by heart attacks or strokes. But cardiovascular diseases are not only a problem in Austria. They have become the predominant cause of death in

many countries and in the whole world claiming 17.1 million lives a year (WHO, 2010). Cardiovascular diseases occur equally in men and women. Known risk factors are tobacco use, unhealthy diet and physical inactivity. These diseases can be prevented by minimizing the known risk factors. Today we can see a decrease of 1.2% over the last ten years, or even of 16% by considering the increase of elder people. Also a reduction of 33% in the death rate of cardiovascular diseases due to improved therapeutic applications and basic research were observed (Statistik Austria, 2009).

1.2 MYOCARDIAL REGENERATION

Heart failure is a result of myocyte hypertrophy and dysfunction as well as the progressive loss of cardiomyocytes. Apoptosis, the programmed cell death plays a critical role in this loss of cardiomyocytes and can rapidly lead to organ destruction (Narula et al., 1996).

Today, the only available therapies to treat a heart failure are cardiac transplantation, remodeling operations and pacing. Cardiac transplantations are the most radical, because the disrupted heart gets replaced by a new functional donor heart. Another possibility is partial transplantation by implanting left ventricular assist devices permanently. Severe heart failures can be surgically treated by remodeling of the left ventricle or by implanting a pacemaker that resynchronizes the heart. All these therapies have their pros and cons so that the research in developing more effective and improved therapies is of great interest. Great hope lies in a recently discovered technique, myocardial regeneration, which allows the repopulation of injured tissues with cells that are able to improve and enhance heart function. The research focuses on finding such cells that represent an adequate source for regeneration of the injured myocardium.

An old dogma, which could be disproved by Kajstura and colleagues (1998), says that cardiac myocytes are not able to divide because of the fact that they are already terminally differentiated. According to this old notion the injured heart is not able to overcome the progressive loss of cardiomyocytes with new self-cardiomyocytes

and consequently the heart do not feature some kind of self-repair mechanisms. But Kajstura and colleagues could disprove the notion of the human heart to be a post-mitotic organ. Indeed, they could show that in normal, healthy myocardium mitosis was extremely infrequent, but in injured myocardium they could see a reenter of cardiomyocytes into mitosis. Unfortunately, this self-repair mechanism of the injured heart is not able to cover up the large deficit of cardiomyocytes. This limitation makes an exogenous supply of cells necessary. An example of such exogenous source of cells represents fetal cardiomyocytes. Fetal cardiomyocytes were used for cell transplantation after a myocardial infarct (Leor et al., 1996). This group could show that this transplanted cardiomyocytes were able to successfully engraft into infracted myocardium thereby expressing gap junction. The transplanted cells were able to survive in the disrupted area and lead to improved cardiac function.

Regardless of the breakthrough with fetal cardiomyocytes, research turned to usage of skeletal myoblasts for cell therapy. With skeletal myoblasts they could overcome the controversial problematic of ethic. Anyway, cells are more available, are more suited for in vitro cultivation and are committed to the cardiac lineage which reduces the prevalence of tumor development. Murry and colleagues (2008) could demonstrate that skeletal myoblasts grafted into injured rat hearts had the potential to develop into muscle tissue. Another study where skeletal myoblasts were engrafted into the infarcted myocardium showed that systolic function and contractility was improved (Taylor et al., 1998). At first glance these cells seem to be perfectly made for cell therapy, but by closer attention these cells exhibit some limitations. One limitation addresses the fact that fetal cardiomyocytes are able to express gap junctions and thereby can interact with neighboring cells, while skeletal myoblasts lack this feature.

A more realistic source of cells for myocardial grafting turned out to be stem cells. Stem cells are known to feature unique characteristics like plasticity which make organs that harbor stem cells possible to get to a certain extent regenerated after injury. Stem cells are able to regenerate tissues like skin, intestinal and pulmonary mucosal and connective tissues. As already mentioned, the heart is considered as a postmitotic organ, but again this notion could be disproved by the behavior of bone

marrow stem cells. Bone marrow stem cells have the capacity to infiltrate into normal and infarcted myocardium. This homing of stem cells is thought to be driven by environmental factors in the injured tissue. Just arrived the infarcted myocardium, bone marrow stem cells gave rise to new myocytes, endothelial cells and smooth muscle cells thereby regenerating the infarcted myocardium (Orlic et al., 2002). Here again, it was shown that the heart feature self-repair mechanisms after injury. Orlic and colleagues were also able to demonstrate a decrease in infarcted area when bone marrow cells were directly transplanted into infarcted myocardium. Autopsies of female hearts who had received sex-mismatched bone marrow transplantation revealed the presence of Y-chromosome-positive cardiomyocytes (Deb et al., 2003). This result indicates that the cardiomyocytes originated from the transplanted bone marrow and thus proved the remarkably potential of bone marrow stem cells to infiltrate infarcted myocardium as Orlic and colleagues already demonstrated. These new comforts revealed the potential of stem cells and consequently raised the interest of further investigations in this area.

1.3 STEM CELLS

Stem cells have two major properties which make them very attractive in clinical research. Firstly, they are provided with an unlimited self-renewing potential and can be kept in an undifferentiated state. Secondly, their plasticity enables them to differentiate into various cell types. These characteristic features make stem cells a unique cell line.

Self-renewal is important to maintain the stem cell pool during injury and throughout life. The process of self-renewal is not an easy one. Complex networks are necessary to balance proto-oncogenes and tumor suppressors (He et al., 2009). Such genes are involved in promoting or limiting self-renewal and are regulated by signals from the stem cell niche. Without signals from the niche stem cells reside in a state of rest with less division potential (Cheshier et al., 1998). But during tissue injury stem cells get activated and enable tissue repair by enhanced self-renewal (Wilson et al., 2008).

So self-renewal is dependent on signals from the niche. Such microenvironments in which stem cells reside are important to balance stem cell activity and without their niche stem cells lose their self-renewal capacity and start to differentiate. Therefore, these niches are not only necessary for tissue repair, they are also important to maintain stem cell identity. The discovery of the importance of such niches emerged firstly by the removal of stem cells from their environment. Without the extrinsic signals provided from the niche, stem cells lost their proliferative potential. Since then, stem cells are thought to need distinct environments where they are associated with tissue-cells and signals emerging from the microenvironment (Schofield, 1978). The term "niche" was created. Today we know about the existence of stem cell niches in the intestinal, neural, epidermal and hematopoietic system (Figure 1.1).
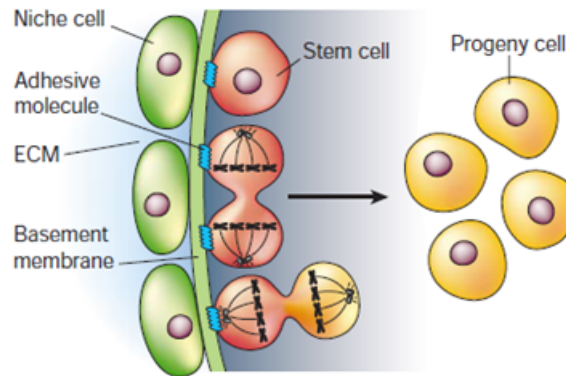
Figure 1.1: Stem cell niches balance stem cell activity. Niche cells interact indirectly with stem cells and control their activity. These cells control the differentiation and division of stem cells.Distinct stimuli activate stem cell division. Thereby one daughter cell remains attached to the niche while the other start the differentiation program (Spadling et al., 2001).

Another special feature of stem cells is pluripotency. So far, three transcriptional factors are known to control stem cell genes involved in maintaining pluripotency or activate genes responsible for repressing differentiation. One of the critical factors is the transcription factor *Oct3/4*. *Oct3/4* controls the fate of embryonic stem cells not simply by an on-off control system, but by the level of *Oct3/4* itself. Niwa and colleagues showed that an up- or downregulation of *Oct3/4* expression results in diverse differentiation programs, while a critical amount is necessary to maintain pluripotency. Further studies on this issue revealed other factors necessary in maintaining

pluripotency. *Nanog* is expressed in undifferentiated murine embryonic stem cells, but absent in differentiated cells (Mitsui et al., 2003). *Nanog* is like *Oct3/4* important for the maintenance of pluripotency and interplays with *Oct3/4* (Chambers et al., 2003). Another today known key factor is *Sox2* which acts on *Nanog*, *Oct3/4* and *Sox2* itself. *Sox2* is maybe not as essential as *Oct3/4* in maintaining embryonic stem cells, but *Sox2* has its critical role in stabilizing cells in the pluripotent state (Masui et al., 2007).

Murine embryonic stem cells have the attractive characteristic to differentiate to every type of cell in vivo promising great hope in cell-based therapies (Murry and Keller, 2008). They can be isolated from the inner cell mass of the blastocyst and can be kept as in vitro cultures (Martin, 1981). In vitro, the cells maintain their differentiation potential and provided with appropriate stimuli they can be induced to differentiate into diverse cell types. Collectively, embryonic stem cell differentiation can be directed into the ectodermal, mesodermal and endodermal lineage (Desbaillets et al., 2000). *LIF/STAT3*-dependent signaling plays a critical role in maintaining pluripotency and self-renewal of in vitro cultivation (Cartwright et al., 2005). To keep embryonic stem cells in an undifferentiated state the presence of *LIF* or feeder layers is indispensable. Differentiation of stem cells into somatic cell types occurs via precursor cells (also often called somatic stem cells). While embryonic stem cells are pluripotent, tissue-specific stem cells are restricted to their lineage. As the term 'tissue-specific' reveals this type of stem cells can only generate cell types of the tissue they reside in.

Today three methods are used to promote differentiation of embryonic stem cells: the culture of ESCs directly on supportive stromal layers, the culture as monolayers and the generation of embryoid bodies. It is debatable which of these methods is classified as the best, but all proved the potential of embryonic stem cells to differentiate in vitro to a wide spectrum of cell types.

1.3.1 Embryoid Bodies

A promising approach in determining appropriate conditions for differentiation of embryonic stem cells was made by the creation of embryoid bodies. Embryoid bodies are 3D spherical structures of cell aggregates hold in suspension, on methylcellulose or as hanging drops. Dependent on the aggregate procedure differentiation reveals distinct cell types (Figure 1.2).

Embryoid bodies mimic early embryonic developmental stages until gastrulation and give rise to most if not all somatic cells of all three germ layers (Desbaillets et al., 2000). Embryoid bodies made it easy to investigate developmental issues and reduced the need of peri-implanted embryos. Further they are suited for the characterization of the function of precursor cells or of given null mutants. But we should be aware that embryoid bodies are restricted in their developmental potential. They possess no polarity or body plan and so no viable embryo can be created what is an important fact in ethical issues.

With the method of hanging drops we are able to create embryoid bodies with defined cell number and shape. This procedure is probably the easiest to control.
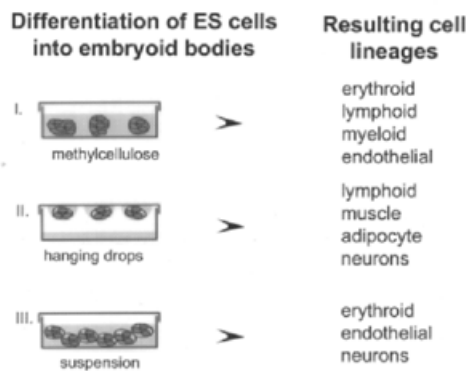
Figure 1.2: Three methods for embryoid body formation. These methods differ in their culture conditions and the following differentiation into distinct cell types. First procedure describes the possibility of aggregates to attach at a methylcellulose layer. Second opportunity is to let aggregates hang from the lid, which separate the aggregates from each other. Last method explains the cultivation in suspension where aggregates can float (Desbaillets et al., 2000).

1.3.2 Differentiation Potential

Developmental biology deals with the formation of organisms and with its associated cellular processes. Gastrulation is an important stage during embryogenesis where intense cell migration proceeds to generate the three germ layers: mesoderm, ectoderm, endoderm. Studies revealed that early lineage commitment occurs not by chance rather by spartial and temporally specification of cell populations (Kinder et al., 1999). During gastrulation the primitive streak is formed transiently at the posterior end of the embryo. This includes also the movement of cells over the primitive streak which in turn gives rise to the mesoderm and the definitive endoderm. The ectoderm does not as mesoderm and definitive endoderm derive through migration of cells through the primitive streak. It derives from the anterior region of the epiblast (Figure 1.3). The primitive streak is distinguished by different expression profiles along its axis (Kinder et al., 2001), whereas some genes like *Brachyury* are expressed over the hole primitive streak (Kispert and Hermann, 1994). Beside the diverse expression profiles, cells of the primitive streak showed also varied differentiation potentials what concludes the presence of a prospective fate map (Smith et al., 1994).
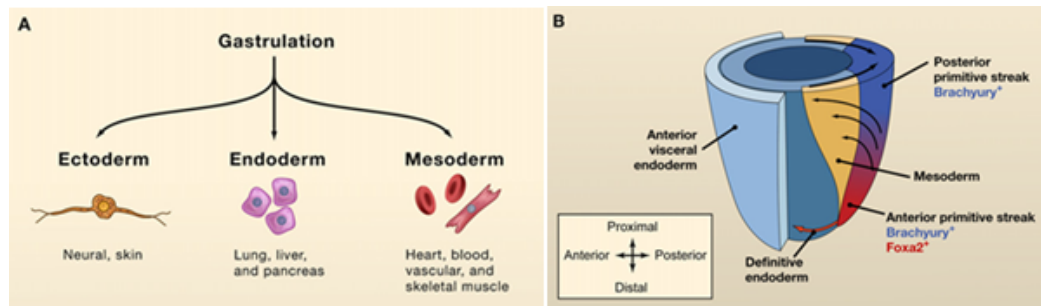
Figure 1.3: Formation of the three germ layers during gastrolation. A: The process of gastrulation leads to the formation of ectoderm, endoderm and mesoderm. Each layer is fated to generate distinct types of cells in further developmental stages. B: Movement of cells located at distinct positions at the primitive streak explains the formation of the three germ layers (Murry and Keller, 2008).

These findings suggested that the regions of the primitive streak differ in their signaling environments, which further concluded the induction of diverse lineages. In vitro studies revealed an insight into the regulatory mechanisms underlying germ layer formation. Different culture conditions mimicking probably distinct signaling

environments lead to the formation of cell types typical for each germ layer.

Embryoid bodies cultured in the presence of activin A or exposed to reduced serum revealed induction of endoderm formation. A population of cells expressing *Brachyury* showed differentiation to endoderm and revealed also a potential for mesoderm formation (Kubo et al., 2003). While *Brachyury+* cells adopt a line between endoderm and mesoderm, *Foxa2+* cells seemed to be more restricted in their differentiation fate (Figure 1.3,B). *Foxa2* promotes an endodermal fate (Burtscher and Lickert, 2009). Endodermal cells emerge to cells comprising the embryonic gut and in following developmental processes form the gastrointestinal tract, liver and pancreas.

The ectodermal layer emerges to the neural lineages and skin. The ectodermal induction proceeds without presence of serum or other primitive streak inducers and is therefore often said as default pathway. Ying et al. demonstrated that neural fate is decided by simple elimination of inductive signals for alternative fates, but requires autocrine fibroblast growth factor (Ying et al., 2003). In vivo, retinoic acid has great influence during developmental decisions affecting mesodermal or ectodermal cell differentiation. It controls the fate of cells to become either cardiac cells or neurons by inducing neuronal differentiation and thereby inhibiting cardiomyogenesis at the same time. While high concentrations of retinoic acid resulted in the development of neurons, low concentrations led to differentiation of cardiomyocytes (Aouadi et al., 2006).

Mice lacking nodal died between E8.5 and E9.5 due to the failure to form mesoderm (Pfendler et al., 2000). Similar results were seen by deletion of *Bmp-5* gene. Because of the observed defects it can be assumed that these two genes are among others important in mesoderm formation. Also an important gene involved in mesoderm formation is *Brachyury T*. Without *Brachyury* not enough mesoderm is produced (Wilkinson et al., 1990). Therefore, an interplay of distinct markers specify the formation of the mesoderm. The formation of beating cardiomyocytes from mouse mesoderm seemed to be directed and enhanced by the cardiac transcription factors, *Gata4* and *Tbx5* which was proved by *alpha-tropomyosin* and *cardiac troponin T*

expression (Takeuchi and Bruneau, 2009). Expression of cardiac marker $cTnT$ is restricted to the mesodermal lineage.

1.4 HEART DEVELOPMENT IN THE MOUSE

One topic of developmental biology deals with heart formation and the origin and role of heart-forming cells. The heart field is explained as the mesodermal area containing the cardiac progenitor cells that are finally destined to form the heart. Such precardiac cells start to migrate from the epiblast through the primitive streak and assemble the myocardial plate (Fishman and Chien, 1997). This is followed by the generation of the heart tube. Chamber formation is driven by looping morphogenesis separating the heart in four different chambers (Christoffels et al., 2000).

The heart is the first functional organ developed during embryonic development and consists of three layers: endocardium, myocardium and epicardium (Manasek, 1969). During gastrulation three germ layers, ectoderm, mesoderm and endoderm are generated that serve as a blueprint for organogenesis. Cells underlie a fate map and are therefore destined to build up distinct organs. One of the germ layers, the mesoderm is known to drive cardiomyogenesis leading to the formation of hematopoietic, vascular, cardiac and skeletal muscle lineages (Brand, 2003). Heart development is a strictly regulated process. Starting with the early mesoderm the cardiac development reaches its final by the formation of the four-chambered organ by continuous remodeling processes that are temporally and spatially controlled (Christoffels et al., 2000). Heart formation is driven by the differentiation of embryonic stem cells to an intermediate stage to the so called precursor cells. The following stepwise commitment of cardiac precursor cells lead to terminally differentiated cells making up the adult heart.

In early stages of embryonic development we can find precursor cells residing in the mesoderm expressing *Brachyury T. Brachyury T* is a marker for the onset of mesoderm induction. During first steps in cardiomyogenic development these cells change their expression profile to *Mesp1* expression. *Mesp1*-null mice featured malformations of the heart indicating that *Mesp1* plays a critical role in early cardiomyogenesis.

Mesp1-expressing cells generate the cardiovascular system, myocardium and endo-
cardium what was revealed by lineage studies (Saga et al., 2000). Mesodermal cells
start to migrate and to expand forming the cardiac crescent. *Mesp1+* cells are fated
to be precursors of cardiac progenitor cells that turn to express *Nkx2.5* and *Isl-1*. By
this, precursor cells got committed to the cardiac lineage irreversibly. *Isl-1*-expressing
cells migrate into the heart and lose most of the expression potential upon differ-
entiation. Sun et al. demonstrated in lineage studies that *Isl-1+* cells encompass
endothelial and smooth muscle cells in the adult heart. This in turn, made *Isl-1* an
adequate marker for cardiac cells in the heart. Mutant *Nkx2.5-/-* embryos showed
abnormal heart development. In conclusion it seemed that *Nkx2.5* is essential for
survival and proliferation of precursor cells (Lyons et al., 1995).

Diverse genes have an important role during heart formation controlling thereby
genetic pathways of embryogenesis. Disruptions in these genetic pathways can lead to
cardiac malformations in humans. Therefore it is not surprising that heart diseases are
associated with abnormal cardiac gene expression profiles. Important transcriptional
regulators are said to be the *Nkx2.5* homeodomain protein, members of the MEF2
family and HLH myogenic proteins (Fishman and Chien, 1997).
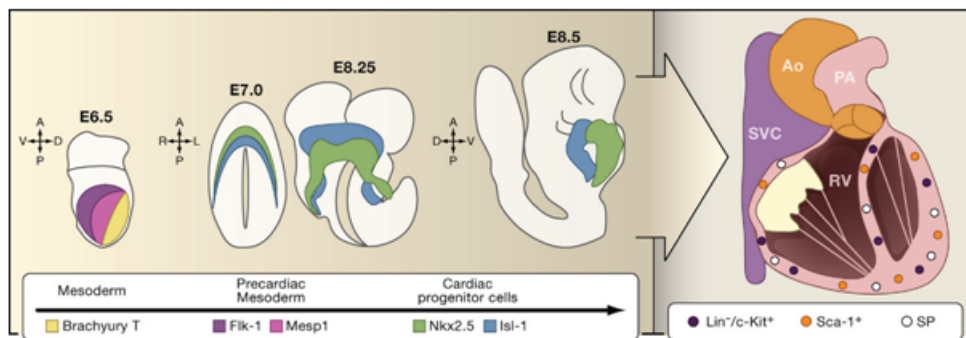
Figure 1.4: Schematic draw of heart development and the role of putative progenitor
cells. Mesodermal cells expressing *Brachyury T* turn to express *Flk-1* and *Mesp1* which
results in the induction of cardiac development. A final commitment is activated by
changing the expression profile to *Nkx2.5* and *Isl-1*. Cells expressing these markers are
assumed to be progenitor cells that form during several differentiation processes the
adult heart (Wu et al., 2008).

1.4.1 *Nkx2.5* Homeodomain Protein

The *Nkx2.5* gene is the vertebrate homolog of tinman and is a cardiac-specific homeobox gene playing a critical role in heart development. As already mentioned mesodermal cells turn to express *Nkx2.5* during heart development, which indicates the first commitment of cells to the cardiac lineage. Therefore *Nkx2.5* can be described as an early marker in cardiac development which is still expressed throughout the developing heart and even in the adult heart. One important enhancer in the activation of *Nkx2.5* expression during heart development seemed to be *GATA4* (Lien et al., 1998).

Mutations in the human *Nkx2.5* gene results in heart disease causing abnormalities of the atrioventricular conduction system and the heart itself (Schott et al., 1998). A study by McElhinney and colleagues showed that only a small percentage of heart diseases originate from mutations in the coding region of the *Nkx2.5* gene. In many cases mutations were missense and observed outside the homeodomain indicating the importance of this region in cardiac development. Tanaka and colleagues demonstrated the effect of *Nkx2.5* gene disruption in the adult heart by revealing its influence on the late differentiation potential of cardiac myocytes.

In summary, *Nkx2.5* plays a critical role in heart development and in cardiac genetic pathways thereby influencing downstream cardiac genes (Lyons et al., 1995).Today it is thought that *Nkx2.5* is critical for cardiac cell fate determination, though it is insufficient to do it all on its own.

A stable CVPC clone A5 cell line called A5-CSX was created by T. Gottschamel (2010) carrying an EGFP reporter gene and a *puromycin* resistence cassette located in the *Nkx2.5* gene.

The A5-CSX cell line was produced by homologue recombination with the pCsx-EGFP-PP-DT vector, which contains homologue sequences to the murine *Nkx2.5* gene which are interrupted by the selection marker *puromycin* and an EGFP reporter

gene. The A5-CSX cell line carries an EGFP marker gene under the control of the *Nkx2.5* promoter. Because EGFP expression correlates with the *Nkx2.5* expression we are able to display differences in *Nkx2.5* expression by detecting the EGFP signal by diverse methods like western blotting, immunofluorescence mircroscopy and FACS analysis. The differentiation as well as the self-renewing potential of A5-CSX cells was not influenced by the knock in (Gottschamel, 2010). Therefore the A5-CSX reporter cell line is an adequate tool for the investigation of factors influencing *Nkx2.5* expression and so cardiomyogenesis.

1.5 CARDIAC PROGENITOR CELLS

The obsolete notion of the adult heart as being a postmitotic organ with the absence of resident stem cell populations is today very well undermined by diverse studies. Results indicated the existence of stem cell-like populations in the fetal and adult heart and abolished the old dogma of a missing self-renewal potential. This assumption is strengthened by the successful isolation of cardiac stem cell-like populations from the adult heart expressing defined markers. By now *Sca-1* or *c-Kit* are common markers for cardiac stem cells that hold good in the identification and isolation of these cells. Cells expressing these markers promise a great regenerative potential of injured tissue.

The number of *Sca-1* expressing cells was enhanced after myocardial infarction indicating their potential in promoting heart tissue repair (Wang et al., 2006). Wang and colleagues succeeded in the isolation of *Sca-1+/ CD31-* cells from the heart of mice. In vitro cultivation and differentiation studies revealed their potential to differentiate to both endothelial and cardiomyocyte cells. Transplantation of these cells into disrupted murine hearts revealed an improvement of heart function as well as an enhancement of cardiomyocyte regeneration.

Transgenic mice featuring *EGFP* under the control of the *c-kit* locus showed a maximum of *c-kit+* cells at postnatal day 2, whereas only very few cells were observed in the adult heart. But disrupted adult hearts expressed *c-kit* positive cells in a higher extent especially in and surrounding the infarct tissue. Isolation of *c-kit+* cells and

further in vitro investigations confirmed the idea of *c-kit+* cells to be precursor cells, because these cells differentiated into endothelial, cardiac and smooth muscle cells during in vitro cultivation (Tallini et al., 2009).

1.6 ISOLATION OF PROGENITOR CELLS

Two different, but similar methods were used by our group to isolate somatic stem cells. To ensure a successful isolation and cultivation of somatic stem cells they were provided with conditions similar with that they are confronted in vivo. Thereby it was attention made on the fact that stem cells need distinct culture conditions to maintain their self-renewal and differentiation potential. Thus, an artificial niche was created to mimic such conditions. This artificial niche consists of both *LIF*-producing fibroblasts and embryonic stem cells. Investigations on the self-renewing potential of embryonic stem cells showed already the importance of the *LIF* signaling pathway (Cartwright et al., 2005). The same necessity of *LIF* was supposed on cardiac stem cells to provide an artificial in vitro niche. Not only feeder cells, but also ESC contributed to the artificial niche by providing distinct growth factors and to ensure physical contact.

For the isolation of cardiovascular progenitor cells (CVPCs) the hearts from new-born 129v mice carrying a *neomycin* resistance cassette in one allele of the HDAC1 locus were cut into several pieces and blood cells were removed by centrifugation. Remaining tissue was dissolved by a mixture of Pancreatin and Collagenase II to obtain separation of cells. Cardiac cells were mixed with ESC AB2.2 cells in a 1:1 ratio and grown on feeder cells for 10 passages according to a 3T3 protocol what says that cells are splitted 1:3 every third day onto new feeder cells. Feeder cells are mitotically inactivated SNL76/7 fibroblasts expressing *LIF* and are resistant to *neomycin*. After the enrichment of putative progenitor cells, cells were exposed to G418, a *neomycin* analogon to get rid of ESC AB2.2 cells. Selection proceeded for 10 days and surviving cells were repeatedly exposed to the selection marker. Finally eleven subclones were maintained and frozen for storage (Figure 1.5, A).

A different strategy was used for the isolation of somatic stem cells (SSCs) from several tissues of neonatal and adult mice. Here single clones were obtained from the brain, pancreas and heart of wildtype mice. Contrary to the first isolation procedure, they worked with a negative selection marker, thymidine kinase carried by ESC Tag3 cells. In general the two procedures are quite similar, except the negative selection with Ganciclovir for 2x4 days instead of G481 for 10 days (Figure 1.5, B).
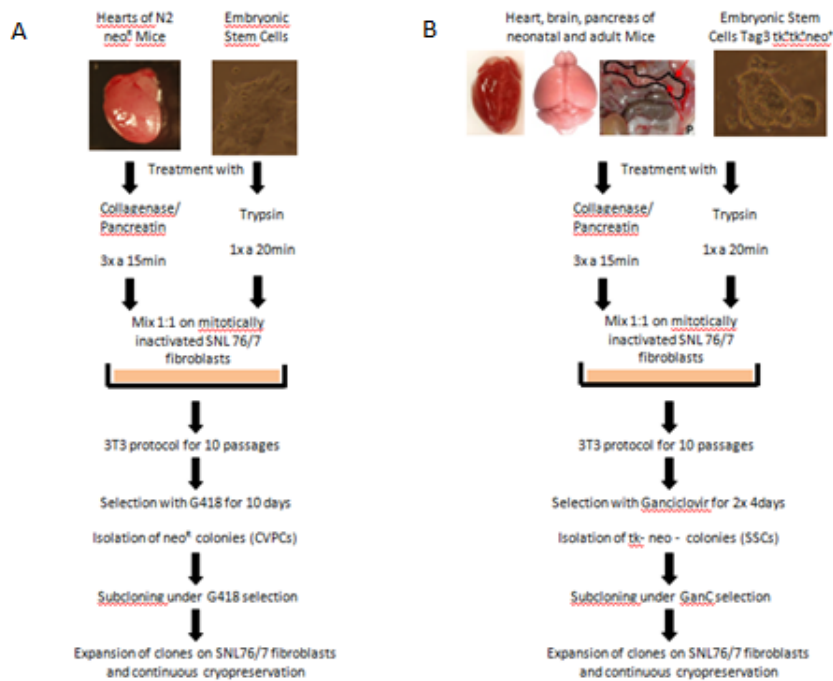
Figure 1.5: Two different procedures for the isolation of progenitor cells. Figure A indicates the isolation of so called cardiovascular progenitor cells (CVPCs) by positive selection of *neomycin* resistance gene. In contrast, for the isolation of so called somatic stem cells (SSCs) from different tissues they selected for *tk- neo-* cells (B).

1.7 MAPK PATHWAY

The mitogen-activated protein kinase (MAPK) cascade seems to control both cell proliferation and differentiation by induction by diverse growth factors and other signals. This cascade consists of several membranal signaling molecules that transmit extracellular signals to diverse cytoplasmic protein kinases. Finally, the signal reaches

the nucleus and activates genes that regulate cellular processes such as proliferation, differentiation and development. The process of transmission of extracellular signals to their intracellular targets is driven by interacting proteins that build up a network leading to serial responses. The signaling process is mediated by receptors, effector molecules and of course by a cascade of kinases. Molecules, such as small GTP binding protein (RAS), adapter molecules (GRB2) and guanine nucleotide exchange factor (SOS) play a critical role in transmitting growth factor signals to the kinases. The subsequent activation of this MAPK signaling cascade results in stimulation of regulatory molecules that in turn initiates cellular processes. But this distinct signaling cascade is not only one restricted pathway. Other pathways are able to use diverse signaling molecules within this MAPK cascade or even can activate this pathway. Diverse phosphorylation processes play a critical role in transmitting the extracellular signals. Starting with phosphorylation events of tyrosyl residues during receptor activation, the pathway is followed and ended by seryl and threonyl phosphorylations of cytoplasmic and nuclear proteins. One of the first kinases that lie upstream of the pathway is named Raf-1. Raf-1 is a serine/threonine kinase activated by various mitogens and directly by RAS. Upon activation Raf-1 gets hyperphosphorylated and in turn phosphorylates MAPKK (MEK-1) on a serine residue that activates MEK-1. Full activation of MEK-1 results in activation of MAPK (ERK-1/2). ERK-1 and ERK-2 are highly conserved and differ only in their substrate specificity. Upon activation threonine and tyrosine residues get phosphorylated (Seger and Krebs, 1995).

Inhibition of MAP kinase pathway by inhibition by SB203580 lead to a reduction of cardiomyogenesis by decreasing the occurrence of cardiomyocytes in P19 cells, while by inhibition of ERK1/2 by PD98059 no effect was visible. Expression levels of mesodermal markers were decreased by SB203580 inhibition (Davidson and Morange, 2000). PD098059 is a synthetic inhibitor of the MAPK pathway by inhibition of MAPK (MEK). This inhibitor is able to cross cell membranes and inhibits MAPK activity through an allosteric mechanism without disturbing other kinase activities. The inhibition by allosteric mechanism explains the selectivity for MEK kinase (Dudley et al., 1995).

2 RATIONAL

Because cardiovascular diseases are quite common in present days and have fatal impact of life quality or can even lead to death, it is important to develop adequate therapies to inhibit such disruptions or find mechanisms that are able to stimulate healing. A heart failure results in a dramatic reduction of cardiomyocytes what finally can lead to organ destruction. Great hope lies in a new therapeutic option, myocardial regeneration where injured tissues get replaced by endogenous or exogenous cells to improve heart function. Though we know today that cardiomyocytes are able to reenter mitosis after a myocardial infarct and that stem cells migrate to injured tissues, this self-repair mechanism of the heart is not sufficient to substitute the loss of cells. Thus, an exogenous source has to be found to completely replace injured tissues and restore proper function of the diseased myocardium. Studies with stem cells showed that they possess a great potential to push myocardial regeneration. Investigations of intrinsic and extrinsic conditions to cultivate and differentiate somatic progenitor cells will contribute to understand the molecular mechanisms that initiate cardiomyogenesis and may help to rescue injured myocardium. The establishment of a proper workflow to isolate progenitor cells will improve the understanding of such mechanisms.

Here we isolated somatic progenitor cells from organs of the mouse, especially from the heart. Today the focus lies in the characterization of these cells, their behavior in culture and their differentiation potential. We determine optimal conditions to drive differentiation to cardiomyocytes to be some day able to isolate human progenitor cells and to differentiate them to cell types residing in the heart.

This diploma thesis deals with the detailed characterization of CVPCs as well as the characterization of SSCs by FACS analysis and confocal immunofluorescence

microscopy. We learned about their spontaneous differentiation potential to generate limited cell types and investigated their behavior in commitment decision in the presence of retinoic acid. Further we analyzed factors that may play important roles affecting cardiomyogenesis by determining the *Nkx2.5* gene expression with FACS analysis and Luciferase assays.

3 ABBREVIATION

Alk3	bone morphogenetic protein receptor, type IA
BMP2	bone morphogenetic protein 2
c-kit	Kit Oncogene
CMC	cardiomyocyte
CMG	cardiomyogenesis
cTnT	cardiac Troponin T
CVD	cardiovascular disease
CVPC	cardiovascular progenitor cell
cDNA	complementary deoxyribonucleic acid
CD31	cluster of differentiation molecule 31
DMEM	dulbecco's modified eagle medium
DMSO	dimethylsulfoxid
dNTP	deoxy nucleotide triphosphate
EB	embryoid body
EDTA	ethylenediaminetetraacetic acid
EGFP	Enhanced Green Fluorescence Protein
ERK1/2	mitogen activated protein kinase 1
ESC	embryonic stem cell
ETC	endothelial cells
FACS	Fluorescence Activated Cell Sorting
FOXA2	Forkhead Box
GATA4	GATA-binding protein 4
GAPDH	glyceraldehyde-3-phosphate dehydrogenase
GFAP	glial fibrillary protein
HDAC	Histone Deacetylase
He2	He2P11K13/5
Hi2	Hi2P11K15/6
IF	immunofluorescence
ILK	integrin linked kinase

Isl 1	Islet-1
LIF	leukemia inhibitory factor
MAPK	mitogen activated protein kinase
MEF2C	myocyte enhancer factor 2c
MEK1	mitogen activated protein kinase 2
Mesp1	mesoderm posterior 1
MHC-alpha	myosin heavy chain-alpha
mRNA	messenger Ribonucleic Acid
neo	neomycin
nkx2.5	NK2 transcription factor related, locus 5
Oct3/4	octamer-binding transcription factor 3/4
PCR	polymerase chain reaction
RA	retinoic acid
RT-PCR	reverse transcription polymerase chain reaction
Sca-1	stem cel antigen-1
SMA	smooth muscle actin
Smad	mothers against decapentaplegic homolog
SMC	smooth muscle cell
Sox2	SRY-related box 2
SPARC	Secreted Protein Acidic and Rich in Cystein
SSC	somatic stem cell
STAT3	signal transducer and activator of transcription 3
tbx5	T box family
TGF-beta	transforming growth factor-beta
tk	thymidine kinase
TU-20	beta3-tubulin
vWF	von Willebrand factor

4 RESULTS

4.1 CHARACTERISATION OF CARDIOVASCULAR PROGENITOR CELLS AND SOMATIC STEM CELLS

Progenitor cell lines, called CVPCs (cardiovascular progenitor cells) and SSCs (somatic stem cells) have been previous isolated from our lab by two different but quite similar methods. Both methods mimicked artificial niches consisting of LIF-producing feeder cells and embryonic stem cells for the successful isolation and cultivation of these progenitor cells. The two procedures differed mainly by their selection method. For the isolation of CVPC a positive selection of neo^R progenitor cells was performed, while in the case of SSCs a negative selection for *tk-neo-* clones was done.

In the recent years focus was on the characterization of these cell lines. Most experiments were performed on CVPCs, the first progenitor cell line isolated by our lab. So far, self renewal and differentiation potential were investigated with interesting results. To maintain their self-renewing potential and to keep cells in an undifferentiated state cells were cultured on LIF-producing feeder layers (Hoebaus, 2009). CVPCs could be already cultured to passage 66 without losing their self-renewal. During this diploma thesis we even reached a passage of 111. Accordingly to Cartwright (2005) embryonic stem cells need LIF/STAT3-dependent signaling pathway to maintain their self-renewal and pluripotency. Same effect was seen in CVPCs. Western blot analysis further showed STAT3 activity (Hoebaus, 2009). To test if CVPCs feature pluripotency they were induced to differentiate. Finally, differentiation studies as monolyer cultures were performed resulting in a restricted differentiation potential. While embryonic stem cells are able to differentiate to any cell types of the body (Desbaillets et al., 2000), stem cells are restricted to their tissue-lineage. CVPCs were isolated from hearts and consequently are assumed to be restricted to the cardiac lineage. Thus, stem cells and the CVPC line are quite similar. Today it is known

that three transcriptional factors are involved in maintaining pluripotency of stem cells as previously mentioned. One of these transcription factors is *Oct3/4* which has to be expressed in a critical amount, while differences lead to diverse differentiation programs (Niwa et al., 2000). Similarly to stem cells, CVPCs express *Oct3/4* indicating the ability for self-renewal (Hoebaus, 2009). In summary, CVPCs act like stem cells in vitro. They possess a self-renewal potential proved by maintaining them in an undifferentiated state over several passages without changing their morphology and by STAT3 activity. Further they spontaneously differentiated only to cells residing in the heart indicating a tissue-specific differentiation potential.

The other cell lines were called somatic stem cells (SSCs) and were isolated from different organs of the mouse (heart, brain). So far, no morphological changes were observed during cultivation on LIF-producing feeder cells. Not much is known concerning differentiation potential and expression profiles.

4.1.1 Differentiation of ESCs in Embryoid Bodies

Embryonic stem cells have unique features that make them conceptually attractive for cell therapy. Beside their ability of unlimited self-renewal they spontaneaously differentiate into various cell types of the organism (He et al., 2009; Desbaillets et al., 2000).

For differentiation of ESCs we made use of the creation of embryoid bodies. Several protocols are available for the aggregation of ESCs that are in general quite similar with few differences (Desbaillets et al., 2000). Our lab optimized its own aggregate procedure to the minutest detail. We apply here a protocol where hanging drops were used for aggregate formation thereby we focused on the creation of conditions adequate for CVPC aggregation. This protocol was used for all cell lines mentioned in this diploma thesis to ensure same culture conditions.

Embryoid bodies are suited for the investigation of early developmental stages in vitro because of their potential to mimic post-implantation embryonic development. The embryoid bodies had a regular sized morphology and when attached to the surface

cells start to spread into the periphery. ESC AB2.2 cell-derived embryoid bodies were able among other cell types to differentiate into neuronal cells and functional skeletal muscle cells (Figure 4.1). Neuronal cells were distinguished by their elongated, thin and branched tubes (presumably neurites) emerging from the cell bodies. Skeletal muscle cells were marked by contracting pipe-like structures consisting of fused cells. Both were seen mainly in the periphery of the aggregates and were quite rare.
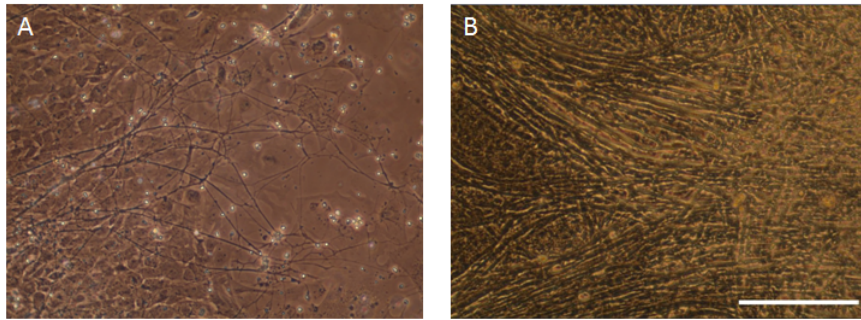
Figure 4.1: Infrequent differentiation of AB2.2 ESC into neuronal cells (A) and skeletal muscle cells (B). AB2.2 ESCs were induced to differentiate in hanging drop cultures. On day 5 of cultivation drops were rinsed onto gelatin-coated plates. Structural changes were checked daily. A: Rare occurrence rate of neuron-like cells seen around day 16 of cultivation. B: Contracting skeletal muscle cells were even more infrequently seen during aggregate development (day 20), (bar=200μm, light microscope).

Frequently, we observed structures like beating cardiomyocytes, smooth muscle cells and endothelial-like cells. But also fibroblast-like cells and hepatocyte cells were observed.

4.1.2 Differentiation of CVPCs and SSCs in Embryoid Body-like Aggregates

CVPCs and SSCs grown in the presence of LIF-producing feeder cells maintain their self-renewing potential and can be kept in an undifferentiated state for several passages. By transferring cells onto gelatin-coated plates they started to differentiate due to the absence of feeder cells. Cells lost their round shape and their ability to form dense and tight colonies. They appeared angular and formed clusters of differentiated cell aggregates. During differentiation as monolayers cell types like cardiomyocytes, smooth muscle cells and endothelial cells were observed, but the number varied highly between experiments and in general formation seemed to be chaotic (Hoebaus, 2009).

To control differentiation in a more effective extent we applied the well known embryoid body system to our isolated precursor cells. This procedure resembles in vivo conditions and mimics early embryonic developmental stages. An adequate concentration of cells (4.5×10^4cells/ml) were dropped onto the lid of a dish and were cultured as hanging drops for a period of five days. During this time period cells start to divide and to form aggregates floating in the drops. The absence of a surface to attach resembles perfectly in vivo conditions. On day five aggregates were rinsed onto gelatin-coated culture dish plates and aggregates started to adhere at the dish surface (Figure 4.2). Medium was changed according to a well adapted feeding protocol in which the medium was changed every third day. To avoid sudden absence of important factors secreted into the medium from the cells themselves, a part of the old medium was always kept and fresh medium was added to ensure new nutrients available in the media.
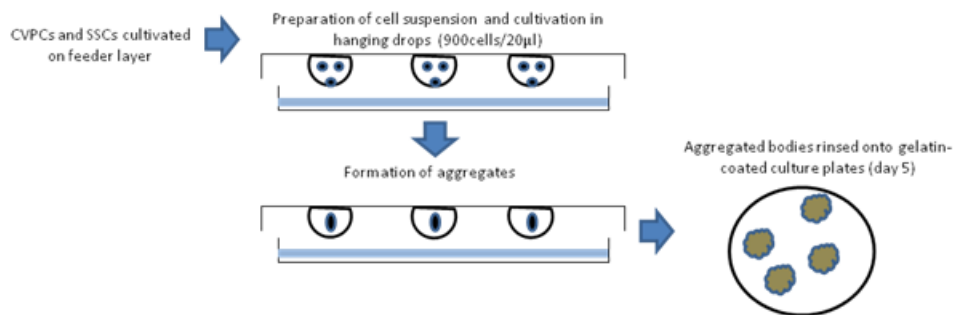
Figure 4.2: Schematic draw of embryoid body-like aggregate generation. Cells were separated from feeder cells to prevent disruption of aggregate formation. Cells were dropped onto the lid of a petri dish with a concentration of 900 cells/$20\mu l$. On day 5 hanging drops were rinsed onto gelatin-coated culture plates. For further cultivation aggregates were fed every third day.

During cultivation aggregates started to differentiate and expanded into the periphery. Three cell types residing in the heart were observed in the course of differentiation: rhythmically contracting cardiomyocytes, slowly contracting smooth muscle cells and endothelium-like cells.

4.1.3 Characterization of Cardiovascular Progenitor Cells (CVPCs)

This topic deals with the differences between differentiated CVPCs and AB2.2 ESCs in aggregate size and morphology as well as the generation of distinct cell types.

Further attention was made on the restricted differentiation potential of CVPC to the cardiac lineage and the differences of cardiomyocyte formation between CVPC clones.

CVPCs - Size and Morphology Characterization

AB2.2 embryoid bodies tended to form horse-shoe like structures after attachment to surface, while aggregated CVPCs seemed to have no such defined morphological structure. CVPC aggregates comprised of cells densely arranged in the middle of the aggregates, which were so compact that they appeared as dark circle in the brightfield microscope (Figure 4.3, white arrows). This compact dark core was also seen in AB2.2 aggregates, but here they were often not centered as seen in CVPC aggregates. This dark core of CVPC aggregates was always surrounded by less dense cell areas arranged as a ring around the core. The outer region was comprised by cells diffusible arranged and spread further into periphery. In general CVPC aggregates were larger and cell spreading into periphery proceeded faster compared to embryoid bodies.
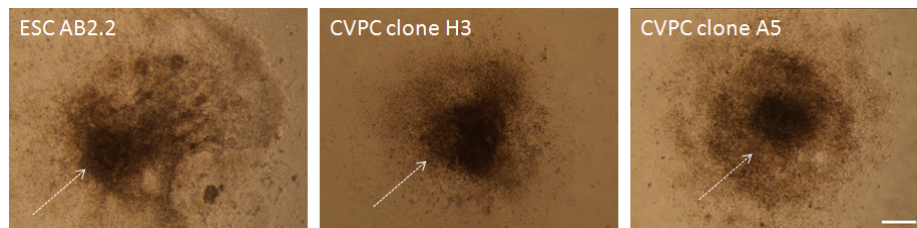
Figure 4.3: Size and aggregate morphology of CVPC aggregates. Size and morphology of CVPC clone A5 and H3 aggregates compared to AB2.2 embryoid body on day 9 of cultivation. Aggregates consisted of a dense inner core, surrounded by less dense cell areas reaching far into periphery. White arrows indicate the compact core, which was centered in CVPC aggregates but not in embryoid bodies (bar=300μm).

CVPC aggregates possessed an inner cell mass of round shaped cells quite dense arranged in the middle of the aggregate. This dense center was surrounded by a less dense intermediate region comprising of differentiated cells. These differentiated cells were characterized by their different cell morphology and elongated further out of the dense center into periphery. Differentiated cells adjacent to and surrounding the dense core, were round or angular shaped and not as densely packed as seen in the core center (Figure 4.4, B, white arrow). The periphery was populated by elongated angular shaped cells (Figure 4.4, C, white dashed arrow).
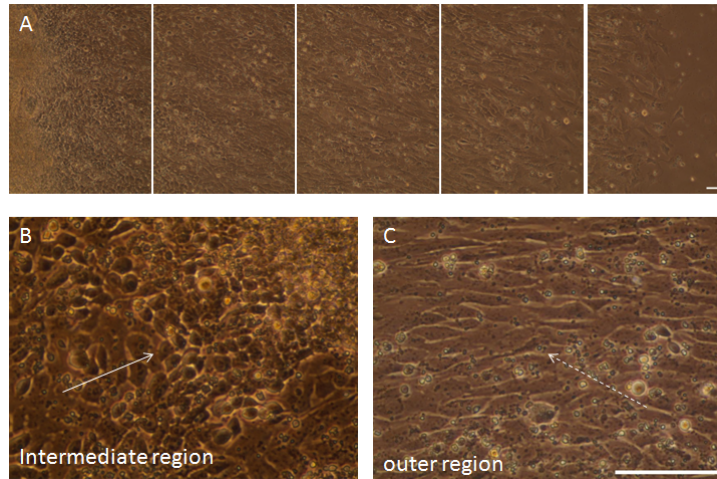
Figure 4.4: Cell morphology characterization of CVPC aggregates. A: CVPC clone A5 (d12) consisting of a dense center bordered by the intermediate region which elongates into the outer region. B and C: Intermediate region, comprising of round and angular shaped cells (B, white arrow) and outer region populated mostly by elongated cells (C, dashed,white arrow)(bar=50μm).

CVPCs - Differentiation Potential

Cardiac lineage commitment of CVPCs was initially assessed by previous studies that revealed that CVPC aggregates differentiate spontaneously into cell types residing in the heart (Hoebaus, 2009). In further differentiation studies we analyzed the potential of CVPC aggregates to differentiate into other cell types not specific for the cardiac lineage. By previous investigations of aggregate development and immunofluorescence experiments we already know that CVPCs are able to differentiate spontaneously into rhythmically beating cardiomyocytes, slowly contracting smooth muscle cells and endothelial-like cells. To exclude differentiation into other lineages we stained CVPC aggregates with antibodies specific for distinct cell types and performed confocal scanning immunofluorescence microscopy and quantitative FACS analysis. Stainings were done with a subset of markers specific for ectoderm, endoderm and mesoderm. Ectodermal markers were provided by both anti-beta3- tubulin and anti-glial fibrillary protein (GFAP) antibodies. Both markers are specific for the neuronal lineage and stain neuronal or glia cells, respectively. For determining cells positive for the endodermal lineage we used anti-FOXA2 and anti- von Willebrand factor (vWF) antibodies. FOXA2 is a member of the forkhead class of DNA-binding proteins and are transcriptional activators for liver-specific transcripts regulating differentiation of

the pancreas and liver. The glycoprotein vWF (also Factor VIII) is produced mainly by endothelial cells and is thereby secreted into the plasma or stored in intracellular granules. It plays an important role in the blood coagulation system and is found in platelet vessel walls. Mesodermal cells were proved by staining with anti-cardiac troponin T (cTnT) and anti-smooth muscle actin (SMA) antibodies.

First, we performed confocal scanning immunofluorescence microscopy with antibodies mentioned above. Therefore we made hanging drop cultures of CVPC clones A5 and H3 and rinsed the aggregates on day 5 onto gelled cover slips and let them grow for further eight days. After this cultivation time aggregates were stained with primary antibodies specific for cell types of the endodermal, ectodermal and endodermal lineage. Addition of fluorescently labeled secondary antibodies (anti-mouse Alexa Fluor 488 and anti-rabbit Alexa Fluor 647) for indirect immunofluorescence was followed. Neither ectodermal cells (beta3-tubulin+ and GFAP+ cells) nor FOXA2 -expressing cells were observed on day 13 of aggregate development. But we obtained vWF-positive cells (Figure 4.5).
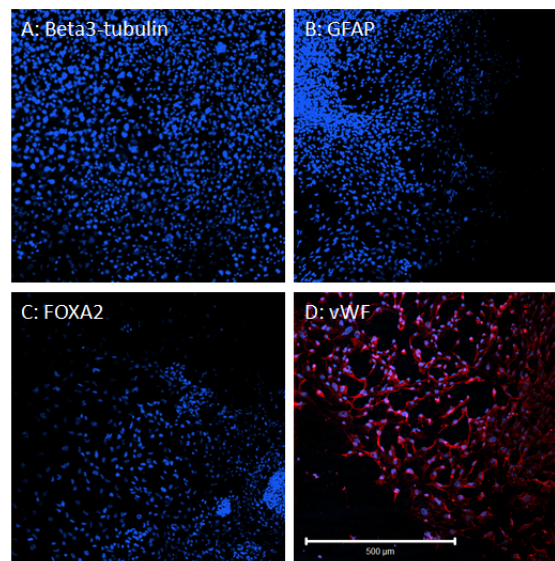
Figure 4.5: Immunofluorescence staining of CVPC aggregates on day 13 of cultivation. Aggregates of CVPC clones A5 and H3 were made and grown onto gelled cover slips until day 13. On day 13 aggregates were stained with primary antibodies against beta3-tubulin, GFAP, FOXA2 and vWF. Secondary antibody staining was followed by either anti-mouse Alexa Fluor 488 (beta3-tubulin) or anti-rabbit Alexa Fluor 647 (GFAP, FOXA2, vWF). (bar = 500μm; LSM-Meta 510 confocal microscope).

Both cardiac marker genes (cTnT, SMA) were expressed by cells of CVPC aggregates. SMA positive cells were circular arranged thereby surrounding the compact center of the aggregates. Presumably these cells represent myofibroblasts. Myofibroblasts have features of both fibroblasts and smooth muscle cells. Cells expressing cTnT were observed near the center of aggregates. While SMA positive cells were exclusively seen in the outer region, cTnT positive cells resided in the intermediate region. Cells expressing cTnT appeared in clusters and were rarely observed individually, they tended to be in groups (Figure 4.6).
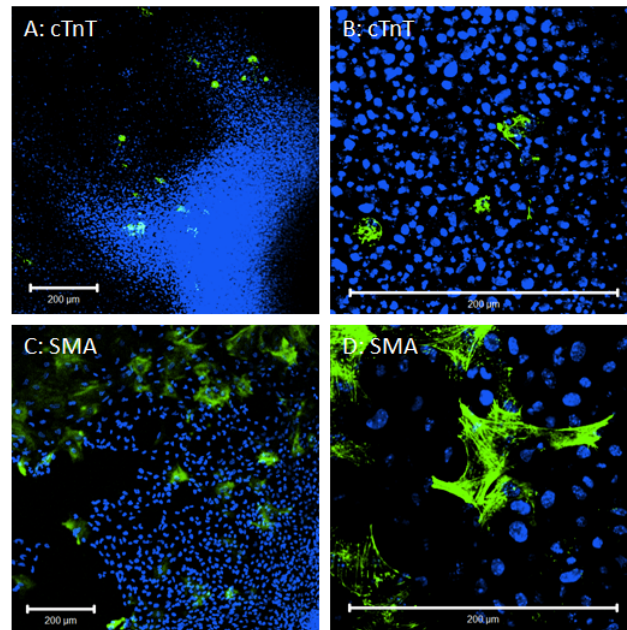
Figure 4.6: Immunofluorescence staining of CVPC aggregates with cardiac markers. Again embryoid body-like aggregates were generated and stained with anti-cTnT and anti-SMA antibodies. Secondary antibody staining was followed by anti-mouse Alexa Fluor 488 (bar = 200μm; LSM-Meta 510 confocal microscope).

Next we analyzed the cell population of CVPC clone A5 and H3 aggregates with quantitative FACS analysis. With this method we wanted to determine the incidence of each cell type mentioned above among a cell population of A5 and H3 aggregates. For FACS analysis aggregates grown on gelatin-coated culture plates were detached from the gelatin-layer and separated into individually cells by trypsinization on day 13. This cell suspension was then fixed with paraformaldehyde and stained with same antibodies used during immunofluorescence microscopy. Surprisingly, the frequency rates of the investigated cell types were enormous and quite different to data obtained

during immunofluorescence microscopy. Therefore, data received by FACS analysis were not reliable due to this great divergence. Figure 4.7 indicates the percentage of cell populations in CVPC clone A5 and H3 aggregates. Beta3-tubulin positive cells were absent in A5 and very low in H3 aggregates. The frequency of GFAP-expressing cells was extremely high with 87.47% in A5 and 51.79% in H3 aggregates, although immunofluorescence microscopy indicated an absence of these ectodermal cell type. Similarly, FACS analysis revealed a presence of FOXA2-expressing cells (A5: 2.51%, H3: 0.97%), while they were also absent during immunofluorescence microscopy. Frequency rate of vWF-expressing cells was nearly 100% during FACS analysis and only few cTnT positive cells (0.49%) could be observed in A5 cell population, whereas H3 aggregates possessed 0.065% cTnT-expressing cells. SMA-expressing cells were seen in both A5 and H3 aggregates. A5 aggregates featured 88.77% SMA positive cells, while H3 aggregates only 48.99%.
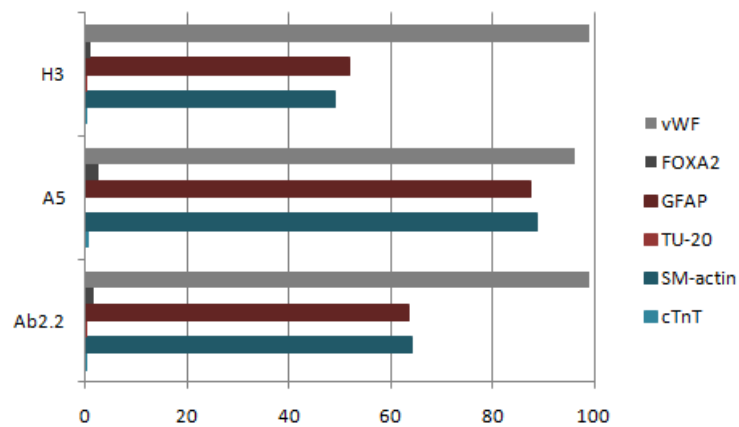
Figure 4.7: Percental distribution of cell types emerging in A5 and H3 aggregates on day 13 of cultivation. Aggregates were separated into single-cell suspensions, fixed with paraformaldehyde and stained with antibodies against beta3-tubulin, GFAP, FOXA2, vWF, SMA and cTnT. Secondary antibody staining was followed by either anti-mouse Alexa Fluor 488 (beta3-tubulin, SMA, cTnT) or anti-rabbit Alexa Fluor 647 (GFAP, FOXA2, vWF)(FACS Calibur).

As already mentioned, data obtained during immunofluorescence studies and data received from FACS analysis were very contradictorily. Cells expressing FOXA2, beta3-tubulin and GFAP were absolutely absent by investigating cover slips under the confocal microscope. While FACS analysis showed extremely high values for the occurrence rate of vWF and GFAP expressing cells. In the assumption that the

error is always the same among the data received from FACS analysis we decided
that it might be possible to compare the occurrence rate of CVPCs with AB2.2
cell population to obtain at least an idea how CVPC aggregates differ from AB2.2
aggregates (Figure 4.8). We did not compare data received from staining with anti-
FOXA2, anti-GFAP and anti-beta3-tubulin antibodies, because no positive signals
were seen during immunofluorescence microscopy.
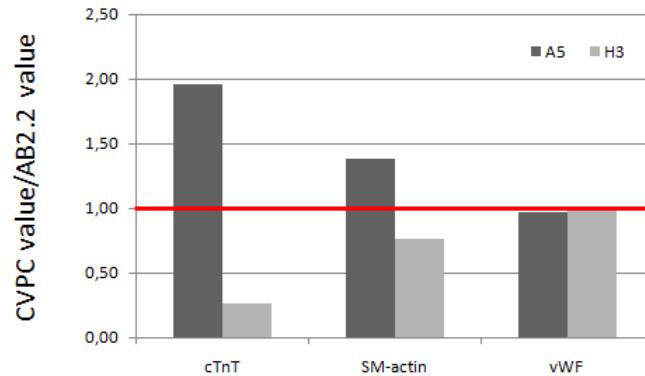
Figure 4.8: Comparison of CVPC and ESC AB2.2 aggregates on day 13. Data of
CVPCs obtained from FACS analysis were divided through AB2.2 data. The value 1
represents the baseline of AB2.2 data (red). Data above this baseline mean a higher
occurrence rate of this cell type compared to AB2.2 and below the opposite.

We can clearly see that CVPC clone A5 showed a higher number of cTnT- and
SMA-expressing cells compared to AB2.2 aggregates. In contrast clone H3 revealed a
lower occurrence rate of these cell types. But vWF expression was nearly the same
as seen in AB2.2 cell population (Figure 4.8).

We also performed FACS analysis with undifferentiated CVPC clone A5 and H3
aggregates as well as ESC AB2.2 aggregates. Therefore cells were grown on LIF-
expressing feeder cells to keep them in an undifferentiated state. For FACS analysis
cells were trypsinized, fixed in 4% paraformaldehyde and stained with same antibodies
used in previous experiments. To compare the composition of cell populations
between the undifferentiated and differentated state we divided data obtained from
analyzing CVPC aggregates by data received from undifferentiated cells. While
vWF expression was not changed dramatically during differentiation of CVPC and
ESC aggregates, other marker showed changes in their expression profiles upon
differentiation. Undifferentiated AB2.2 cells showed a high expression level of beta3-

tubulin reaching nearly 100% while CVPC clones only reached about 50% (not shown). In general, during aggregate development neuronal differentiation is strongly reduced as seen with GFAP and with beta3-tubulin (TU-20). Expression of cTnT was reduced in differentiated AB2.2 and H3 cells. Data from A5 cells are missing due to the fact that a division through 0 is not possible. So differentiated A5 cells showed a higher cTnT expression compared to undifferentiated cells. SMA expression was reduced during aggregate development in AB2.2 and CVPC aggregates. Also FOXA2 expression was reduced upon differentiation in AB2.2 and H3 cells, but was increased in differentiated A5 cells (Figure 4.9).
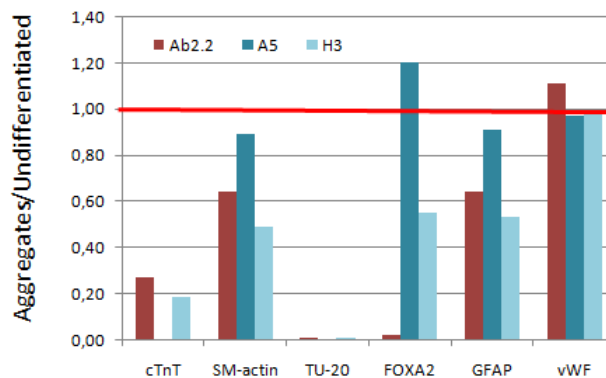
Figure 4.9: Comparison of cell populations of CVPC aggregates and undifferentiated cells. Data received from analyzing CVPC aggregates are divided by data of undifferentiated cells. Value 1 represents the baseline of undifferentiated cells (red). Data above this baseline mean a higher expression of markers in differentiated cells compared to undifferentiated cells and below the opposite.

CVPCs - Cardiomyocyte Development

Not only a divergence between AB2.2 ESC and CVPC aggregate morphology was observed, but also beating efficiency and onset of cardiomyocyte formation was different in AB2.2 ESC and CVPCs and even among CVPC clones. Although CVPC clones originate from the same clone, they vary among themselves. This was indicated by unequal mRNA expression profiles (Hoebaus, 2009) and different beating capacity of cardiomyocytes. Already in early days of aggregate development first differences in beating capacity were seen among these cell lines. First cardiomyocytes in AB2.2 aggregates started to beat around day 8 and rapidly reached almost hundred percent,

whereas beating cardiomyocytes in A5 aggregates were not seen until day 11. And CVPC clone H3 hardly ever showed beating cardiomyocytes (Figure 4.10).
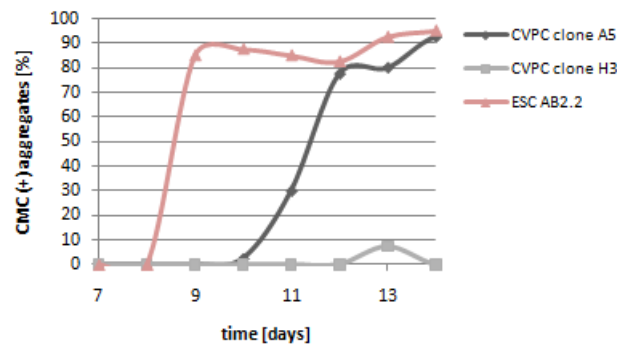
Figure 4.10: Cardiomyogenesis in CVPC clone aggregates. Aggregates of CVPC clones A5, H3 and ESC AB2.2 aggregates were made and the appearance of beating cardiomyocytes was checked every day. Data are means of 40 counted aggregates from 4 culture plates (10 counts per culture plate).

All in all, we could see that cardiomyogenesis was delayed in CVPC clones. But cardiomyocytes maintained their beating capacity over a longer time period in CVPC A5 aggregates, while they already started to disappear in AB2.2 aggregates (Gottschamel, 2010). The low occurrence rate of beating cardiomyocytes in H3 aggregates go along with data seen in FACS analysis where cTnT expressing cells were nearly absent (Figure 4.7).

4.1.4 Characterization of Somatic Stem Cells (SSCs)

SSCs - Size and Morphology Characterization

SSC clone Hi2P11K15/6 was isolated from the brain of two day old mice, while He2P11K13/5 from the heart. Aggregates of SSC clones (Hi2P11K15/6, He2P11K13/5) featured also different morphological structures compared to embryoid bodies. They were much larger as AB2.2 aggregates and even larger as CVPC aggregates. SSC clone He2P11K13/5 aggregates mostly seemed to have a cell cluster that radiated from the center of the aggregate to the periphery. While the inner cell mass of CVPC clones is round shaped, He2P11K13/5 aggregates often had a stellar shaped core. Often we observed in He2P11K13/5 aggregates a defined edge in contrast to Hi2P11K15/6 and CVPC aggregates where there was a continuous transition of cells moving from

the center to the periphery. But sometimes we could also see no such structural separation in He2P11K13/5 aggregates and then they possessed similar structural morphologies as seen in Hi2P11K15/6 aggregates. Hi2P11K15/6 aggregates had a diffuse structure comprising of a core of dense cells, which was infrequently seen in the center of the aggregate but rather was located out of the middle. In the less dense areas often gaps of cells were observed (Figure 4.11). SSC clone He2P11K13/5 aggregates often possessed more elongated cells in the intermediate region while SSC clone Hi2P11K15/6 and CVPC clones showed a higher number of round and angular shaped cells. As seen in CVPC clones both SSC clone aggregates featured mostly elongated cells in the outer region (Figure 4.11,B).
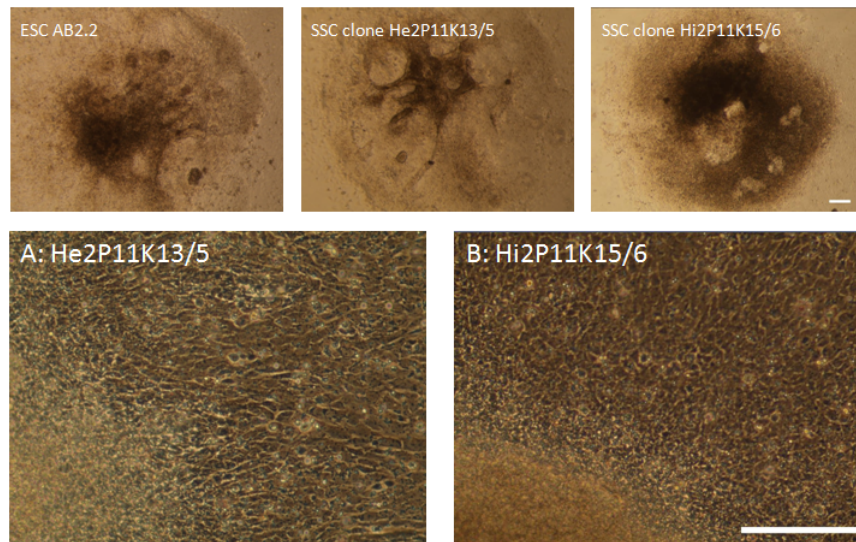
Figure 4.11: Morphological differences between ESC AB2.2 and SSC aggregates. Aggregate morphology of AB2.2 and SSC clones He2P11K13/5 and Hi2P11K15/6 aggregates on day 9 of cultivation. A and B: Intermediate region of SSC clone aggregates on day 12 of cultivation (bar=200μm).

SSCs - Differentiation Potential

SSC clone aggregates not only differed in size and morphology from CVPC clones, their differentiation potential seemed not as restricted to the cardiac lineage as seen in CVPC clones. While aggregates of CVPC clones spontaneously differentiated only to cells residing in the heart, SSC clone aggregates possessed also cells from other lineages. Rarely, we could see cells with structures reminding of neuronal cells (Figure 4.12).
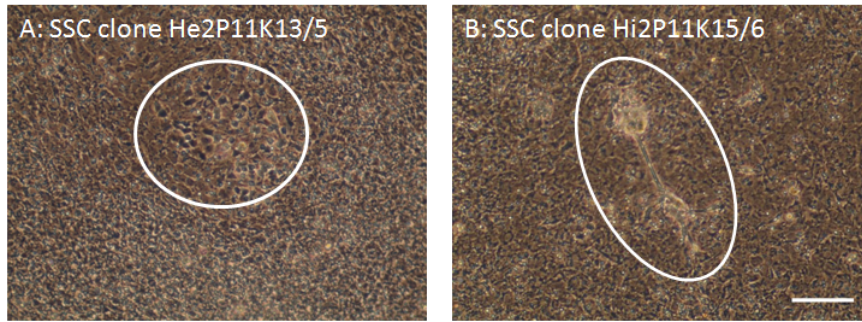
Figure 4.12: Neuronal differentiation in aggregates of SSC clones He2P11K13/5 (A) and Hi2P11K15/6 (B). Outer region of aggregates (d17) comprising neuron-like cells possessing a cell body with neurites. White circles indicate presence of neuron-like cells (bar=100μm).

Because of the isolation of Hi2P11K15/6 from the murine brain we expected a tendency to neuronal differentiation and therefore we were not surprised by the appearance of neuron-like cells. Whereas we did not expected the presence of neuron-like cells in SSC clone He2P11K13/5 cells. Because of the ability of spontaneous neuronal differentiation in He2P11K13/5 cells we concluded that these cells were not restricted to the cardiac lineage as seen in CVPC clones, although they were isolated from the murine heart too.

Here, we also performed differentiation studies to investigate lineage commitment of SSC clones. Same experiments and conditions were used as already described in differentiation studies with CVPC clones. We analyzed appearance of cells expressing beta3-tubulin, GFAP, FOXA2, vWF, SMA and cTnT with immunofluorescence microscopy and determined their incidence in the cell population of SSC aggregates with FACS analysis. Again, primary antibodies against beta3-tubulin, GFAP, FOXA2, vWF, SMA and cTnT and secondary antibodies anti-mouse Alexa Fluor 488 and anti-rabbit Alexa Fluor 647 were used. Aggregates of He2P11K13/5 and Hi2P11K15/6 (d13) were prepared for FACS analysis or immunofluorescence microscopy, respectively.

Aggregates of Hi2P11K15/6 and He2P11K13/5 revealed already the presence of neuron-like cells by investigations under the light microscope. Indeed, FACS analysis proved the appearance of beta3-tubulin expressing cells in Hi2P11K15/6 with 7.14% (Figure 4.13), but IF studies showed no positive fluorescence signal (not shown).
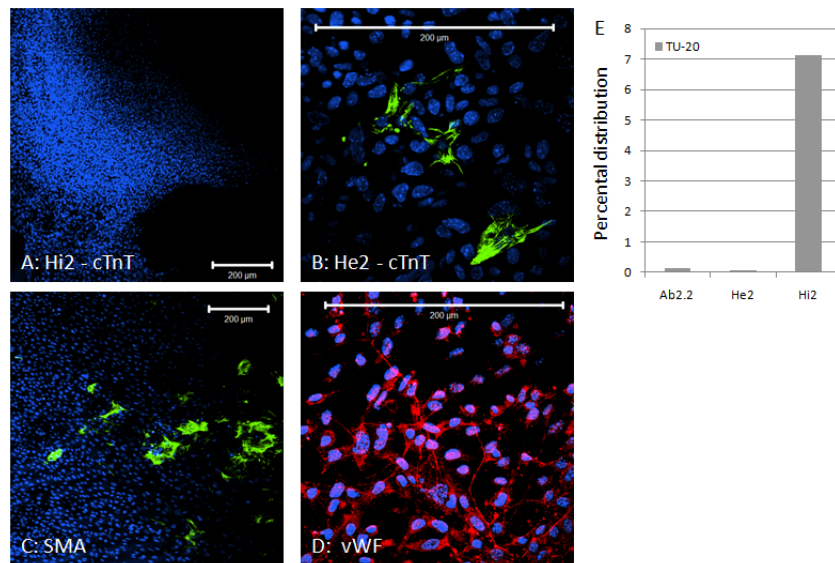
Figure 4.13: Occurrence or absence of diverse cell types in cell populations of SSC clones He2P11K13/5 and Hi2P11K15/6. A-D: Immunofluorescence microscopy of SSC aggregates on day 13 with primary anti-cTnT, SMA and vWF and secondary anti-mouse Alexa Fluor 488 (cTnT, SMA) and anti-rabbit Alexa Fluor 647 (vWF) antibodies, respectively (bar= 200μm). E: Quantitative FACS analysis of He2P11K13/5, Hi2P11K15/6 and AB2.2 aggregates on day 13 of cultivation. Chart represents the percental distribution of beta3-tubulin expressing cells in the cell population of aggregates as indicated.

Although we classified the neuron-like cells seen in He2P11K13/5 aggregates during investigation under the light microscope as neurons we were not able to prove the presence of such cells with anti-beta3-tubulin antibodies. In general, SSC aggregates (d13) complied with CVPC aggregates in their differentiation potential. Immunofluorescence microscopy showed no positive signals for the ectodermal markers beta3-tubulin and GFAP. Further only vWF expressing cells were recognized, while FOXA2 positive cells were absent. SMA positive cells were observed in the same arrangement and in a more or less similar extent as seen in immunofluorescence studies with CVPC aggregates. He2P11K13/5 aggregates possessed cTnT-expressing cells, while Hi2P11K15/6 aggregates were the only cell line that lacks this cell type. This indicates a decreased potential or even a prevention of cardiomyogenesis in Hi2P11K15/6 cells isolated from the murine brain.

In SSC aggregates (d13), the same discrepancy between data received from immunofluorescence microscopy and FACS analysis was observed as seen in experiments with

CVPC aggregates. Percentage of markers like vWF, GFAP and SMA obtained during FACS analysis were extremely high, ranging from 70% to nearly 100% (not shown), but this was contrary to results received from immunofluorescence microscopy. There we could indeed prove the presence of vWF and SMA-expressing cells, but they were not as prevalent as quantitative FACS analysis revealed. For GFAP actually, we even could not obtain one single positive signal for GFAP during immunofluorescence studies. Interestingly, we could observe a higher number of FOXA2 expressing cells (ranging from 10-15%) and of beta3-tubulin expressing cells in Hi2P11K15/6 aggregates during FACS analysis what indicated differences to CVPC aggregates. Again we decided to compare the expression relation of SSC aggregates with ESC aggregates. By comparing expression levels of SSC aggregates to ESC aggregates we could see few differences in SMA, GFAP and vWF. FOXA2 expressing cells were higher in both He2P11K13/5 and Hi2P11K15/6 than in ESC aggregates. In Hi2P11K15/6 cell population we recognized a higher number of cTnT and beta3-tubulin (TU-20) expressing cells compared to He2P11K13/5 aggregates (Figure 4.14).
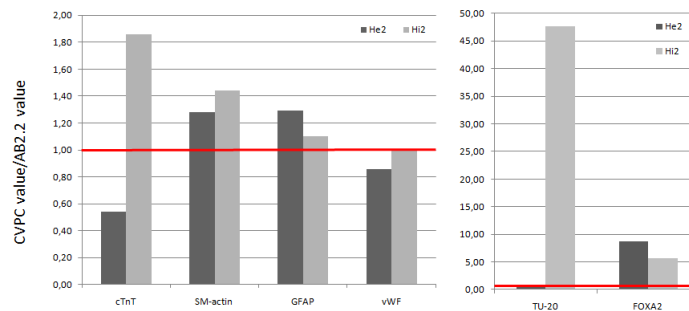
Figure 4.14: Expression relation of differentiated SSC clones to differentiated ESC. Data of SSC aggregates on day 13 obtained from FACS analysis were divided through ESC data (A, B). The value 1 represents the baseline of AB2.2 data (red). Data above this baseline mean a higher occurrence rate of this cell type compared to AB2.2 and below the opposite.

Next, we compared cell populations of differentiated SSC aggregates on day 13 to undifferentiated SSCs (Figure 4.15). Upon differentiation a decline in the incidence of cardiac (cTnT, SMA) and ectodermal markers (TU-20, GFAP) was observed, while the frequency of vWF-expressing cells was to a greater or lesser extent maintained. But the incidence of FOXA2-expressing cells in He2P11K13/5 cells rapidly increased during differentiation.
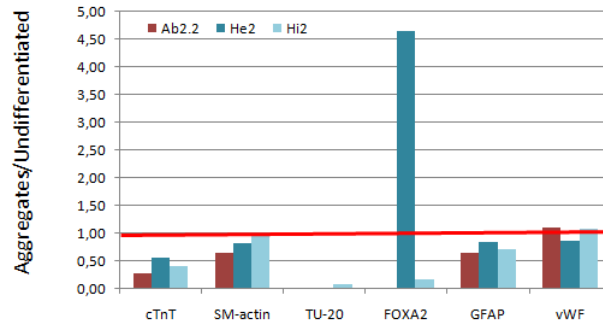
Figure 4.15: Comparison of cell populations of SSC aggregates (d13) and undifferentiated SSCs. Data received from analyzing SSC aggregates on day 13 are divided by data of undifferentiated cells. Again value 1 represents the baseline of undifferentiated cells (red). Data above this baseline mean a higher expression of markers in differentiated cells compared to undifferentiated cells and below the opposite.

Though immunofluorescence showed no presence of neuronal cells in Hi2P11K15/6, we proved their appearance by investigation under the light microscope and FACS analysis. So we assumed that Hi2P11K15/6 have a restriction to the neuronal lineage. Whereas Hi2P11K15/6 cells showed a commitment to their tissue lineage they were isolated from, He2P11K13/5 cells seemed to possess a less limited potential. Because of their isolation from the murine heart we assumed He2P11K13/5 cells to be restricted to the cardiac lineage, but morphology investigations under the light microscope revealed an appearance of neuron-like cells which could however not been confirmed by immunofluorescence and FACS analysis.

SSCs - Cardiomyocyte Development

Because SSC clone He2P11K13/5 cells were isolated from the murine heart we expected a high occurrence rate of beating cardiomyocytes, instead we had to recognize an absence of beating aggregates (Figure 4.16). We expected that Hi2P11K15/6 were not able to undergo cardiomyogenesis due to the fact that they were isolated from the murine brain. These results were confirmed by an absence of beating cardiomyocytes (Figure 4.16) and a lack of cTnT-expressing cells observed during immunofluorescence studies (Figure 4.13).
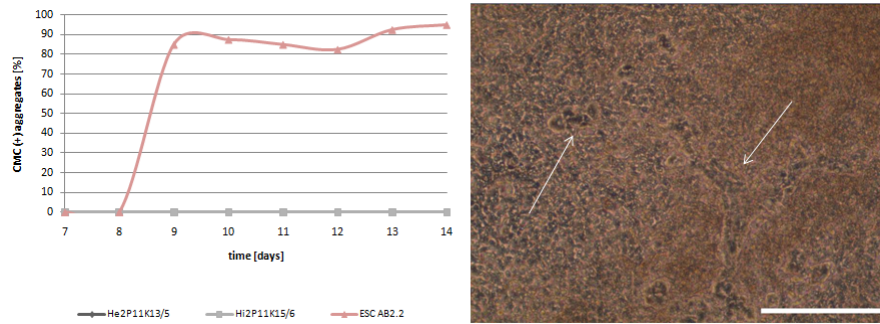
Figure 4.16: Cardiomyogenesis in SSC clone aggregates. Aggregates of SSC clones He2P11K13/5 and Hi2P11K15/6 as well as ESC AB2.2 aggregates were made and the occurrence rate of beating cardiomyocytes was determined during aggregate development (A) Data are means of 40 counted aggregates from 4 culture plates (10 counts per culture plate). B: Presence of non-contracting cardiomyocytes in He2P11K13/5 aggregates on day 26 of culitvation (see white arrows) (bar=50μm).

4.1.5 Induction of Neuronal Differentiation by Retinoic Acid

Retinoic acid is known to induce neuronal differentiation in mouse embryonic stem cells, because ESC aggregates exposed to retinoic acid differentiated to neuron-like cells (Bain et al., 1995). While gene expression of neuronal markers was enhanced during retinoic acid induction, they could see a repression of mesodermal gene expression (Bain et al., 1996). But induction of neuronal differentiation is not simply driven by exposure to retinoic acid alone, in fact it is dependent on its concentration. Retinoic acid influences the commitment of embryonic stem cells in a dose-dependent manner. Teratocarcinoma cells exposed to low concentrations of retinoic acid (10^{-9} M) are driven to the cardiac differentiation, while high concentrations ranging from 10^{-7} to 10^{-5} M resulted in the formation of neurons and glia cells (Edwards and McBurney, 1983).

Though we already had proven that CVPCs are restricted to the cardiac lineage and could only differentiate spontaneously into cells residing in the heart we wanted to investigate whether cells are capable to give rise to cell types of other lineages. Here, we tested the influence of high concentrations of retinoic acid on the differentiation potential of CVPCs and SSCs.

AB2.2 ESC, CVPC and SSC aggregates were made and five days after cultivation as

hanging drops they were rinsed onto gelatin-coated culture plates. Addition of retinoic acid (5×10^{-7} M) to the aggregates started on day 5 of cultivation. Aggregates were fed every third day and so retinoic acid was replaced by fresh one to ensure a constant concentration present during the whole cultivation.

Effect of Retinoic Acid on Aggregate Morphology

Retinoic acid induction caused alterations in aggregate morphology indicating an inhibiting influence on aggregate formation. First distinguishable morphological differences between aggregates untreated and treated with retinoic acid were observed already three days after rinsing the hanging drops onto gelatin-coated culture plates (Figure 4.17). On day 8, treated aggregates were much smaller in size compared to untreated ones. Cells in the middle of the aggregates maintained their round and dense arrangement and did not expand into periphery. So the aggregates seemed to be more compact and cell spreading into periphery was reduced compared to untreated aggregates. The decreased cell spreading might be due to a reduced cell differentiation.
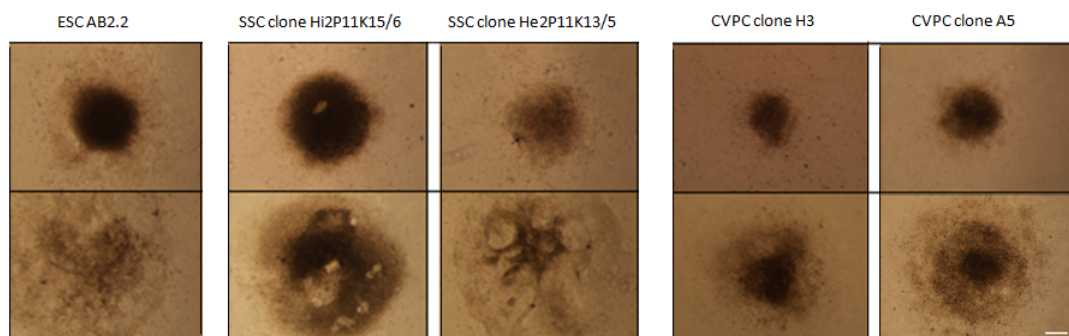
Figure 4.17: Pictures of treated (first row) and untreated (second row) aggregates on day 8 of cultivation. (bar=300μm, light microscope).

Effect of Retinoic Acid on Cardiomyogenesis

Due to the fact that retinoic acid induction impaired cell differentiation it is hardly surprising that it also had an effect on cardiomyogenesis. Both SSC and CVPC aggregates treated with retinoic acid developed cardiomyocytes to a lesser extend and beating capacity was strongly reduced. Addition of retinoic acid from day 5 to day

20 resulted in a reduction of cardiomyocyte formation and a decreased frequency of beating aggregates in all cell lines, ESC (AB2.2), CVPC (clone A5) and SSC (clone He2P11K13/5) (Figure 4.18; Figure 4.19).
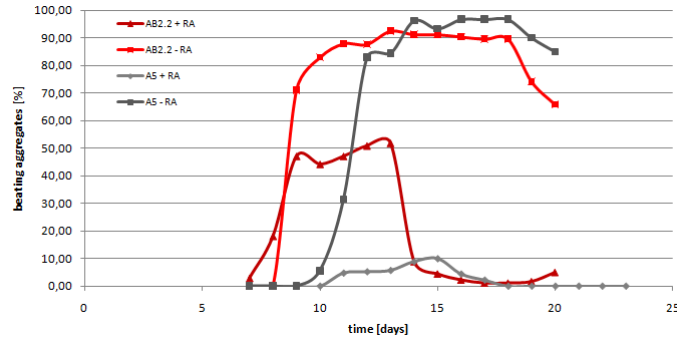
Figure 4.18: Influence of retinoic acid on beating CVPC aggregates on day 13. CVPC clone A5 and ESC AB2.2 cells were cultured as hanging drops for five days and were rinsed onto gelled culture plates. From day 5 on aggregates were exposed to retinoic acid (5×10^{-7} M) to induce neuronal differentiation. Beating efficiency of aggregates was determined form day 5 to 20. Data are means of 4 independent experiments with 100 counted aggregates, each untreated and treated in summary.
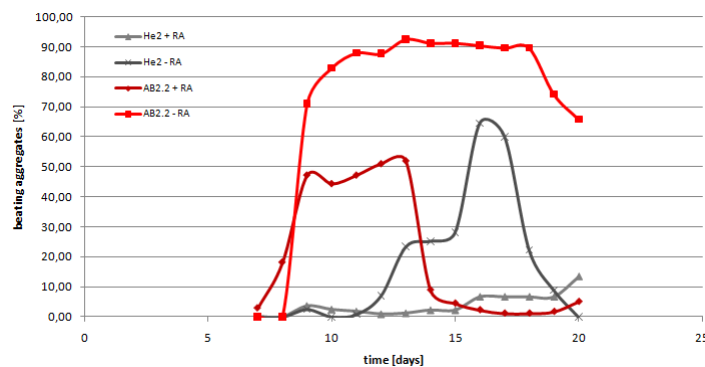
Figure 4.19: Influence of retinoic acid on beating SSC aggregates.Data are means of 4 independent experiments with 120 counted aggregates, each untreated and treated in summary.

Untreated aggregates possessed beating cells located mainly in the periphery which were getting bigger during cultivation, compared to cardiomyocytes exposed to retinoic acid. These cardiomyocytes hardly ever beat and the few beating ones were located in the compact center and marginally increased in size. Interestingly, these cardiomyocytes featured a higher beating frequency compared to untreated ones. During our investigation on beating efficiency in retinoic acid-treated aggregates we could recognize a correlation between aggregate size and the incidence of beat-

ing cardiomyocytes. Indeed, treated aggregates were always smaller compared to control, but aggregate size varied among treated aggregates. Aggregates that were somewhat bigger as usual possessed more beating cardiomyocytes. The same effect was observed for smooth muscle cells (not shown). They hardly contracted, were more infrequently seen and formation was dependent on the size of treated aggregates.

Immunofluorescence studies revealed an absence of cTnT-expressing cells in retinoic acid-treated aggregates (AB2.2, SSC, CVPC) on day 13 of cultivation (Figure 4.20, A). These data confirmed the extremely low frequency of beating cardiomyocytes observed during investigations on the beating capacity under the light microscope. In summary, the presence of retinoic acid seemed to disrupt aggregate-expansion and prevents cardiomyogenesis.
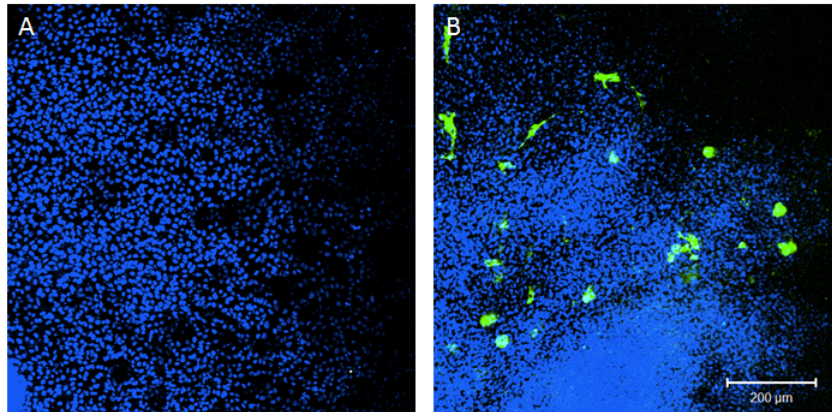
Figure 4.20: Immunofluorescence staining of SSC aggregates on day 13. Aggregates were stained with cTnT antibody and secondary anti-mouse Alexa Fluor 488 antibody. A: Immunofluorescence staining of He2P11K13/5 aggregates treated with retinoic acid on day 13 of cultivation. B: Immunofluorescence staining of untreated He2P11K13/5 aggregates possessing cardiomyocytes (bar=00μm).

Effect of retinoic acid on Nkx2.5 gene expression

Further we tested the negative influence of retinoic acid on cardiomyogenesis by FACS analysis. The stable A5-CSX cell line carries an EGFP reporter gene located in the *Nkx2.5* gene and is therefore a suitable tool for the investigation of the effect of retinoic acid on cardiomyogenesis by FACS analysis. Undifferentiated A5-CSX (clone 2) cells were transferred onto gelatin-coated plates and retinoic acid was added for 3

hours, 24 hours and 3 days. For control A5 cells not carrying the EGFP promoter and A5-CSX cells not treated with retinoic acid were used (Figure 4.21).
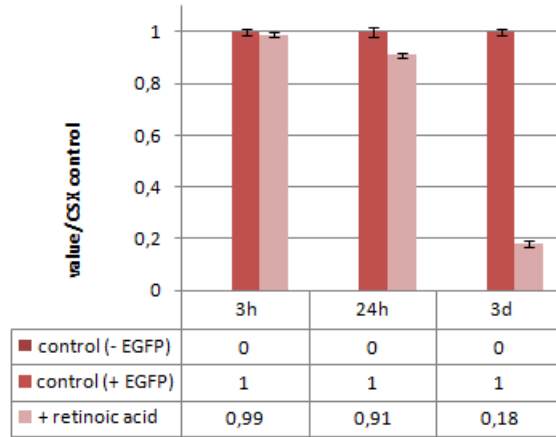
Figure 4.21: FACS analysis of undifferentiated CVPC clone A5-CSX treated with retinoic acid for 3h, 24h and 3d. A5 cells carrying an EGFP reporter gene were treated with retinoic acid (5×10^{-7} M) for indicated time intervals. EGFP signal correlates with the activation/repression of Nkx2.5 gene. FACS values were divided by mean value of control (+EGFP) to compare the effect of retinoic acid among each time interval. This division is necessary due to slight fluctuations in *Nkx2.5* gene expression during the indicated time intervals. Data are means of one experiment with duplicates. For standard deviation see Appendix.

Retinoic acid induction reduced the *Nkx2.5* expression. A continuous decline in the EGFP expression was observed with greatest effect seen by adding retinoic acid for three days.

We repeated the experiment with differentiated A5-CSX cells. For this A5-CSX cells were aggregated in hanging drops using the embryoid body model. Aggregates were rinsed onto gelatin-coated culture plates on day 5. On day 13 of cultivation retinoic acid (5×10^{-7}) was added for 3h and 24h (Figure 4.22). Aggregates were trypsinized and prepared for FACS analysis.

Again a reduction in the *Nkx2.5* gene expression was observed. While addition of retinoic acid for 3h days resulted in a minimal significant reduction, the addition of retinoic acid for 24 hours had a great effect.
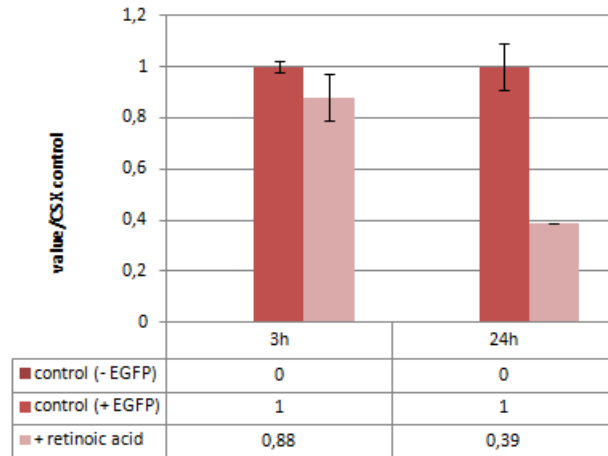
Figure 4.22: FACS analysis of differentiated CVPC clone A5-CSX (day 13) treated with retinoic acid for 3h and 24h. A5 cells carrying an EGFP reporter gene were aggregated in hanging drops and rinsed onto gelatin-coated plates. On day 13 of cultivation the aggregates were treated with retinoic acid ($5x10^{-7}$ M) for indicated time intervals. FACS values were divided by mean value of control (+EGFP) to compare the effect of retinoic acid among each time interval. This division is necessary due to slight fluctuations in *Nkx2.5* gene expression during aggregate development. Data are means of one experiment with duplicates. For standard deviation see Appendix.

Morphology of Neuron-like Cells

An ordinary neuronal cell possesses a central spherical region often called soma or cell body, where general cellular processes take place and it also consists of neurites that enables this cell type to conduct information over long distances. Neurites (axons, dendrites) are thin tubes that arise from the cell body and are the most obvious difference to regular cells which makes neurons easily distinguishable to other cell types.

Neuron-like cells observed in aggregates treated with retinoic acid resemble neurons of the brain (Figure 4.23). The neuron-like cells observed during investigations under the light microscope feature quite similar morphological characteristics, like a spherical body and thin tubes arising from this central region. These thin tubes (presumably neurites) often branch and some connect to other tubes to from very simple "networks". Because the neuron-like cells share this typical neuronal characteristics we concluded that upon retinoic acid induction the cells were driven to neuronal differentiation thereby forming neuron-like cells.
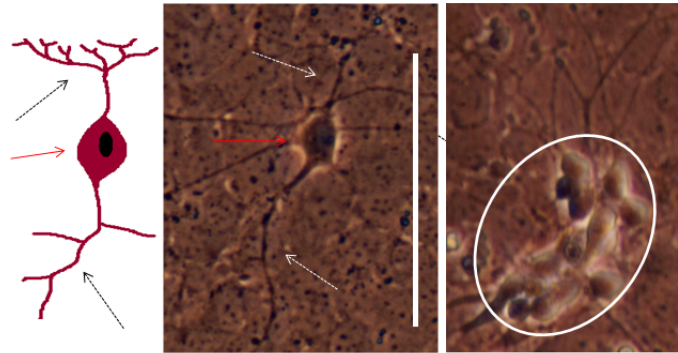
Figure 4.23: Morphological similarities between neuronal cells in the brain and neuron-like cells observed during retinoic acid induction. As typical neurons the neuron-like cells observed in treated aggregates possessed a cell body (indicated by red arrow) and neurites (indicated by dashed arrows, black and white). White circle marks clusters of neuron-like cells that presumably connect to each other (bar = 50μ).

Because neuron-like cells were never observed in the dense center of the aggregates, just only in the periphery we concluded that neuronal differentiation proceeds exclusively at the periphery of retinoic acid-treated aggregates. Usually, several thick tubes radiated away from the aggregate center into the periphery over quite long distances (Figure 4.24). The more common neuron-like cells located directly at the periphery were in general not as thick as those arising from the aggregate center.
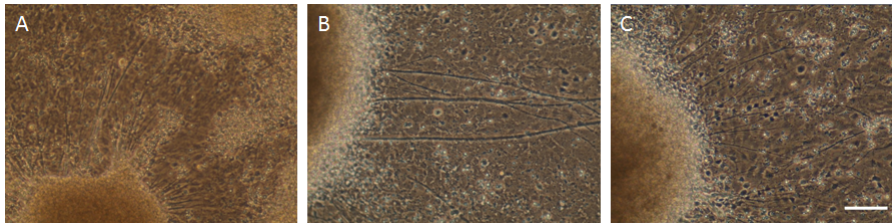
Figure 4.24: Pictures represent cuts of aggregates treated with retinoic acid on day 11. All aggregates treated with retinoic acid possessed thick tubes arising from the center into the periphery (A: AB2.2, B: CVPC, C: SSC)(bar=100μm).

Immunofluorescence studies of CVPC, SSC and ESC aggregates on day 13 exposed to retinoic acid was performed to prove the presence of neuron-like cells with anti-beta3-tubulin antibodies. Unfortunately, any positive signal for this neuronal marker was absent (Figure 4.25, A). We could exclude a dysfunction of this antibody itself as well as an incorrect staining procedure due to the ability of the anti-beta3-tubulin antibody to recognize neuron-like cells in untreated AB2.2 aggregates on day 20.

Therefore we can not confirm that the cells indicated as neuron-like cells were actually neuronal cells, although investigations under the light microscope revealed neuron-like phenotypical structures.
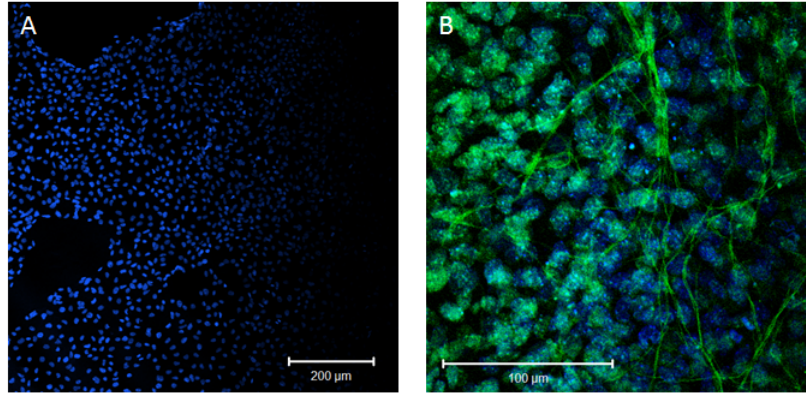
Figure 4.25: Immunofluorescence staining of SSC aggregate (He2P11K13/5) on day 13 treated with retinoic acid. Aggregates were stained with anti-beta3-tubulin antibodies and with secondary antibodies Alexa Fluor 488 (A) or anti-mouse FITC (B), respectively. Here, diverse secondary antibodies were used, but same results were achieved by using identical secondary antibodies. A: He2P11K13/5 aggregate on day 13 treated with retinoic acid. B: ESC aggregate on day 20 not exposed to retinoic acid. (LSM-Meta, confocal microscope).

Occurrence of Neuron-like Cells

The appearance of neuron-like cells was checked every day from day 6 till day 20 during the cultivation of aggregates. Aggregated ESCs treated with retinoic acid showed first appearance of neuron-like cells on day 9. The percentage of aggregates possessing neuronal cells increased continuously and reached hundred percent within the next five days. On day 14 of cultivation all ESC aggregates possessed neuron-like cells, which were still seen on day 20. Though the initiation of neuronal differentiation seemed to be stronger induced by retinoic acid in CVPC aggregates compared to ESC aggregates, the incidence of aggregates possessing neuron-like cells fell continuously in later developmental stages whereas ESC aggregates maintained their occurrence rate. So the effect of retinoic acid did not hold on as long as seen in ESC aggregates. Compared to ESC aggregates neuron-like cells seen in CVPC aggregates appeared one to two days earlier, hardly never reached hundred percent and started to disappear prior as to neuron-like cells seen in ESC aggregates (Figure 4.26, A).

Minor morphological differences between neuron-like cells seen in treated CVPC aggregates and ESC aggregates were detected (Figure 4.26, B-D). While neuron-like cells originated from CVPC clone A5 and H3 possessed quite similar structures, we could distinguish them from neuron-like cells observed in ESC treated aggregates. ESC derived neuron-like cells were often not as elongated as cells seen in treated CVPC aggregates. Generally, they possessed shorter tubes radiating from the cell body and tended to occur mainly in clusters compared to neuron-like cells in CVPC aggregates that were often seen individually.
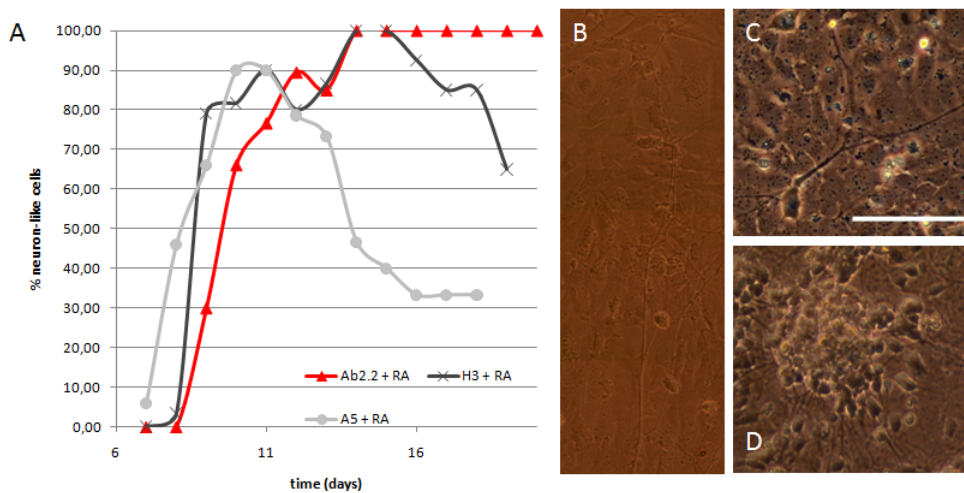
Figure 4.26: Percentage of neuron-like cells observed in CVPC aggregates treated with retinoic acid. Retinoic acid was added from day 5 ($5\text{x}10^{-7}$ M). A: Percentage of aggregates possessing neuron-like cells was determined from day 6 to 20. First appearance of neuron-like cells were observed on day 7 of CVPC clone A5, day 9 of CVPC clones H3 as well as in AB2.2 ESC aggregates. Data are means of 3 independent experiments with 80 counted aggregates (AB2.2, H3) and 2 experiments with 50 counts in A5. B-D: Morphological differences of neuron-like cells in A5 (B), H3 (C) and AB2.2 (D) aggregates.

Determining the occurrence rate of retinoic acid-treated SSC aggregates possessing neuron-like cells revealed similar results as obtained from studies with CVPC aggregates. Also here, SSC aggregates showed a strong induction in the first days of cultivation, while it fell in later developmental stages (Figure 4.27, A). Both treated SSC clone aggregates featured neuron-like cells similar to that observed in treated CVPC aggregates as well as those seen in ESC aggregates (Figure 4.27, B and C). Though CVPCs and SSCs are able to be induced to differentiate to neuron-like cells
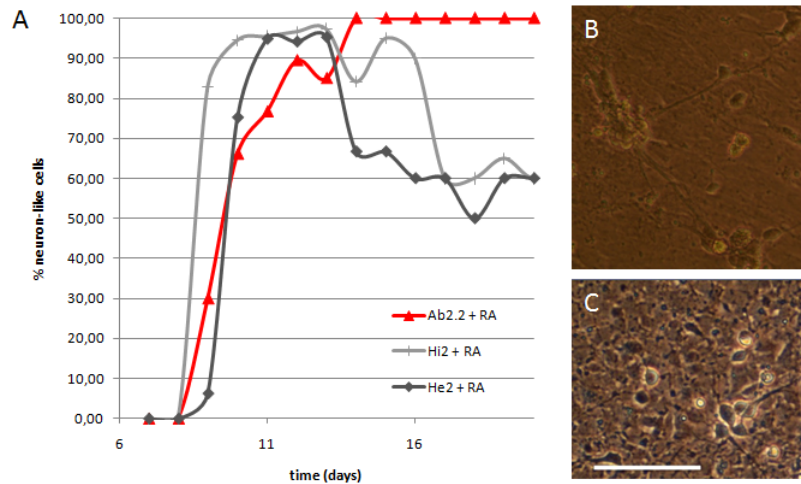
Figure 4.27: Influence of retinoic acid on neuron-like cell formation in SSC aggregates exposed to retinoic acid. SSC clones He2P11K13/5 and Hi2P11K15/6 aggregates formed neuron-like cells after several days of exposure to retinoic acid. A: Percentage of aggregates possessing neuron-like cells was determined from day 6 to 20. Percentage of neuron-like cells was highest during days 10 to 13 and decreased in later developmental stages to around 60%. Data are means of 3 independent experiments with 110 counted aggregates (He2, Hi2). B-C: Morphological differences of neuron-like cells in He2P11K13/5 (B) and Hi2P11K15/6 (C) aggregates.

by retinoic acid, without induction we could never observe spontaneous neuronal differentiation, at least in CVPC aggregates. Untreated Hi2P11K15/6 aggregates were supposed to differentiate to neuron-like cells, because of their isolation from the murine brain. Because we could prove the presence of neuron-like cells in untreated Hi2P11K15/6 aggregates we were able to confirm the assumption of these cells to have a neuronal differentiation potential. Surprisingly, untreated He2P11K13/5 cells were also able to differentiate to neuron-like cells without induction (Figure 4.28, A). So without induction by retinoic acid CVPC aggregates were never driven into neuronal differentiation, while AB2.2 ESC, He2P11K13/5 and Hi2P11K15/6 aggregates showed even without induction neuron-like cell formation. The difference in neuron-like cells occurrence rate of untreated and treated aggregates falls into place especially by looking at figure 4.28,B.

Comparing phenotypical differences of neuron-like cells of treated and untreated SSC aggregates revealed only minor differences (Figure 4.29). Great differences were only seen by comparing neuron-like cells of untreated and treated AB2.2 aggregates. Here, untreated neuron-like cells possessed thin tubes that arose from the center of the
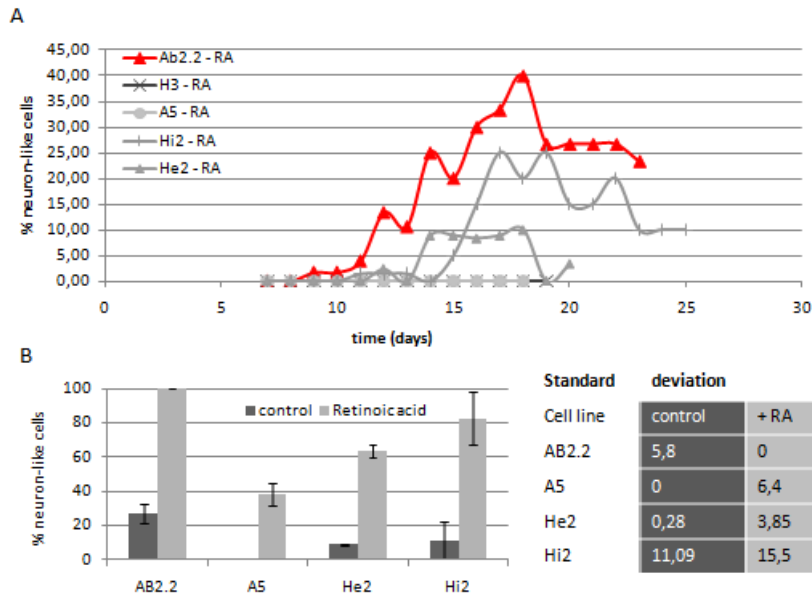
Figure 4.28: Percentage of neuron-like cells observed in untreated aggregates. A:
Percentage of aggregates possessing neuron-like cells was determined from day 6 to
25. First appearance of neuron-like cells were observed on day 9 (AB2.2), day 12
(He2P11K13/4) and day 15 (Hi2P11K15/6). CVPC clones never showed spontaneous
formation of neuron-like cells. B: Chart represents mean value of neuron-like cell frequency
between day 14 to 17 in untreated and retinoic acid-treated AB2.2, A5, He2P11K13/5
and Hi2P11K15/6 aggregates. Data are means of 3 experiments with 110 counts (He2,
Hi2), 3 experiments with 80 counts (AB2.2,H3) and 2 experiments with 50 counts for
A5.

aggregate and reached far into the periphery. Such morphological characteristics
could also be observed in treated AB2.2 aggregates, but here, the tubes seemed to be
much thicker. Whereas neuron-like cells could be also observed in the periphery of
treated aggregates, in untreated aggregates such cells were absent and neuron-like
cells exclusively originated from the center. As far as we can say, the only differences
in untreated and treated neuron-like cells in He2P11K13/5 was that in treated
aggregates neuron-like cells were widely distributed throughout the aggregate, while
in untreated aggregates the occurrence of neuron-like cells was mainly restricted to
one part of the aggregate. Neuron-like cells of untreated Hi2P11K15/6 aggregates
were often seen distributed over the whole aggregate and the tubes were often shorter
as compared to neuron-like cells in treated aggregates.
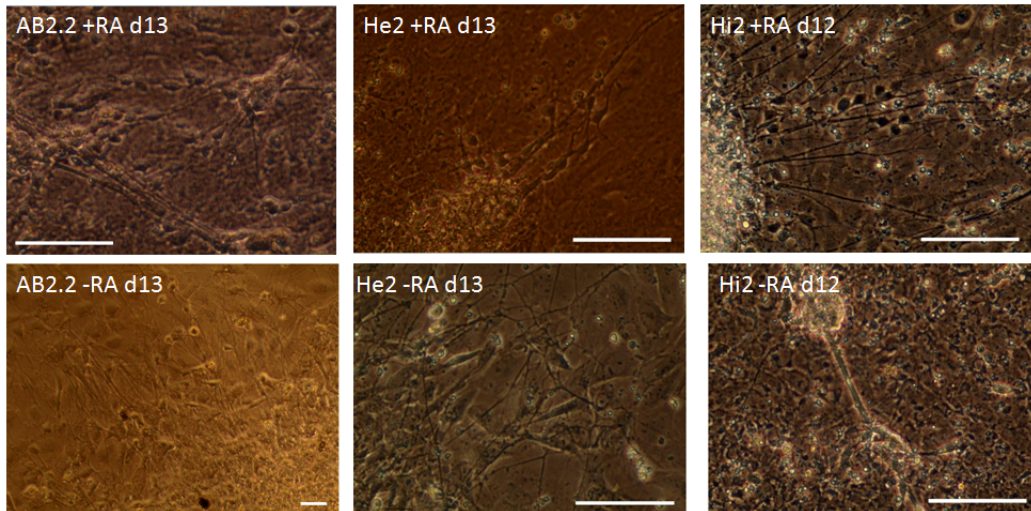
Figure 4.29: Morphological differences of neuron-like cells in untreated and treated AB2.2 and SSC aggregates on day 13 and 12 of cultivation. First row represent examples of neuron-like cells observed in aggregates exposed to retinoic acid. Second row shows neuron-like cells of untreated neuron-like cells.

Effect of retinoic acid on neuronal marker expression

Further we analyzed the expression level of neuronal markers in aggregated cells. Therefore RNA of undifferentiated, untreated and treated aggregates on day 15 were isolated and transcribed into cDNA. RT-PCR analysis was done with primer pairs for tyrosine hydroxylase (TH) and glial fibrillary protein (GFAP) to prove the presence of neuronal cells (Figure 4.30).

RT-PCR revealed that ESC AB2.2 possessed no TH-expressing cells whether in an undifferentiated state or upon differentiation. Even in the presence of retinoic acid no bands for TH were visible. But RA-treated AB2.2 aggregates revealed the presence of GFAP expressing cells. CVPC clone A5 aggregates showed under RA exposure tyrosine hydroxylase expression, but no GFAP expression, while in CVPC clone H3 aggregates the opposite effect was seen. Undifferentiated CVPC clone A5 possessed no bands for both neuronal markers, in contrast to undifferentiated CVPC clone H3 that showed a pale band for GFAP. In both CVPC aggregates not treated with RA no bands were visible. This concludes that upon differentiation CVPC possessed no TH- or GFAP- expressing cells, while treated with RA a different subset of genes was activated. Similar results were seen in SSC clone He2P11K13/5 cells. Undifferentiated He2P11K13/5 cells showed no expression of TH, but a low amount of GFAP. Upon
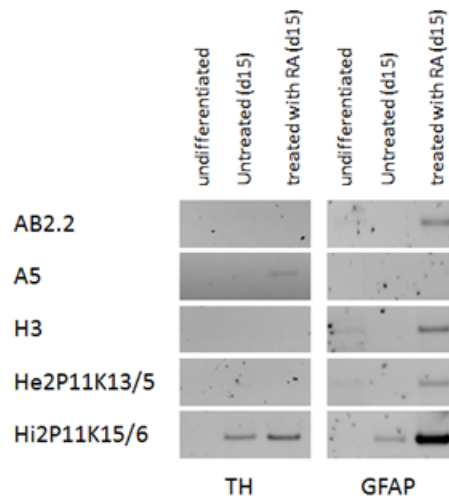
Figure 4.30: Expression profiles of ESC AB2.2, CVPCs and SSCs. Undifferentiated cells, untreated aggregates and RA-treated aggregates (d15) were analyzed by RT-PCR for the expression of TH and GFAP as indicated.

differentiation expression of neuronal markers was absolutely absent. Aggregates treated with retinoic acid behaved like H3 aggregates and expressed GFAP. The SSC clone Hi2P11K15/6 was the only cell clone that behaved quite different. This clone, isolated from the murine brain, showed upon differentiation in aggregates expression of both neuronal markers. The expression of these two markers was increased by exposure to retinoic acid. Interestingly, CVPC clones and SSC clone He2P11K13/5 showed either TH or GFAP expression, but both markers were never expressed at the same time, whereas we observed expression of both markers in Hi2P11K15/6. CVPC clone H3 and SSC clone He2P11K13/5 cells showed the same expression profile as seen in ESC AB2.2.

4.2 INFLUENCE OF MAPK CASCADE PATHWAY ON CARDIOMYOGENESIS

The MAPK cascade is an important pathway for cell proliferation and differentiation (Seger and Krebs, 1995). Especially during differentiation its activity is critical for cell fate decisions of embryonic stem cells (Aouadi et al., 2006). Aouadi and colleagues demonstrated in their differentiation studies that MAPK activity is necessary to induce cardiomyogenesis.

To study the involvement of mitogen-activated protein kinases (MAPKs) in car-

diomyogenesis of CVPCs, aggregated CVPC clone A5 cells were treated with MEK1 inhibitor PD98059. To investigate the influence of PD98059 on the formation of cardiomyocytes the percentage of beating aggregates was determined daily over a period of twenty days. CVPC clone A5 cells were cultured as hanging drops for five days followed by rinsing them onto gelled culture plates. The inhibitor (10μM) was added for different time intervals, from days 0-5, 5-7, 7-10 and 10-13. The experiment indicated an influence of PD98059 at very early developmental stages (0-5), whereas later no effect was visible. A decrease in the number of beating cardiomyocytes and a delayed onset for two days was observed from days 0-5 (Gottschamel, 2010). Though the MEK1 inhibitor was shown to negatively influence cardiomyogenesis, it had no effect on morphology of aggregates when added on days 0-5 (Figure 4.31).
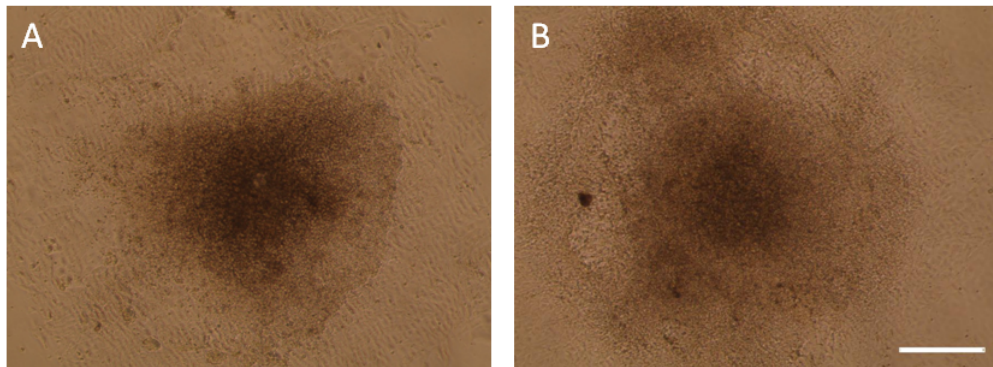
Figure 4.31: Morphology of untreated (A) and treated (B) aggregates. PD98059 (5μM) was added to CVPC clone A5 aggregates on days 0-5.Images were made on day 7 of cultivation (bar=500μm).

These results were verified by repeating the previous experiment using half of the PD98059 concentration (5μM). Although we even reduced the concentration the same effect was visible. Only by adding the MEK1 inhibitor on days 0-5 we obtained a reduction in beating capacity (Figure 4.32).

Here we could prove the influence of PD98059 (5μM) on cardiomyogenesis only in early stages of development. Even by increasing the concentration of the inhibitor to 20μM did not change the fact that PD98059 is only effective in early developmental stages (Figure 4.33).
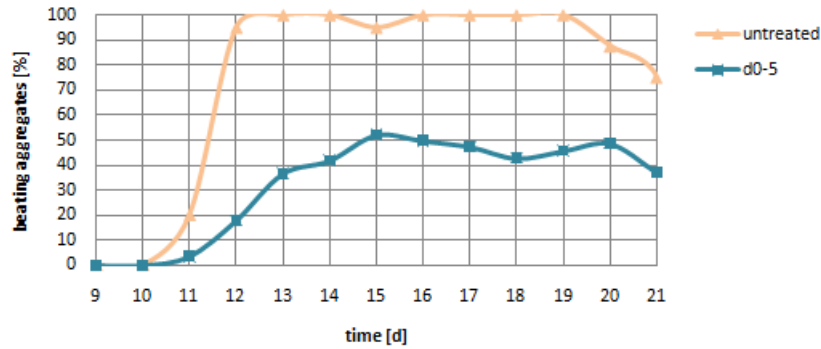
Figure 4.32: Influence of 5μM PD98059 on beating aggregates. PD98059 was added on days 0-5. CVPC clone A5 aggregates were made and percentage of beating aggregates was determined over a period of 21 days. Data are means of 4 culture plates (10 counts per plate) each treated and untreated.
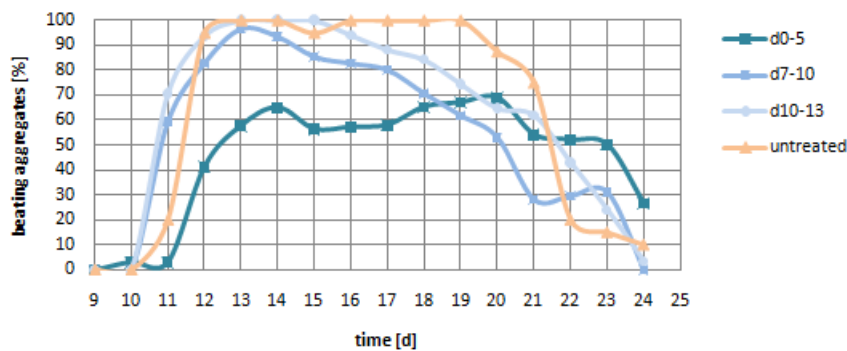
Figure 4.33: Influence of 20μM PD98059 on beating aggregates. CPVC clone A5 aggregates were cultured as hanging drops for five days. They were rinsed onto gelatin-coated culture plates. The MEK1 inhibitor was added from days 0-5, 7-10, 10-13. Percentage of beating aggregates was determined every day for a period of 24 days. Data from days 5-7 are not included in the figure, because aggregates were smaller than normal and therefore beating capacity was already reduced independently of the presence of inhibitor. Data are means of 4 culture plates (10 counts per plate) each treated and untreated.

Next we investigated the influence of PD98059 on cardiomyogenesis by adding the inhibitor for longer time periods. Aggregated CVPC clone A5 cells were treated with the MEK1 inhibitor (5μM) on days 5-13 and 0-13. Though the inhibitor was given for the long period of nine days (days 5-13) no reduction in the occurrence of beating aggregates was seen. While adding PD98059 from days 0-13 again a strong inhibitory effect was visible (Figure 4.34).

As assumed cardiomyogenesis was not influenced by adding the MEK1 inhibitor
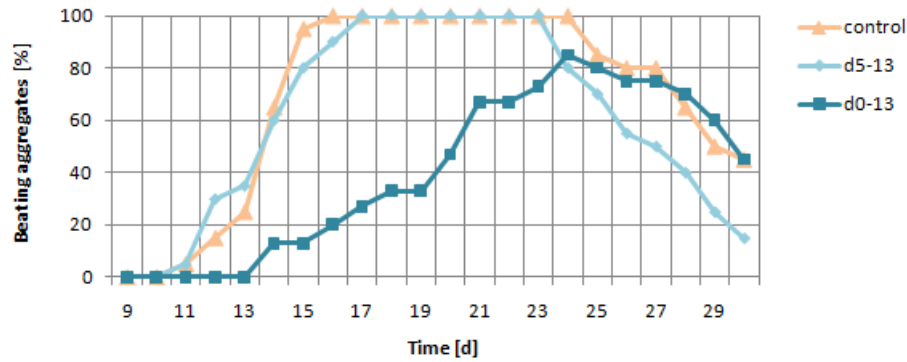
Figure 4.34: Effect of 5μM PD98059 when added for longer time periods. CVPC clone A5 aggregates were treated with PD98059 for days 5-13 and 0-13.

on days 5-13. Now we can really exclude a negative effect of PD98059 in later developmental stages. Even when the inhibitor is present over a longer period no effect on cardiomyogenesis was determined. During the investigations we recognized not only an influence on beating cardiomyocytes, also contracting smooth muscle cells seemed to be influenced by PD98059 (Figure 4.35). By adding the inhibitor in early stages of development a significant reduction in contracting smooth muscle cells was determined, while the presence of the inhibitor on days 5-13 showed a slight enhancement of contractions. This indicated a time dependent action of the MEK1 inhibitor on smooth muscle cell formations.
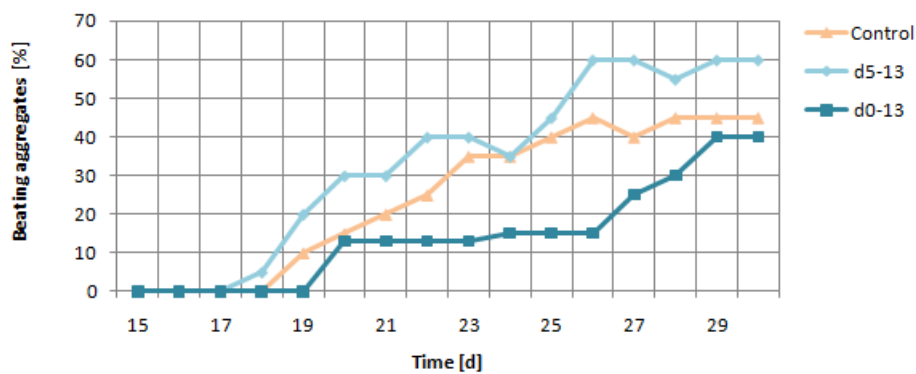
Figure 4.35: Effect of PD98059 on contracting smooth muscle cells. The inhibitor was added from days 5-13 and 0-13.

4.2.1 Effect of MEK 1 Inhibition on Nkx2.5 gene Expression

Because we could observe an influence of PD98059 on cardiomyogenesis, we investigated also the effect of the inhibitor on *Nkx2.5* gene expression. The *Nkx2.5* gene is a cardiac marker involved in cardiomyogenesis. To determine gene expression we made use of the A5-CSX reporter cell line by detecting the EGFP signal which correlates with the *Nkx2.5* expression by FACS analysis. Due to the fact that the MEK1 inhibitor is only effective by adding it in early stages of aggregate development we added PD98059 on days 0-7. Before the formation of hanging drops the inhibitor was added in a concentration of 5μM. After five days of cultivation of CVPC clone A5-CSX aggregates as hanging drops we rinsed them onto gelatin-coated 10cm culture plates. FACS analysis was performed on days 7, 13 and 20 and percentage of EGFP positive cells was determined (Figure 4.36). On day 7 the *Nkx2.5* expression was significantly reduced compared to control, while FACS analysis on days 13 and 20 showed no change in expression profile. The presence of the inhibitor at early developmental stages not only decreased the occurrence of beating cardiomyocytes, also a strong decrease in *Nkx2.5* gene expression was obtained.
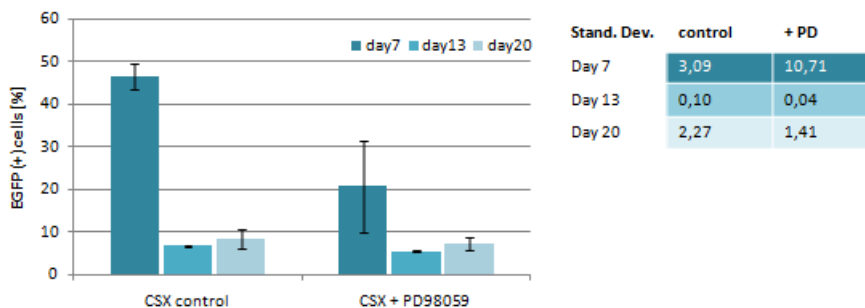
Figure 4.36: Effect of PD98059 on *Nkx2.5* gene expression. FACS analysis of undifferentiated and differentiated CSX A5 cells on day 7, 13 and 20. Data are means of duplicates. (Stand.Dev. .. standard deviation)

4.3 INFLUENCE OF SPARC, ANIT-SPARC, BMP2/4 AND ANTI-BMP2/4 ON NKX2.5 EXPRESSION

Here, we concentrated on the investigation of the *Nkx2.5* gene expression in CVPCs. The *Nkx2.5* gene becomes important during heart development and its activation

depicts commitment of cells to the cardiac lineage (Lyons et al., 1995). Therefore, *Nkx2.5* is an adequate marker for the identification of cardiac progenitor cells.

To study *Nkx2.5* gene expression we made use of the EGFP-*Nkx2.5* reporter cell line, called A5-CSX (Gottschamel, 2010). This cell line was exclusively used in the following experiments where we investigated the *Nkx2.5* gene expression during the course of differentiation by FACS analysis. Additionally, we studied the influence of cardiomyocyte-stimulating factors, like recombinant SPARC and BMP2/4 in undifferentiated and differentiated A5-CSX cells.

4.3.1 Nkx2.5 Gene Expression during Emrbyoid Body-like Aggregate Development

Here we concentrated on the investigation of the *Nkx2.5* gene expression in CVPCs. The A5-CSX reporter cell line was used to measure *Nkx2.5* gene expression during the course of differentiation by FACS analysis. Therefore A5-CSX cells were cultured as hanging drops for five days followed by rinsing them onto gelled 10cm culture plates. For control A5 cells not carrying the EGFP marker gene were treated and analyzed the same way. Aggregates were measured on days 5, 7, 10 and 13 by FACSCalibur.

Undifferentiated (day 0) CVPC clone A5-CSX showed a strong expression of *Nkx2.5*, while upon initiation of differentiation an almost linear decrease in expression was observed (Figure 4.37).

These results are contrary to previous results from RT-PCR experiments that revealed an upregulation of *Nkx2.5* mRNA upon differentiation (Hoebaus, 2009). A possible explanation could lie in the complex transcription and translation machinery. While RT-PCR is based on mRNA and reflect the process of gene transcription, the results determined by using A5-CSX reporter cell line and FACS analysis also include the process of translation. We assume that undifferentiated A5-CSX cells produce adequate amounts of *Nkx2.5* mRNA followed by fast translation into protein, which would explain the high percentage of cells expressing EGFP and the accompanied loss of mRNA. During differentiation less Nkx2.5 protein is required, therefore we
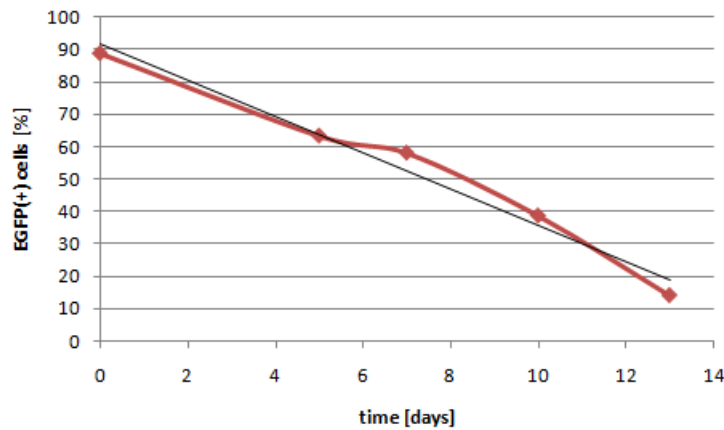
Figure 4.37: The *Nkx2.5* expression during aggregate development. Undifferentiated and differentiated A5-CSX2 cells were analyzed by FACS. Therefore aggregates were made and *Nkx2.5* expression was determined at different time points (days 0, 5, 7, 13). Almost 90% of the measured undifferentiated cell population expressed EGFP, while cell aggregates on day 13 possessed only 14% EGFP(+) cells. Data are means of duplicates.

can see a decrease in EGFP (+) cells and an increase on mRNA-level. It might be the explanation why we obtained different results.

4.3.2 Effect of BMP2/4 on Nkx2.5 gene Expression

Recent studies on ALK3 receptor expression by RT-PCR analysis revealed that CVPCs use BMP signaling and presumably plays a critical role during differentiation and cardiomyogenesis (Hoebaus, 2009). Other studies suggested also the need of BMP signaling during cardiac development (Zhang and Bradley, 1996). To get deeper insights of the importance of BMP signaling we tested CVPCs for the expression of BMP2/4. RT-PCR analysis was performed with primer pairs for BMP2/4 (Figure 4.38). All tested CVPC clones expressed high levels of BMP2/4 in the undifferentiated state. Expression rate of CVPC clones were higher compared to ESC AB2.2 cells.
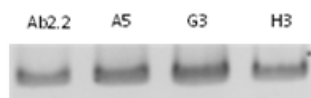
Figure 4.38: RT-PCR analysis of undifferentiated CVPC clones A5, G3 and H3 and ESC AB2.2 cells with primer pairs for BMP2/4.

Previous experiments with CVPCs revealed a positive effect of BMP2/4 on cardiomyogenesis by increasing the number of beating cardiomyocytes, while anti-BMP2/4

antibodies slightly inhibited cardiomyogenesis (Hoebaus, 2009). Therefore we next focused on the effect of BMP2/4 on *Nkx2.5* gene expression.

To investigate the influence of BMP2/4 and anti-BMP2/4 on *Nkx2.5* expression un-differentiated A5 and A5-CSX cells were trypsinised and 3×10^5 cells were transferred onto gelatin-coated 24-well culture plates. After 24 hours BMP2/4 (0.1 μg/ml) and anti- BMP2/4 (1.5 μg/ml) were added for 3 hours, 24 hours and 3 days and the quantitative differences in the EGFP expression was measured by FACS analysis. Because cells were not longer cultured on feeder layers, but as a monolayer cultures we could observe differences in the *Nkx2.5* gene expression compared to control cultures (3h, 24h, 3d) (Figure 4.39, A). The observed reduction on *Nkx2.5* gene expression might be due to the fact that cells were grown as monolayer culture in the absence of LIF-producing feeder cells for different time periods. Without LIF, cells start to differentiate resulting in changed *Nkx2.5* expression profile. To compare the effect of BMP2/4 and anti- BMP2/4 it was necessary to created a base line by dividing FACS values through the mean value of CSX control. Neither treatment with BMP2/4 nor with anti-BMP2/4 resulted in a significant difference in *Nkx2.5* gene expression in undifferentiated CVPC clone A5-CSX cells. Even the presence of these factors for three days showed no effect (Figure 4.39, B).

Next we analyzed the influence of these factors in differentiated CVPCs. Therefore A5 and A5-CSX cells were cultured as hanging drops and were rinsed on day five onto gelatin-coated 10cm culture plates. Because *Nkx2.5* expression was lowest on day 13 of aggregate cultivation BMP2/4 (0.1μg/ml) and anti-BMP2/4 (1.5μg/ml) were added at this time point for 3 and 24 hours and the *Nkx2.5* expression was determined by FACS analysis. Differentiated cells treated with BMP2/4 and anti-BMP2/4 for three and 24 hours showed an effect on *Nkx2.5* gene expression. Addition of BMP2/4 for 3 hours resulted in no significant change in expression, but presence of BMP2/4 for 24 hours resulted in a downregulation in expression. Unexpectedly presence of anti-BMP2/4 showed an enhancement in *Nkx2.5* gene expression during the first 3 hours, but after 24 hours a significant decrease in *Nkx2.5* gene expression was detectable (Figure 4.39, C).
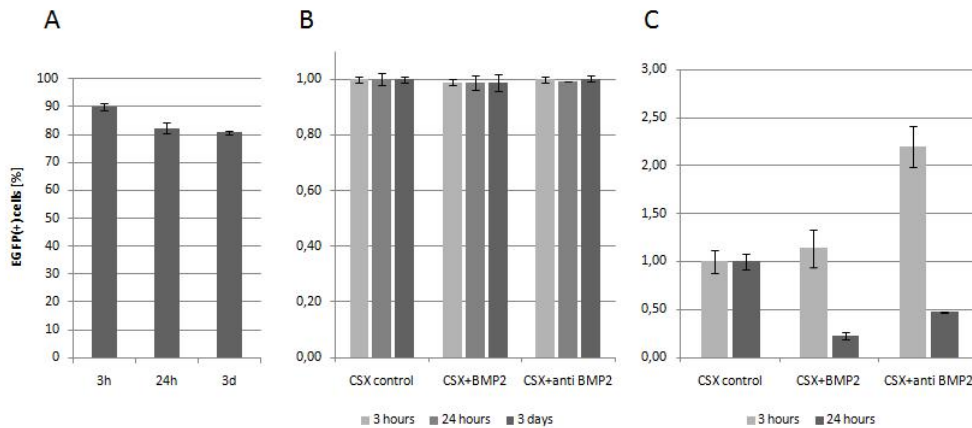
Figure 4.39: Influence of BMP2/4 on *Nkx2.5* gene expression. A: Differences in *Nkx2.5* gene expression in CSX control cultures. While cells cultured as monolayer for three hours showed 90% EGFP(+) cells, a slight reduction in *Nkx2.5* gene expression was observed in monolayers deprived of LIF for 24 hours and three days (81%). B: Undifferentiated A5-CSX cells were treated with BMP2/4 and anti-BMP2/4, respectively for indicated time intervals. C: A5-CSX cells were cultured as hanging drops for five days and were rinsed onto gelled culture plates. Addition of BMP2/4 (0.1μg/ml) and anti-BMP2/4 (1.5μg/ml) on day 13 of aggregate formation for the indicated time periods. FACS values were divided by mean value of CSX control to obtain a constant basis line to compare the effect on *Nkx2.5* gene expression. Data are means of duplicates. For standard deviation see Appendix.

4.3.3 Effect of SPARC on Nkx2.5 gene Expression

Here we determined the influence of SPARC (3 μg/ml) and anti-SPARC (1:100) on the *Nkx2.5* gene expression of undifferentiated and differentiated CVPCs with FACS analysis. Thereby the same procedure was used as previously mentioned and the quantitative difference in EGFP expression of A5-CSX cells was measured again.

Analysis of CVPCs in an undifferentiated state revealed similar results as seen by addition of BMP2/4. Neither recombinant SPARC nor anti-SPARC had an influence on *Nkx2.5* gene expression of undifferentiated CVPC clone A5-CSX (Figure 4.40).

Previous transfection experiments confirmed our findings. Undifferentiated CVPCs exposed to SPARC for 48 hours lead to no significant differences in *Nkx2.5* gene expression (Hoebaus, 2009). This observations let us assume that the *Nkx2.5* gene expression in undifferentiated CVPCs is too high to be affected by SPARC or anti-SPARC. It also might be possible that SPARC and anti-SPARC have no influence on
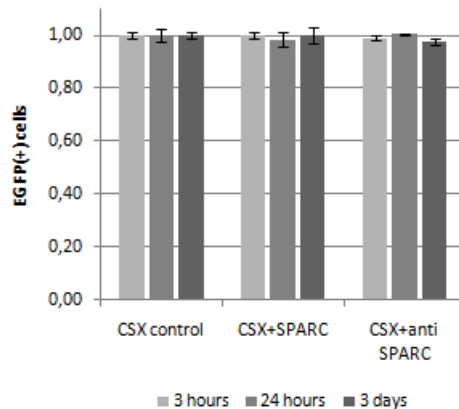
Figure 4.40: The *Nkx2.5* gene expression in undifferentiated CVPC clone A5-CSX in presence of SPARC and anti-SPARC. Addition of SPARC (3μg/ml) and anti-SPARC (1:100) for the indicated time periods. Data are means of duplicates.

gene expression at this time point. But it seemed that CVPCs gain their accessibility toward SPARC during differentiation (Gottschamel, 2010). Here, CVPC aggregates exposed to SPARC from days 5-7 showed an increase in cardiomyogenesis, while anti-SPARC negatively influenced cardiomyogenesis.

Because CVPCs are susceptible toward SPARC during aggregate development, we next studied the effect of SPARC and anti-SPARC in CVPC aggregates on day 13 of cultivation. Differentiated cells exposed to SPARC for 3 hours showed an enhancement of *Nkx2.5* gene expression. But this activation of gene expression elapsed rapidly and after 24 hours a decreased expression was left. This initial enhancement comprised 0.7-fold more EGFP(+) cells with SPARC as without SPARC (Figure 4.41, A).

Similar results were achieved by using the transfection protocol adapted for CVPCs and performing luciferase assays (Figure 4.41, B). Again hanging drops were made with CVPC clone A5. On day 5 the formed aggregates were rinsed onto gelled 10cm culture dishes. Aggregates were cultured till day 9 and were next trypsinized and disseminated onto a gelled 48-well-plate with a concentration of 6 x 10^4 cells/ 500μl. After 24 hours cells were transfected with a *Renilla* plasmid used as internal control encoding a *Renilla luciferase* reporter gene that is constantly expressed in each cell.

Renilla (*reniformis*) luciferase originates from the sea pansy and is used to determine transfection efficiency. Additionally cells were transfected with a control *pGL3*-Basic vector encoding a *luciferase* gene without a promoter region. To make visible the effect of SPARC and neutralizing anti-SPARC on the *Nkx2.5 gene* expression, cells were further transfected with a *NKE24* plasmid. The *NKE24* plasmid is identical to *pGL3b* plasmid, but contains an insert of the *Nkx2.5* promoter region in front of the *luciferase* reporter gene. Lipofectamine 2000 reaction was stopped after 3 hours. 48 hours after transiente transfection SPARC (3μg/ml) and anti-SPARC (1:100) were added for 4 and 24 hours. Luciferase assays were made and Renilla and Firefly values were measured with a luminometer to determine the expression level of the reporter gene.
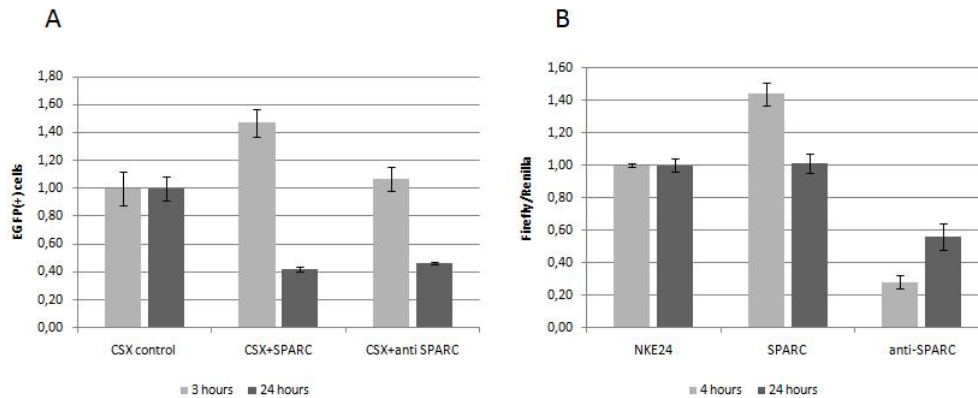
Figure 4.41: The *Nkx2.5* gene expression in differentiated CVPC clone A5. A: FACS analysis. A5-CSX cells were cultured as hanging drops for five days and were rinsed onto gelled culture plates. Addition of SPARC (3μg/ml) and anti-SPARC (1:100) on day 13 of aggregate formation for the indicated time periods. FACS values were divided by mean value of CSX control to obtain a constant basis line that make it able to compare the effect of SPARC and anti-SPARC on *Nkx2.5* gene expression. Data are means of duplicates. For standard deviation see Appendix. B: Luciferase gene expression. CVPC clone A5 aggregates were trypsinized on day 9 of cultivation and were seeded (6 x 10^4 cells/ 500μl) onto gelled 48-well-plates. Transient transfection was performed with Lipofectamine 2000. Plasmid DNA (1000ng) to Renilla DNA ratio was 100:1. Values are mean of duplicates and are indicated as firefly/renilla ratios.

Data obtained from luciferase experiments are similar to FACS results. Addition of SPARC for 4 hours resulted in an increase of luciferase activity and therefore in an enhancement of *Nkx2.5* expression. While FACS analysis showed that anti-SPARC had no effect on *Nkx2.5* expression not before an incubation time of 24 hours is

reached, luciferase assay data revealed a significant inhibition of expression even after 4 hours. These differences could be explained by the fact that in both cases a different sample of anti-SPARC was used.

4.3.4 Effect of SPARC on CVPC gene Expression

It was already shown that undifferentiated CVPC clone A5 cells express to a very low extent *GATA4* on mRNA level. This expression of the myocardial marker indicated a commitment of CVPCs to the cardiac lineage. Upon differentiation of CVPC clone A5 aggregates the expression profile gets altered. Aggregates showed a strong enhancement in *GATA4* expression compared to undifferentiated A5 cells (Hoebaus, 2009).

Next we determined the effect of SPARC on the expression of defined genes in undifferentiated CVPC clone A5 cells. SPARC was added for three hours and RT-PCR analysis with primer pairs for *BMP2, GATA4, TBX5* and *ILK1* was performed. SPARC was able to enhance expression of the genes *GATA4, TBX5* and *ILK1*, whereas gene expression of *BMP2* was slightly decreased (Figure 4.42).
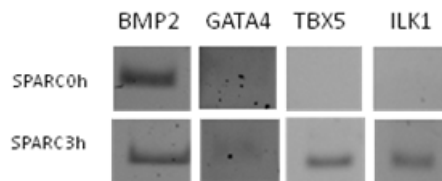
Figure 4.42: Influence of SPARC on genes *BMP2, GATA4, TBX5* and *ILK1* in undifferentiated CVPC clone A5 cells. RT-PCR analysis with indicated primer pairs were performed on untreated A5 cells and cells treated with SPARC for three hours.

5 DISCUSSION

5.1 DIFFERENTIATION POTENTIAL OF CVPCs

5.1.1 Morphological Differences upon Differentiation

In the presence of LIF-producing feeder cells CVPCs maintain their self-renewing potential. Under LIF deprivation cells start to differentiate into three types residing in the heart. Thereby their change their morphology and form cardiomyocytes, smooth muscle cells and endothelial cells (Hoebaus, 2009). For differentiation studies we used the well known embryoid body system by generating embryoid body-like CVPC aggregates and determined morphological changes compared to embryoid bodies with ESC AB2.2 and between CVPC clones itself. As figure 4.3 shows we can observe a difference in aggregate size between ESC AB2.2 and CVPC aggregates. While AB2.2 embryoid bodies tended to form horse-shoe-like shaped dense areas in the center of the aggregates, CVPC embryoid body-like aggregates possessed never such defined structure. CVPC aggregate morphology seems to be more chaotic. We can distinguish AB2.2 aggregates from CVPC aggregates by investigating the location of the dense core, which seems to be in CVPC aggregates in the middle of the aggregates, while in embryoid bodies it is not centered. Between CVPC clones itself no morphological differences were observed, except that CVPC clone H3 aggregates seemed often smaller compared to A5 aggregates. During aggregate development cells start to spread from the core to the periphery thereby differentiating to diverse but limited cell types. The compact core consists of round shaped cells which are surrounded by less dense differentiated cells with elongated, round or angular shaped structure (Figure 4.4).

5.1.2 CVPCs are Restricted to the Cardiac Lineage

FACS analysis and confocal scanning immunofluorescence microscopy proved a limited differentiation potential of CVPCs. With both methods we analyzed the potential of CVPC aggregates to differentiate spontaneously into distinct cell types of the three germ layers ectoderm, endoderm and mesoderm. Therefore, we stained aggregates with antibodies against FOXA2, vWF, GFAP, beta3-tubulin, cTnT and SMA on day 13 of cultivation.

Confocal scanning immunofluorescence microscopy revealed a very limited differentiation potential of CVPCs. Figure 4.5 shows an absence of cells expressing beta3-tubulin and GFAP. These two markers are specific for the ectodermal layer, especially for the neuronal lineage. The absence of any positive signal indicates that CVPC lack the potential for neuronal differentiation at least on day 13 of cultivation. Even in later days of cultivation (d20) no beta3-tubulin expressing cells could be observed in CVPC clone A5 aggregates (not shown). Surprisingly, quantitative FACS analysis revealed data contrary to immunofluorescence microscopy. Here, GFAP-expressing cells were quite common among the CVPC population, while immunofluorescence microscopy depicted an absence of these cells. Beta3-tubulin positive cells were absent in A5 and very low in H3 aggregates. This extremely low incidence in H3 aggregates can be declined as background signals during FACS measurement. Immunofluorescence microscopy revealed an absence of FOXA2-expressing cells in CVPC aggregates, but FACS analysis showed an occurrence rate of 1-2 % in H3 and A5 cell populations. Cells expressing vWF could only be observed during immunofluorescence microscopy by electronic amplification of the output signal. This output signal seemed to be too weak to be recognized only by the naked eye. Indeed, we could recognize a wide distribution of vWF-expressing cells in CVPC aggregates, but data received from FACS analysis revealed an occurrence rate of nearly 100%, which seemed to be too high. Importantly, we could observe cTnT and SMA expressing cells during immunofluorescence microscopy and even FACS analysis proved the presence of these cell types.

Unfortunately data from immunofluorescence staining and FACS analysis were very contradictorily. We can exclude that the reason for this contradiction are due to the antibodies, because in both experiments the same primary and secondary antibodies were used. Maybe, FACS analysis was more sensitive to fluorescence signals and therefore measured even background signals. This would explain the high occurrence rates and the presence of signals, which were more infrequent or even absent during immunofluorescence microscopy. Another possibility for the divergence could be the different methods used to prepare aggregates for staining and the staining procedure itself. For FACS analysis cells were exposed to harsh mechanical stress during separation of cells and during staining procedure. While for microscope analysis aggregates itself were stained and therefore were more gently treated. One important fact to mention is the method of detaching cells from the layer by trypsin. Trypsin may have an effect on cell morphology and expression profile. So we decided to trust more datas received from immunofluorescence microscope analysis than FACS data. We more or less concluded that the FACS analysis is not well suited as the method for analyzing the distribution of cell types and the quantitative determination.

These results indicated an absence of the ability of CVPCs to spontaneously differentiate to cells of the ectodermal lineage. We could already observe the absence of such cell types under the light microscope. We could also show that CVPCs are restricted in their endodermal differentiation potential. While we could observe vWF-expressing cells, we never observed FOXA2 positive cells. Investigations under the light microscope also revealed the presence of rhythmically beating cardiomyocytes, slowly contracting smooth muscle cells and endothelial-like cells. Stainings with anti-cardiac troponin T, anti- smooth muscle actin and anti-vWF antibodies showed the presence of cells expressing these markers. Other groups already succeeded in the isolation of precursor cells expressing cardiac markers and thereby demonstrating the commitment to the cardiac lineage (Tallini et al., 2009; Pfister et al., 2005).

By comparing cardiac cells derived from AB2.2 and CVPC clones A5 and H3, respectively we could recognize that A5 aggregates possessed more cTnT- and SMA-expressing cells compared to AB2.2, while H3 aggregates revealed a lower frequency

(Figure 4.8). These findings were confirmed by data received during the study of beating capacity of A5 and H3 aggregates under the light microscope. There, a different frequency of beating cardiomyocytes could be observed among CVPC clones. Although immnofluorescence microscopy proved the presence of cTnT-expressing cells in both CVPC clones, H3 seemed to have a reduced cardiomyogenese compared to A5 aggregates.

5.1.3 CVPCs can be Induced to Neuronal Differentiation by Retinoic Acid

Here we wanted to test if CVPCs are able to form neuron and glia cells by induction by retinoic acid. Addition of high concentrations of retinoic acid to aggregates resulted in the formation of neuron-like cells (Figure 4.26). Investigation of CVPC aggregates under the light microscope revealed the presence of cells with typical structures seen in neuronal cells of the brain. Because of the similar phenotypical appearance we concluded that the observed cells are neuron-like cells. Neuron-like cells possessed a cell body with neurites arising from the cell body and reaching far into periphery. Such cells were mainly seen in the periphery of aggregates and never in the dense center. Unfortunately, we were not able to absolutely define these cells as neuron-like cells, because of the absence of any positive signal for antibodies specific for neuronal differentiation. Immunofluorescence staining with anti-beta3-tubulin and anti-GFAP antibodies was negative for cells expressing these neuronal markers (Figure 4.25). But RT-PCR analysis bared the expression of neuronal markers like tyrosine hydroxylase and glial fibrillary protein upon exposure of aggregates to retinoic acid (Figure 4.30). Interestingly, we recognized a diverse expression profile among A5 and H3 embryoid body-like aggregates. While ESC AB2.2 embryoid bodies showed a slow increase of neuron-like cells during first days of aggregate development, neuron-like cells occurrence proceeded faster in CVPC aggregates. Compared to embryoid bodies, CVPC aggregates were not able to maintain the continuous presence of neuron-like cells, because in later days the occurrence rate fell. In contrast to AB2.2 embryoid bodies, CVPC aggregates hardly never reached hundred percent (Figure 4.26). Differences in the formation of neuron-like cells could also be observed among CVPC aggregates.

A5 cells seemed to have a more reduced potential to keep their neuron-like cells alive compared to H3. Although in A5 clone neuron-like cells were observed already on day 8 (compared to H3 one day after), they decreased more rapidly compared to CVPC clones H3 (Figure 4.26). Without treatment with retinoic acid we never observed the formation of neuron-like cells in both CVPC clones (Figure 4.28). In conclusion, data support the notion that CVPCs can not give rise to ectodermal somatic cells without induction.

5.1.4 Retinoic Acid is Able to Inhibit Cardiomyogenesis in CVPC Aggregates

CVPC aggregates treated with retinoic acid were much smaller in size compared to untreated aggregates (Figure 4.17). It seemed that retinoic acid prevents differentiation and cell spreading into the periphery. Cardiac differentiation was clearly inhibited as observed by immunofluorescence staining and determining the percentage of beating aggregates. Cells expressing cTnT were absolutely absent in aggregates treated with retinoic acid (Figure 4.20, A). This observation was proved by the strong reduction of beating cardiomyocyte formation resulting in fewer beating aggregates (Figure 4.18). With a CVPC cell line carrying an EGFP reporter gene under the control of the *Nkx2.5* promoter and FACS analyzing we observed a reduction in *Nkx2.5* gene expression upon exposure to retinoic acid. Either adding retinoic acid to undifferentiated CVPCs or to differentiated aggregates resulted in a decrease in expression (Figure 4.21; Figure 4.22). This explains the dual potential of retinoic acid to promote neuronal differentiation by preventing cardiomyogenesis at the same time.

5.2 REGULATION OF CARDIOMYOGENESIS

Cardiomyogenesis is a complex network of regulated gene expression and signal transduction. Extracellular signals are involved in the activation of transcription factors that enter the nucleus and activate a subset of genes involved in cardiomyogenesis.

5.2.1 Inhibition of MAPK Cascade Resulted in a Reduction of Cardiomyogenesis

The mitogen-activated protein kinase (MAPK) pathway is a signaling cascade that convert extracellular signals into intracellular activation of distinct transcription factors involved in cell proliferation and differentiation. Studies have revealed the influence of MAPK pathway in cardiomyocyte differentiation in P19 cells (Eriksson and Leppä, 2002). Here, similar results on cardiomyogenesis were achieved by adding PD98059, the MEK1 inhibitor to CVPC aggregates. While MEK1 inhibition showed no effect on aggregate morphology, we observed a negative effect on cardiomyogenesis. Addition of the inhibitor resulted in a reduced beating capacity. Low concentrations of the inhibitor already decreased the occurrence rate of beating cardiomyocytes in first days of aggregate development (Figure 4.32). Even by increasing the concentration of the inhibitor to 20μM did not change the fact that PD98059 is only effective in early developmental stages (Figure 4.33). In general, the onset of contraction was delayed and 50-60 % less beating aggregates could be observed. Inhibition at later stages of aggregate development did not affect cardiomyogenesis. Even adding the inhibitor for longer time periods resulted in no reduction of beating capacity. Only the presence of the inhibitor at the time point of aggregation (d0) resulted in a delayed onset of cardiomyogenesis (Figure 4.34). So we can really exclude an influence on cardiomyogenesis in later stages of development, whether increasing the concentration nor adding the inhibitor for longer time intervals. We further could recognize a time dependent action of the MEK1 inhibitor on smooth muscle cell formation. While the presence of PD98059 from day 0 on resulted in a prevention of contracting smooth muscles, the addition of the inhibitor from day 5 on enhanced SMC formation (Figure 4.35).

We could confirm a prevention of cardiomyogenesis also by observation of *Nkx2.5* gene expression during MEK1 inhibition. We recognized a significant reduction of *Nkx2.5* expression in first days of aggregate development(Figure 4.36).

These facts indicated that the MAPK cascade plays an important role in cardiomyogenesis by influencing the onset as well as the occurrence rate of beating cardiomyocytes

and contracting smooth muscle cells. Thereby the MAPK signal transduction pathway positively influences the differentiation of CVPCs to cardiomyocytes and smooth muscle cells during early developmental stages and simultaneously inhibits contractions of smooth muscle cells in later phases of development.

5.2.2 Influence of SPARC, anti-SPARC, BMP2/4 and anti-BMP2/4 on Nkx2.5 Expression

The *Nkx2.5* gene is known as a cardiac marker with important functions during heart development. First commitment of cells to the cardiac lineage is indicated by the expression of *Nkx2.5* (Jamali et al., 2001). Progenitor cells residing in the heart are shown to express *Nkx2.5* (Saga et al., 2000) and this expression seems to be essential for survival and proliferation of precursor cells (Lyons et al., 1995). Undifferentiated CVPCs are characterized by high expression levels of *Nkx2.5*. Upon differentiation it came to an almost linear decrease in expression (Figure 4.37). These findings indicate CVPCs to be cardiac progenitor cells that are already committed to the cardiac lineage due to their expression of *Nkx2.5* in their undifferentiated state.

Bone morphogenetic protein (BMP) belongs to the subfamily of the TGF-beta superfamily and plays important roles in proliferation, differentiation and migration. BMPs are expressed during heart development and the interplay of BMP repression and stimulation is critical for cardiomyocyte differentiation (Yuasa and Fukuda, 2008). BMP2 has the potential to specify cells to the cardiac lineage (Lough et al., 1996) and is critical for the specification of the cardiogenic mesoderm (Schlange et al., 2000). The BMP-signaling pathway activates Smad1 by phosphorylation and this results further in the activation of cardiac genes (Callis et al., 2005). Inhibition of BMP signaling resulted in a prevention of cardiomyocyte differentiation in *Flk1+* progenitor cells (Yamashita et al., 2005). Also our isolated CVPC cell line revealed the importance of BMP2. Undifferentiated CVPCs express high amounts of BMP2 what was seen during RT-PCR analysis. Previous experiments revealed the positive influence of BMP2 on cardiomyogenesis in CVPCs (Hoebaus, 2009). Here, we were

not able to show a positive effect of BMP2 signaling on the *Nkx2.5* gene expression, although we assumed an upregulation in expression due to findings that revealed BMP2 as a positive regulator for cardiomyogenesis. Neither in undifferentiated nor in differentiated CVPC clone A5 aggregates we could see the presumed positive effect. Instead, we had to recognize that BMP2 had no effect in undifferentiated cells at all, but a negative effect in differentiated cells exposed to BMP2 for 24 hours. Unexpectedly, presence of anti-BMP2/4 during later stages of differentiation showed an enhancement in *Nkx2.5* gene expression after 3 hours, but decreased rapidly after 24 hours (Figure 4.39).

Previous experiments revealed already the positive effect of SPARC on cardiomyogenesis (Gottschamel, 2010). *Nkx2.5* gene expression in undifferentiated CVPCs was not influenced by the presence of SPARC or anti-SPARC. However, experiments on differentiated CVPCs revealed an enhancement of *Nkx2.5* gene expression after 3 hours, while anti-SPARC showed a decrease in expression after 24 hours (Figure 4.41). The positive influence of SPARC on cardiomyocyte differentiation revealed also an upregulation of cardiac markers like *Nkx2.5*, troponin, BMP-2 and MHCalpha (Hrabchak et al., 2008). Undifferentiated CVPCs exposed to SPARC revealed altered gene expression profiles concerning *BMP2, GATA4, TBX5* and *ILK1*. While it seemed that BMP2 expression was decreased, *GATA4, TBX5* and *ILK1* expression was enhanced upon SPARC exposure. The T-box gene *tbx5* is like BMP2 expressed during heart development. Expression of *tbx5* proceeds early in the developing heart together with *Nkx2.5* and *GATA4* expression (Liberatore et al., 2000). The *GATA4* gene is expressed in the primary and secondary heart field and presumably plays an important role during heart development (Waldo et al., 2001). The *Nkx2.5* gene is known to have binding sites for *GATA4* and elimination of this binding sites results in a loss of early cardiac gene activation. This hints at a GATA-dependent controlling of *Nkx2.5* gene expression (Searcy et al., 1998). Interestingly, treatment of undifferentiated CVPCs with recombinant SPARC resulted in an increase of *GATA4* gene expression.

In conclusion, CVPCs expressed cardiac transcription factors like *Nkx2.5* and *BMP2*

in their undifferentiated state and possessed a decreased *Nkx2.5* gene expression upon differentiation. These results defined CVPCs to be presumably cardiac progenitor cells. Further findings demonstrated that recombinant SPARC is able to enhance expression of diverse cardiac genes, which in turn indicated SPARC as a positive regulator of cardiomyogenesis.

5.3 SUMMARY

So far we know that CVPCs can be kept in an undifferentiated state by cultivation on LIF-producing feeder cells thereby activating STAT3 signaling pathway and preventing differentiation (Hoebaus, 2009). From RT-PCR analysis we know that CVPCs have both embryonic and cardiac character by expressing stemness transcription factors like *Oct4, Sox 2* and *Nanog* as well as myocardial transcription factors such as *Brachyury*, *Nkx2.5*, *GATA4* and *Isl1* (Hoebaus, 2009). As proved by immunofluorescence microscopy we conclude that CVPCs are able to differentiate to cell types residing in the heart exclusively. They spontaneously differentiate to cardiac troponin T-expressing cardiomyocytes, contracting smooth muscle cells expressing SMA and vWF-expressing endothelial cells. Presumptive ectodermal cells could only be observed by induction with high concentrations of retinoic acid. This resulted in the formation of neuron-like cells, which however, never expressed neuron specific genes except on mRNA level.

5.4 DIFFERENTIATION POTENTIAL OF SSCs

5.4.1 Morphological Differences Upon Differentiation

As seen in CVPCs, SSCs cultured on LIF-producing feeder cells maintain their undifferentiated state and start to differentiate under LIF deprivation. Upon differentiation SSCs change their cell structure and form distinct cell types. While He2P11K13/5 cells were isolated from the murine heart, Hi2P11K15/6 cells were isolated from the brain. Because of their diverse origin we assumed that cells could differentiate to different cell types. For Hi2P11K15/6 we believed a restriction to the neuronal lineage

based on their isolation from the murine brain and He2P11K13/5 were assumed to be committed to the cardiac lineage as seen in CVPC clones.

Embryoid body-like aggregates of Hi2P11K15/6 and He2P11K13/5 were the largest one compared to AB2.2 embryoid bodies and CVPC aggregates (Figure 4.11). Hi2P11K15/6 aggregates often seemed to have a very diffuse structure where the dense core was often not centered. He2P11K13/5 aggregates often possessed a stellar shaped core and a defined edge in the outer peripheral area. But also aggregate structures as seen in Hi2P11K15/6 could be observed in He2P11K13/5. An expert eye could distinguish these two SSC aggregates by their morphological differences. Upon differentiation cells spread from the dense core to the periphery and start to differentiate to several cell types. As seen in CVPC aggregates the compact core consists of round shaped cells which is passed to less dense elongated, round or angular shaped cells. SSC aggregates can be distinguished easily from CVPC aggregates in their morphological differences. Another difference could be observed by investigating their differentiation potential. While CVPC aggregates seemed to be restricted to the cardiac lineage, SSC aggregates seemed to have a more extended differentiation potential. In both SSC clones we could observe cells with structures identical to neuronal cells. Although such cells could only be observed infrequently, they possessed the potential for neuronal differentiation (Figure 4.12).

5.4.2 SSC Clone Hi2P11K15/6 is More or Less Restricted to The Neuronal Lineage

Differentiation studies revealed the potential of Hi2P11K15/6 to spontaneously differentiate to neuron-like cells. Because of the isolation from the murine brain we were not surprised by the appearance of neuron-like cells during investigations under the light microscope. Neuron-like cells featured a cell body and dendrites emerging from the body. Further we recognized expression of the neuronal markers GFAP and TH in aggregates, while no expression was seen in CVPC aggregates (Figure 4.30). The occurrence rate of neuron-like cells was slightly lower than in AB2.2 embryoid bodies and first appearance of these cells was delayed in Hi2P11K15/6

aggregates (Figure 4.27). The potential to differentiate to neuron-like cells could further be confirmed by the mRNA expression pattern of neuronal markers. AB2.2 aggregates treated with retinoic acid showed only expression of GFAP. Surprisingly, Hi2P11K15/6 aggregates expressed both markers. Hi2P11K15/6 cells were the only cell line that expressed neuronal markers without induction by retinoic acid. So we could exclude the possibility of Hi2P11K15/6 to be embryonic stem cells. Although immunofluorescence staining never showed beta3-tubulin- or GFAP-expressing cells, we could observe an occurrence rate of 7.14% beta3-tubulin-expressing cells by FACS analysis. In comparison to AB2.2 embryoid bodies, Hi2P11K15/6 aggregates revealed a higher percental distribution of beat3-tubulin expressing cells (Figure 4.14). Further investigation on their differentiation potential revealed the presence of vWF and SMA expressing cells. Due to the fact that Hi2P11K15/6 cells were isolated from the brain we expected a prevention of cardiomyocyte formation which was confirmed by a lack of cTnT-expressing cells. We could also see an absence of beating cardiomyocytes (Figure 4.18) what is attended by the lack of cTnT-expressing cells. Because of the appearance of neuron-like cells and the absence of beating cardiomyocytes we concluded that Hi2P11K15/6 cells are restricted to the neuronal lineage.

5.4.3 SSC Clone He2P11K13/5 is Not Resctricted to The Cardiac Lineage

Because of the isolation of He2P11K13/5 from the murine heart we expected a restriction to the cardiac lineage as seen in CVPC clones. But differentiation studies revealed the potential to spontaneously form neuron-like cells what was not seen in CVPC aggregates. Because of the ability of neuronal differentiation we concluded that these cells are not restricted to the cardiac lineage and are therefore multipotent. Although the spontaneous formation of neuron-like cells was fewest in He2P11K13/5 aggregates among SSC clone Hi2P11K15/6 and AB2.2 embryoid bodies, they have the potential for neuronal differentiation (Figure 4.28). The occurrence rate of He2P11K13/5 aggregates possessing neuron-like cells never passed 10%. We were not able to classify neuron-like cells as neurons because of the absence of positive signals during FACS analysis and immunofluorescence microscopy. We assumed that

the absence of positive signals might be due to the time-dependent appearance of neuron-like cells. Because neuron-like cells were seen only after passing day 13, we believe that antibody staining failed because of the absence of neurons. Neuronal formation proceeded principal in later developmental stages. Indeed, we tried to stain neuron-like cells on day 20 of aggregate cultivation, but we failed to get meaningful IF pictures due to the rare occurrence rate of these cells. Immunofluorescence microscopy revealed the presence of vWF-, cTnT- and SMA-expressing cells. Compared to CVPC clone A5, He2P11K13/5 aggregates showed a lower beating capacity of cardiomyocytes. While CVPC clone A5 reached nearly 100 % of aggregates possessing beating cardiomyocytes on day 13, He2P11K13/5 showed only maximal 65 %.

5.4.4 SSC Aggregates Enhanced Neuron-like Cell Formation by Exposure to Retinoic Acid

Addition of retinoic acid to SSC aggregates resulted in a decrease in aggregate size as seen in RA-treated CVPC aggregates and embryoid bodies (Figure 4.17). RA-treated aggregates seemed to be more compact and cell spreading into periphery was strongly reduced. Compared to He2P11K13/5 aggregates treated with retinoic acid, Hi2P11K15/6 aggregates were some bigger. SSC aggregates exposed to high concentrations of retinoic acid formed a high number of neuron-like cells as seen in RA-treated CVPC aggregates. The formation of neuron-like cells was enormous enhanced by addition of retinoic acid. Neuron-like cells were again mainly seen in the periphery of aggregates and thick tubes radiated away from the center to the periphery (Figure 4.24). RA-treated Hi2P11K15/6 aggregates possessed neuron-like cells on day 8, while first appearance of these cells was observed on day 10 in He2P11K13/5. Compared to AB2.2 embryoid bodies we could recognize a decrease of neuron-like cells from day 14 on (Figure 4.27). Investigations on the mRNA expression of neuronal markers revealed that He2P11K13/5 aggregates treated with retinoic acid expressed GFAP, but not TH as seen in CVPC clone H3 and AB2.2 embryoid bodies. In contrast RA-treated Hi2P11K15/6 aggregates expressed both markers, but they expressed these markers also in untreated aggregates, but addition of retinoic acid enhanced the

expression (Figure 4.30). Again, we were not able to absolutely define these cells as neuron-like cells, because of the absence of any positive signal for antibodies specific for neuronal differentiation. Immunofluorescence staining with anti-beta3-tubulin and anti-GFAP antibodies was negative.

5.4.5 Retinoic Acid is Able To Inhibit Cardiomyogenesis in SSC Aggregates

Rarely we could observe beating cardiomyocytes in SSC aggregates treated with retinoic acid. The few observed cardiomyocytes hardly contracted and retinoic acid also seemed to inhibit smooth muscle formation. Immunofluorescence microscopy showed an absence of any cTnT-expressing cells in SSC aggregates treated with retinoic acid (Figure 4.20, A). Because Hi2P11K15/6 aggregates never possessed beating cardiomyocytes even if they were not treated with retinoic acid, we could only demonstrate the decrease in beating cardiomyocytes on the example of He2P11K13/5 aggregates. Here, we could see a prevention of cardiomyogenesis by a great reduction of beating aggregates induced by retinoic acid (Figure 4.19). We assume that this prevention is due to a decrease of *Nkx2.5* expression what was demonstrated in CVPC clone A5.

5.5 FUTURE

CVPCs and SSCs are stable cell lines that can be maintained in an undifferentiated state and possess self-renewing potential. These cell lines were isolated by two different methods that resulted in diverse limited differentiation potentials of these cells. While CVPCs are restricted to the cardiac lineage, SSCs seemed to be multipotent. Optimizing the isolation method could improve the yield of progenitor cells which are restricted to cardiac lineage. Proper in vitro investigations of molecular mechanism involved in CVPC differentiation will help to understand cardiomyocyte development in the embryonic and adult heart.For this purpose the in vitro embryoid body system is an adequate tool to mimic early cardiomyogenesis. It remains to be investigated which signal transduction pathways are involved during cardiomyogenesis and especially in

cardiomyocyte differentiation. This would further enhance the finding of adequate cardiomyocyte-stimulating factors to enrich cultures with cardiomyocytes. Insights in these molecular pathways could reveal how stem cells residing in heart are activated to differentiate to cardiac cells and how the homing of these cells to the injured myocardium proceeds. For future in vivo experiments it would be necessary to understand the differentiation process of CVPCs. Then, it might be possible to inject exogenous cardiomyocytes into infarcted myocardium and to determine grafting efficiency as well as their differentiation potential in vivo. So we could determine the regenerative potential of CVPCs in injured hearts.

6 MATERIAL

6.1 ENZYMES

Table 6.1: Enzymes

Chemical	Company
Collagenase	Wothington, USA
DNase I, RNase free	Fermentas, Lithuania
Pancreatin	Sigma, USA
Proteinase K	Fluka, CHA
RiboLockRNase Inhibitor	Fermentas, Lithuania
RevertAidTM M-MuLV RT	New England Biolabs, USA
Taq DNA Polymerase	Fermentas, Lithuania
Trypsin	Life Technologies, USA

6.2 PROTEINS AND INHIBITOR

Table 6.2: Proteins and Inhibitors

Chemical	Company
BMP2/4	R and D Systems
M-LIF	Purified from insect cells (Wiedner, 2008)
Recombinant SPARC	Sigma, USA
PD98059	Cayman, USA

6.3 GENERAL CHEMICALS

Table 6.3: General Chemicals

Chemical	Company
Acetic acid	Merch, D

Acryl amide	BioRad, USA
Agarose Biozyme LE	Biozyme, D
Beta-Mercaptoethanol	Loba Feinchemie, A
BSA	Roth, D
DABCO	Sigma, USA
DAPI	Invitrogen USA
DNA ladder (gene ruler, 100bp, 1kb)	Fermentas Lithuania
dNTPs Fermentas	Lithuania
Dimethylsulfoxid (DMSO)	Acros, B
Dithiothreitol (DTT)	Acros, B
EDTA	Acros, B
Ethanol	Merch, D
Ethidiumbromide	Fluka, CH
Formaldehyde	Merck, D
Glycerine	Merck, D
Glycin	Sigma, USA
Hydrochloric acid (HCl)	Acros, B
Lithiumchloride	Merck, D
Lipofectamine 2000	Invitrogen USA
Loading dye	Fermentas Lithuania
Methanol	Merck, D
Magnesiumchloride	Fermentas, Lithuania
Magnesiumsulfate	Fluka, CH
Mowiol	Hoechst, D
Nalgene Filter	Nalagene Labware, USA
PCR-buffer without MgCl2	Fermentas, Lithuania
Pepstatin	Roche, D
Polyacrylamide	Merck, D
Proteinase Inhibitor	Roche, D
Reverse Transcriptase Buffer	Invitrogen, USA
Sodiumazid	Acros, B
Sodiumbicarbonate	Sigma, USA
Sodiumhydrogencarbonate	Life Technologies, USAA
Sodiumhydrogenphosphate	Roth, D
Sodiumhydroxide	Merck, D

Sodiumthiosulfate	Merck, D
Trichloracetic acid	Merck, D
Tris Base	Life Technologies, USA
Triton X100	Sigma, USA

6.4 CHEMICALS FOR CELL CULTURE

Table 6.4: Chemicals for cell culture

Chemical	*Company*
Beta-Mercaptoethanol	Loba, A
D-Glucose	Acros, B
DMEM powder	Gibco, USA
DMSO	Sigma, USA
Fetal Bovine Serum (FBS)	HyClone, USA
Fetal Bovine Serum (FBS)	Gibco, USA
Fetal Bovine Serum (FBS)	Sigma, USA
Gelatine	Difco, USA
Glycine	Applichem, D
L(+) - Glutamin	Gibco, USA
Lipofectamine 2000	Invitrogen, USA
Mitomycin C	Acros, B
Penicillin /Streptomycin (P/S)	Gibco, CH
Streptomycin	Sigma, USA

6.5 KITS

Table 6.5: Kits

Chemical	*Company*
Endo Free Plasmid Maxi Kit	Qiagen, D
RNeasy Mini Kit	Qiagen, D
Dual Luciferase Reporter System	Promega, USA

6.6 PLASMIDS

6.6.1 RENILLA PLASMID
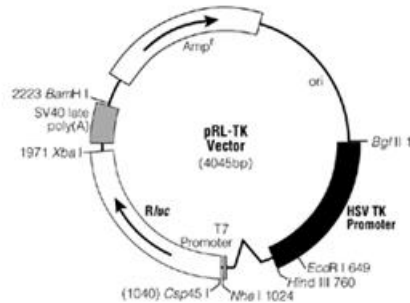
Figure 6.1: Renilla Plasmid

The pRL-TK vector (here often called as Renilla plasmid) is used as internal control to determine transfection efficiency. This plasmid carries a Renilla luciferase reporter gene under the control of T7 promoter that is constantly expressed in the cells. For selection it additionally carries an Ampicillin resistance gene.

6.6.2 pGL3-BASIC PLASMID

The control pGL3-Basic Vector contains a firefly luciferase gene that is promoterless. Again we can find an Ampicillin resistance gene.
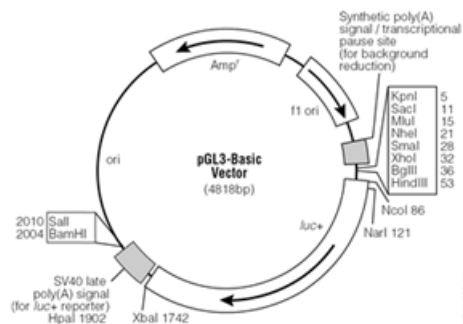
Figure 6.2: Promega pGL3-Basic Plasmid (E1751)

6.6.3 NKE24 PLASMID

The NKE24 plasmid is identical to pGL3-Basic vector, but contains an insert of the
Nkx2.5 promoter region in front of the luciferase reporter gene. This vector was
obtained by Dr. Katherine Yutzey (USA).
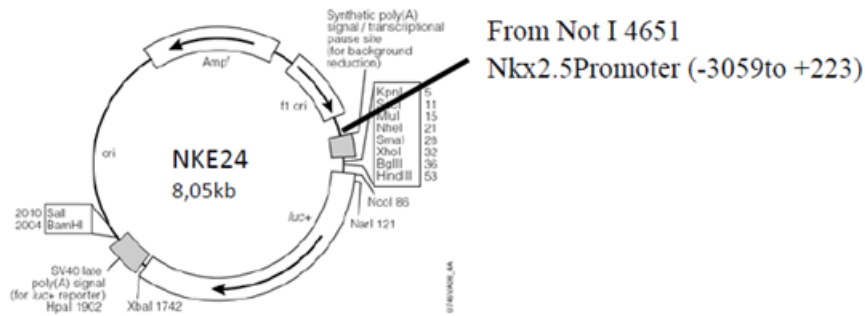
Figure 6.3: pGL3-Basic vector containing a Nkx2.5 promoter

6.7 PRIMERS

Table 6.6: Primers

Name	Direct.	Sequence	Temp	Cycles	bp
BMP2	Fwd	5' - GTTTGTGTTTGGCTTGACGC - 3'	57.5°C	34	719
	Rev	5' - AGACGTCCTCAGCGAATTTG - 3'			
GATA4	Fwd	5' - GCCTGTATGTAATGCCTGCG - 3'	53°C	31	500
	Rev	5' - CCGAGCAGGATTTGAAGAGG - 3'			
GAPDH	Fwd	5' - CGTCCTTCACCACCATGGAGA- 3'	55°C	29	300
	Rev	5' - CGGCCATCACGCCACAGTTT- 3'			
ILK	Fwd	5' - CTCTGCGGTGGTTGAAAT- 3'	52.5°C	35	190
	Rev	5' - GAAACATGCATAGTGAAGTGG- 3'			
MEF2c	Fwd	5'-GGCCATGGTACACCGAGTACAACGAGC-3'	66°C	34	395
	Rev	5'-GGGGATCCCTGTGTTACCTGCACTTGG-3'			
Nkx2.5	Fwd	5' - AGCAACTTCGTGAACTTTG- 3'	48°C	30	345
	Rev	5' - CCGGCCAGTGTGGA- 3'			
Mesp1	Fwd	5' - AGAAACAGCATCCCAGGAAA- 3'	52°C	32	346
	Rev	5' - GTGCCTGCTTCATCTTTA- 3'			
Isl 1	Fwd	5' - CGGTGCAAGGACAAGAAA- 3'	49°C	38	346

	Rev	5' - CAATAGGACTGGCTACCA- 3'			
MLC1v	Fwd	5' - TCAGGAAGCCCAGGGCAGGC - 3'	56°C	38	86
	Rev	5' - GGAGTCCGAACCACTCCTTC - 3'			
GFAP	Fwd	5' - AGGAGCCAGCAGAGGCAGGG - 3'	72°C	35	852
	Rev	5' - CTTGGCTTGGCGGAGCAGCT - 3'			
TBX5	Fwd	5' - GTTCCAGCACGGAGCACCCC - 3'	55°C	31	422
	Rev	5' - CCCGCACTGCCTGACCACAG - 3'			
TH	Fwd	5' - CGTCTCAGAGCAGGATACCAAGCAG - 3'	71°C	35	835
	Rev	5' - CAGTAGACCGGCCACGGGTC - 3'			

6.8 ANTIBODIES

Table 6.7: Antibodies

Chemical	Company
anti-rabbit Alexa Fluor 647 Conjugate	Cell Signaling 4414
anti-mouse Alexa Fluor 488 Conjugate	Cell Signaling 4408
anti-mouse Troponin T-C (CT3)	Santa Cruz Biotechnology I2208
anti-mouse FITC	Dianova 715-095-151
Human BMP-2/4	R and D Systems MAB3552
Mouse LIF	R and D Systems AF449
anti-rabbit FITC	Jackson Labs 711-095-152
anti-mouse Smooth muscle actin	Sigma A2547
SPARC	Santa Cruz 25574 /Sigma S5174
anti-rabbit Von Willebrand Factor	Sigma F-3520
anti-mouse Beta-3-tubulin (TU-20)	Cell Signaling 4466S
anti-rabbit Glial fibrillary protein (GFAP)	Sigma Aldrich SL09462
FOXA2/HNF3beta	Cell Signaling 3143S

6.9 CELL LINES

6.9.1 SNL76/7- Fibroblasts

Allan Bradley established the murine SNL76/7 fibroblast cell line, which derives from the murine STO fibroblast cell line and contains a neomycin-resistence and LIF gene (McMahon and Bradley, 1990).

6.9.2 Bacteria Strain XL1-Blue

Bacteria strain XL1-Blue was used to multiply different plasmids (Stratagene, USA).

6.9.3 Embryonic stem cells

AB2.2

The embryonic stem cell line AB2.2 originates from 129v mice and was isolated by Allan Bradley (Soriano et al., 1991).

DC6

This cell line overexpresses Desmin and was obtained by Sonja Puz (Puz, 1999).

6.9.4 Cardiovascular progenitor cells

The CVPC cell line was isolated from the heart tissue of neonatal HDAC1 +/- mice (N1-2 neoR) by Georg Weitzer and Wolfgang Weber. Because of the presence of a neomycin resistance gene in one allel of the HDAC1 locus cells are resistant to neomycin and neomycin analogs like G418. Isolated cells were co-cultured with the embryonic stem cells AB2.2 and feeder cells for 10 passages according to a 3T3 protocol. Selection with G418 resulted in survival of cells carrying a neomycin resistance. The survived cells are named cardiovascular progenitor cells (CVPCs) and consists of eleven subclones (A3, A5, B3, B5, C3, D3, D5, E3, F3, G3 and H3). In this study CVPC clones A5 and H3 were used.

A5-CSX

This CVPC cell line contains an EGFP reporter gene under the control of Nkx2.5 promoter region. The pCsx-EGFP-PP-DT plasmid was inserted into the Nkx2.5 locus of A5 cells by homologue recombination (Gottschamel, 2010)

6.9.5 Somatic stem cells

The somatic stem cell lines (SSCs) were isolated from several tissues of neonatal and adult mice. Single clones were obtained from the brain, pancreas and the heart of wildtype mice. This isolation method uses embryonic stem cells (Tag3) carrying the selection marker thymidine kinase. Isolated cells were co-cultured with ESCs (Tag3) and feeder cells for 10 passages according to a 3T3 protocol. Negative selection was performed with Ganciclovir for 2x4 days and resulted in the isolation of SSC clones. In this diploma thesis, He2P11K13/5 (isolated from the heart) and Hi2P11K15/6 (isolated from the brain) cells were used for experiments.

7 METHODS

7.1 CELL CULTURE

7.1.1 Washing of glass pipettes

Because ESCs and CVPCs are sensitive to any kind of contamination, glass pipettes are washed only with hypochlorite and tapwater to avoid contamination with soap and other organic substances. Cotton plugs of used glass pipettes is removed and pipettes are put into vessels containing a mixture of hypochlorite and tapwater. Glass pipettes are then washed with tapwater for at least four hours and are kept in milliQ-H2O overnight. The next day pipettes are dried at 60°C for about 3 hours and are stuffed with new cotton plugs. They are placed into pipette boxes and backed at 180°C for 8 to 10 hours.

7.1.2 Washing of cell culture glass ware

Used glass ware for tissue culture work is filled with tapwater and hypochlorite. After 15 to 30 minutes glass ware is rinsed out with tapwater until no hypochlorite is left. Glass ware is rinsed out with milliQ-H2O to ensure no tapwater is left. It is then filled with milliQ-H2O and left overnight. The next day glass ware is dried and autoclaved at 120°C and 1 bar.

Other tissue culture appliances are also washed with hypochlorite and tapwater, followed by rinsing them with milliQ-H2O. It is important that they never come in contact with soap.

7.2 BUFFER AND SOLUTIONS

10x PBS (phosphate buffered saline)

1.37 M NaCl

14.7 mM KCl

78.1 mM Na2HPO4x7H2O

26.8 mM KH2PO4

80g NaCl, 2g KCl, 10,72g Na2HPO4x7H2O and 2g KH2PO4 was dissolved in 800ml MilliQ water and pH was adjusted to 7.2 with a saturated Na2HPO4x7H2O solution. After the buffer is filled up to the 1l mark with MilliQ the solution is sterile filtered (Nalgene Filter, Nalgene Membrane; 0.22μm pore width) and stored at room temperature.

1x PBS

10x PBS is diluted 1:10 with MilliQ and stored at room temperature.

100x GPS (Glutamine-Penecillin-Streptomycin)

4.25 g NaCl

1.5 g Penicillin

2.5 g Streptomycin

14.6 g L-(+)-Glutamine

Ingredients are dissolved in 500 ml MilliQ and sterile filtered. Aliquots of 40 ml are transferred into 50 ml Falcon tubes and stored at -20°C. Aliquot in use is stored at 4°C (to dissolve the pellet during thawing it is commended to mix and put it on 37°C till pellet is completely thawed)

100x ß-Mercaptoethanol

200 ml 1x PBS

144 μl beta-Mercaptoethanol

Sterile filtration and aliquoting in 50ml Falcon tubes. Storage at -20°C. Aliquot in use is stored at 4°C.

Trypsin

3.5g NaCl

0.5g D-Glucose

0.09g Na2HPO4x7H2O

0.185g KCl

0.12g KH2PO4

0.2g EDTA

1.25g Trypsin

1.5g Tris Base

Ingredients were dissolved in 500ml MilliQ water and pH was adjusted to 7.6 with concentrated HCl. The solution is sterile filtered and stored at -20°C. Aliquot in use is stored at 4°C.

1% gelatin stock solution

10g gelatin is dissolved in 1l of MilliQ water and autoclaved. Storage at room temperature

0.1% gelatin solution

1x stock solution is diluted 1:10 with MilliQ and stored at room temperature.

Dulbecco's Modified Eagle Medium (DMEM)

4.5 l MilliQ are poured into a 5 l Erlenmeyer flask and 66.9 g of DMEM are added (magnetic stirrer). 18.5 g (3.7 g/l) NaHCO3 are added, the pH of 7.4 is adjusted with concentrated HCl and the flask is filled up to the 5 l mark with MilliQ. The medium is sterile filtered and stored at 4°C. Aliquots of 3 ml are pipetted into a 6 well culture dish and incubated at 37°C, 5% CO2. These aliquots are checked for bacterial growth or other contamination daily until the medium is used.

Culture media

M15Hi medium	M15Si medium	M10Gi medium	Freezing medium
15% HyClone FBS	15% Sigma FBS	10% Gibco FBS	60% DMEM
1% beta- Mercap- toethanol	1% beta- Mercap- toethanol	1% beta- Mercap- toethanol	20% FBS
1% GPS	1% GPS	1% GPS	20% DMSO
83% DMEM	83% DMEM	88% DMEM	

Gelatin coating of cell culture plates

To obtain a adequate surface matrix for cells to attach we coat cell culture plates with 0,1% gelatine solution two hours prior to use. Before cells are added remaining solution is aspirated.

7.3 SNL76/7

7.3.1 Thawing of SNL76/7

Aliquots are stored in cryotubes in liquid nitrogen. For thawing aliquots are put into a 37°C water bath and thawed until a tiny ice cube is left. The tube is disinfected with 70% ethanol, put into the lamina flow and flamed at a Bunsen burner. The total volume of the cryotube is transferred into a 50ml Falcon tube and M10Gi medium is added drop by drop until to the 12.5ml mark. After each drop the tube is shaked carefully to ensure consistent dispersion of M10Gi medium. Drops were added not

too fast and not too slow. When added too fast cell will burst due to osmotic shock and when added too slow cells are kept too long in DMSO rich medium what will kill them. After addition of M10Gi the Falcon tube is centrifuged for 7 minutes at 1000rpm at room temperature (Heraeus Biofuge, swing out buckets) and the pellet is resuspended in 1ml M10Gi and transferred onto bacterial dishes. Residual cells are washed out with another 3ml M10Gi and solution is added to the dish. SNL76/7 fibroblasts are kept at 37°C at 5%CO2.

7.3.2 Cultivation of SNL76/7

Cells are cultivated at 37°C at 5%CO2. Medium change is often not necessary, but must be done when pH indicator switches to orange. If the cells are confluent they have to be splitted onto new dishes. Cells were generally splitted on Mondays in a ratio of 1:6 and on Fridays 1:3. Before splitting cells are washed with 4ml 1xPBS to get rid of any traces of medium which will inhibit trypsin action. For detaching SNL76/7 cells from the matrix 2ml trypsin is added for five minutes at 37°C. Detachment is checked under the light microscope. Round shaped cells are indicators for detachment and trypsin can be inactivated by adding fresh M10Gi. For 1:3 splitting trysin is inactivated by adding 3ml of M10Gi and 1ml of this solution is transferred onto new dishes containing already 7ml M10Gi medium.

7.3.3 Freezing of SNL76/7

Confluent cells are washed with 1xPBS twice and 0.7ml trypsin is added for 7 minutes at 37°C. Trypsin is inactivated by 2ml M10Gi and cell suspension is transferred into a 15ml Falcon tube. 2.7ml freezing medium (FBS Gibco) are added drop by drop. Content is transferred into two cryotubes and stored for 48 hours in a tightly sealed styropor box at -80°C. Finally cryotubes can be transferred to a liquid nitrogen tank. Freezing medium consists of 60% DMEM, 20% Gibco FBS Serum and 20% DMSO.

7.3.4 Generation of feeder cells

One confluent SNL76/7 10cm plate is sufficient to obtain two 24 well plates. Medium of a confluent plate is aspirated until 4ml is left. Therefore it is the best to use a glass pipette and take up the whole medium and return 4ml to the cells. For mitotic inactivation of SNL76/7 fibroblast 80ml Mitomycin C is added for 3-4 hours at 37°C and 5%CO2. Supernatant is removed and cells are washed twice with 1xPBS before addition of trypsin for five minutes at 37°C. Trypsin is inactivated after addition of 5ml M10Gi medium. Cells are pooled in a 50ml Falcon tube and centrifuged for 7 minutes at 1000rpm (Heraeus Biofuge, swing out buckets). Pellet is resuspended in 10ml M10Gi medium and cell number is determined with a cell counter chamber. Cells are diluted in a 50ml Falcon or when necessary in a 150ml glass bottle with M10Gi until a cell concentration of 35 x 10^4 cells/ml is achieved. Feeder cells are transferred onto gelatine-coated culture plates and stored at 37°C and 5%CO2. Feeders can be used the next day and up to two weeks and have to be fed once a week with M10Gi.

Table 7.2: seeding of feeder cells

Culture plate	ml transferred
96 well plate	100 μl / well
24 well plate	500 μl /well
6 well plate	2 ml/ well
6 cm dish	4 ml / well
10 cm dish	12 ml / well

7.4 EMBRYONIC STEM CELLS, CARDIOVASCULAR PROGENITOR CELLS AND SOMATIC STEM CELLS

7.4.1 Thawing of ESC, CVPC and SSC

Before thawing feeder cells must be fed with M15Hi medium 2 hours prior to adding thawed cells. Selected cryotubes are removed from the liquid nitrogen tank and put in a 37°C water bath until a tiny ice cube is left. Tube is disinfected with 70% ethanol and flamed before content is transferred into a 15ml Falcon tube. M15Hi medium is added drop by drop under pivoting until the 12.5ml mark is reached.

Drops were added not too fast and not too slow. When added too fast cell will burst due to osmotic shock and when added too slow cells are kept too long in DMSO rich medium what will kill them. After addition of M15Hi Falcon is centrifuged for 7 minutes at 1000rpm at room temperature (Heraeus Biofuge, swing out buckets) and pellet is resuspended in 1ml of pre-fed feeder cell medium and transferred back onto the feeder cells. Cells are kept at 37°C at 5%CO2 and must be fed after 24 hours.

7.4.2 Culture of ESCs, SSCs and CVPCs

The cells are cultivated at 37°C and 5% CO2 and are fed every 24 hours with fresh M15Hi. To keep the cells in an undifferentiated state they are co-cultured with feeder cells expressing leukemia inhibitory factor (LIF) to maintain their self-renewing potential. Cells cultivated in 24-well plates are fed with 1 ml to 2 ml M15Hi depending on their confluence. Cells must be split when the well is confluent.

7.4.3 Splitting of ESCs, SSCs and CVPCs

Feeder cells and ESCs (CVPCs/ SSCs) must be fed with fresh M15Hi two hours prior to splitting. The appropriate number of Feeder-wells on which the ESCs (SSCs/ CVPCs) are cultivated after splitting are fed with 2ml M15Hi to enrich the medium with enough LIF. ESCs (SSCs/ CVPCs) are fed with 0.5ml M15Hi. After two hours the medium of the ESCs (SSCs/ CVPCs) is aspirated and the cells are washed once with 1x PBS. After removal of PBS by aspiration, trypsin is added to the cells (100μl/48 well; 200μl/24 well; 800μl/6 well; 2ml/10cm) and the cells are placed at 37°C and 5% CO2. After an incubation time of 20 minutes trypsin is inactivated by resuspending the cells in medium from the pre-fed feeder cells (at least thrice the amount of trypsin is used: 500μl/100μl trypsin; 1ml/200μl trypsin). In general cells are splitted in ratios of 1:2 or 1: 3 and the appropriate volume of this suspension is transferred back onto the new feeder cells. Splitting ratio depends on the confluence of the cells.

7.4.4 Freezing of ESCs, CVPCs and SSCs

Cells have to be fed two hours prior to freezing. Cells grown on 24 wells are washed with 1xPBS and $200\mu l$ trypsin is added to detach cells from surface for 20 minutes at 37°C and 5%CO2. To inactivate trypsin 1ml M15Hi is added to the cells. Freezing medium (FBS HyClone) is added in a 1:1 ratio therefore a volume of $1200\mu l$ is added to the cells drop by drop. For the first $200\mu l$ a $200\mu l$ pipette is used and one drop after another is added carefully. After each drop the well is shaked carefully. Next a $1000\mu l$ pipette is used and again the freezing medium is added drop by drop. To ensure a homogenous distribution the pipette is used to stir within the well carefully. Each $800\mu l$ of the suspension are transferred into a cryotube and stored for 48 hours in a tightly sealed styroform box in a -80°C freezer. After 48 hours cryotubes are transferred into liquid nitrogen tank.

Freezing medium consists of 60% DMEM, 20% HyClone FBS Serum and 20% DMSO.

7.4.5 Generation of Embryoid Body (EB) like aggregates

ESCs/CVPCs/SSCs cultured on feeder cells in 24 wells must be split 1:2 24 hours before aggregate formation to be in log phase. The cells are fed with 1ml fresh M15Si two hours prior to EB/CB formation and 6 well plates are coated with gelatin (0,1%). After two hours cells are washed with 1x PBS and $200\mu l$ of trypsin are added to the cells for 20 minutes at 37°C and 5% CO2. Cells are resuspended in $800\mu l$ M15Si to inactivate trypsin. To get rid of the feeder cells, which would disturb aggregate formation, the suspension is transferred to the gelatin coated 6 well and incubated for 45 minutes to 1 hour at 37°C and 5% CO2. Because the feeder cells adhere faster than embryonic stem cells (SSCs/CVPCs) it is possible to separate the ESC (CVPCs/SSCs) from feeder cells by preabsorption. The supernatant is transferred to a 50ml Falcon and is expanded with M15Si to a final concentration of about 4.5 x 10^4 cells/ml. Sterile bacteria plates are filled with autoclaved milliQ-H2O and each $20\mu l$ of the all supernatant is dropped on the lid of plates until the lid is densely covered with drops. The lid is put back carefully onto the dish filled with water,

thereby creating hanging drops. The plates are incubated at 37°C and 5% CO2 for 4.7 days and then rinsed with 6 ml M15Si onto gelled 10 cm cell culture plates. The aggregates are dispersed well and with care and incubated at 37°C and 5% CO2.

7.4.6 Culture of aggregates

Aggregates are fed on day 7 for the first time. From then on they get fed on every third day. Thereby the medium is partially removed and an appropriate volume of fresh M15Si is added.

Feeding protocol:

Table 7.3: feeding protocol

day	old medium kept	fresh medium added	old medium kept	fresh medium added
	10 cm culture plate		60 mm culture plate	
7	3 ml	8 ml	1.5 ml	4 ml
10	3 ml	8 ml	1.5 ml	4 ml
13	4 ml	10 ml	2 ml	5 ml
16	4 ml	10 ml	2 ml	5 ml
19	4 ml	10 ml	2 ml	5 ml
22	4 ml	10 ml	2 ml	5 ml
25	5 ml	12 ml	2.5 ml	6 ml
28	5 ml	12 ml	2.5 ml	6 ml
31	5 ml	12 ml	2.5 ml	6 ml

7.5 FIXATION AND IMMUNOFLUORESCENCE

7.5.1 Fixation

Embryoid body-like aggregates grown onto gelatin-coated cover slips were fixed on day 20 of cultivation. Therefore cover slips were transferred carefully into a 6 well, which was prior treated with a hot forceps to create protuberances. The resulting unevenness makes it easier to remove cover slips later from the well. Gently, 2 ml of 1x PBS are added and cells were washed. Again 1xPBS is added but this time for

two minutes and on ice. During this time period cover slips were transported to the lab carefully. 1x PBS is aspirated thereby avoiding to get too close to the aggregates and 2 ml of EtOH (-20°C) is added carefully drop by drop. It is important to do not drop directly onto cells, but to rinse EtOH along the edge into the wells. Cover slips are stored for 20 minutes at -20°C. After that 800μl ddH2O are dropped to the aggregates under pivoting the well thereby a concentration of 70% EtOH is reached. Again cover slips are stored at -20°C for 20 minutes. Fixed aggregates are stored in 70% EtOH at 4°C and are ready to use for immunofluorescence staining. To avoid evaporation wells are sealed with parafilm.

7.5.2 Immunofluorescence-method 1

70% EtOH is aspirated and cover slips are washed three times with 2ml 1x PBS for five minutes. It is important to rinse any liquid gently and slowly along the edge of the wells to avoid disruptions of aggregates. First antibody is diluted (generally 1:200) with 1x PBS and 100μl of the antibody solution is dropped onto the lid of a 6 well plate. Next cover slips are put onto these antibody drops for 1h 30 minutes. To avoid drying small wet pieces of paper are put into the wells and the plate is put into a wet chamber. Cover slips are washed three times with 2ml 1x PBS for ten minutes. Secondary antibody is diluted and also dropped onto the lid of a culture plate. Cover slips are kept for 45 minutes on the antibody solution in a wet chamber. Cover slips are again washed with 1x PBS for ten minutes and DAPI is added in a concentration of 1:1000 for 5 minutes. To get rid of DAPI aggregates were washed twice with 1xPBS for 10 minutes. Cover slips are fixed onto a microscope slide with mowiol (40-80μl depending on the size of cover slips). Mowiol may be shortly heated to 37°C before use. Cover slips and slides are dried over night in the dark. The next day the edges of the cover slips are sealed by nail polish and stored at 4°C.

7.5.3 Fixation and Immunofluorescence-method 2

Appropriate cover slips are selected for immunofluorescence. Cover slips were transferred carefully into a 6 well, which was prior treated with a hot forceps to create protuberances. Embryoid body -like aggregates are washed with 1x PBS and were fixed in 4% Paraformaldehyde (2ml) for 20 minutes at room temperature under pivoting. Cover slips were washed twice with 1x PBS to get rid of paraformaldehyde. Next 0.1% Saponin (1ml) is added to the aggregates for 20 minutes at room temperature under pivoting to permeabilize cells. Again aggregates were washed twice with 1x PBS. For blocking we used 2% BSA in PBS (1ml) for 10 minutes at room temperature. First antibody is diluted in 2% BSA/PBS as prescribed $100\mu l$ of the antibody solution is dropped onto the lid of a 6 Well plate. Next cover slips are put onto these antibody drops for 1 hour at 4°C. To avoid drying small wet pieces of paper are put into the wells and the plate is put into a wet chamber. Cover slips are washed three times with 2ml 1xPBS for ten minutes under gentle pivoting. Secondary antibody is diluted and also dropped onto the lid of a culture plate. Cover slips are kept for 1 hour on the antibody solution in a wet chamber. Cover slips are again washed with 1x PBS for ten minutes and DAPI is added in a concentration of 1:1000 for 5 minutes. Cover slips are washed twice with 1x PBS for 15 minutes. Cover slips are fixed onto a microscope slide with mowiol (40-$80\mu l$ depending on the size of cover slips). Cover slips and slides are dried over night in the dark. The next day the edges of the cover slips are sealed by nail polish and stored at 4°C. To visualize fluorescent staining a LSM - Meta 510 (Zeiss) Microscope is used.

Mowiol

6 g Glycerin

2.6 g Mowiol 2-88

5 % DABCO

6 ml ddH2O

The ingredients are mixed together and incubated at room temperature for 2 hours.

Addition of 12 ml 0.2M Tris/HCl pH 8.5 was followed and incubation for 10 minutes at 50°C is performed. Centrifugation for 15 minutes at 5000 rpm was continued and aliquots are stored at -20°C.

7.6 mRNA ISOLATION FROM CELLS (ESC/SSC/CVPC) with RNeasy Mini Kit (Quiagen)

7.6.1 RNeasy Mini Kit

Before RNA isolation the bench is carefully cleaned with soap and ethanol to get rid of RNases as much as possible. During the whole isolation process a set of pipettes is used uniquely for RNA. Cells are fed with medium 2 hours prior to isolation. Cells are washed with ice cold 1x PBS twice and are scraped with a scraper. The supernatant is transferred into a 15 ml Falcon tube and centrifuged for 5 minutes at 1000 rpm. The supernatant is aspirated and the pellet is resuspended in 600μl RLT buffer - beta-mercaptoethanol (100:1). Suspension is loaded onto the shreeder column (violet) and centrifuged for 2 minutes at 14000 rpm and at room temperature. 70% EtOH is added in a ratio of 1:1 (600μl) to the flow through and mixed by pipetting. 600μl of this suspension is transferred onto a RNeasy Mini Spin Column (pink) and results in RNA binding to the column. Column is centrifuged for 15 seconds at 14000 rpm and flow through is discarded. The remaining 600μl suspension is loaded onto the same column and centrifugation step is repeated. 700μl RW1 buffer is loaded onto the column and is centrifuged for 15 seconds at 14000 rpm. Flow through and tube is discarded and column is put in a fresh tube. 500μl RPE (with EtOH) is added and centrifuged for 15 seconds at 14000rpm. Again flow through and tube is discarded. RPE treatment is once again performed, but this time centrifugation step proceeds for 2 minutes. Column is now put into a 1.5 ml eppendorf tube and 30μl RNase free water was added directly onto the membrane. To elute RNA, water was incubated for 1 minute and afterwards column is centrifuged for 1 minute at 14000 rpm.

7.6.2 DNA digestion

For DNA digestion, 3.75 μl DNase I buffer and 3.75 μl DNase I buffer are added to the eluate and the tube is kept at 37°C for 30 minutes. To stop digestion 3.75 μl EDTA are added to the tube and is kept for 10 minutes at 65°C on a shaker. RNA eluate is stored at -80°C. DNA digestion was controlled by a GAPDH PCR. No bands visible at 300bp (GAPDH) indicate a successful DNA digestion.

7.6.3 Reverse Transcription

To determine RNA concentration we performed a Nanodrop measurement.Ideally the concentration should be 0.5 μg/μl or larger. If the concentration of RNA was lower than 0.5 μg/μl a different procedure was used.

1. c $<$ 0.5 μg/μl

2. c $=$ 0.5 μg/μl; c $>$ 0.5 μg/μl

Ad 1. **RNA concentrations lower than 0.5 μg/μl:**

Because the RNA concentration is too low it is necessary to adopt the whole volume of the mRNA solution. So we deal now with a volume of 70 μl instead of 50 μl. This means a factor of 1.4 which is multiplied with substances applied during RT to maintain the ratio. Whole volume of mRNA solution is used. 1.4 μl d(T) are added to the sample for 10 minutes at 70°C, followed by incubation on ice for 3 minutes. Tube is centrifuged for 30 seconds at 13000 rpm. Reverse transcription - Mix is added to the sample and an end volume of 25.9 μl is reached. RT - Mix is incubated for 2 minutes at 42°C. After this 1.4 μl Revert Aid Reverse Transcriptase is added and incubated for 50 minutes at 42°C. Next the sample was incubated for 15 minutes at 70°C and put on ice for another 5 minutes. Tube is centrifuged for 2 minutes at 13000 rpm and stored at -20°C.

Ad 2. **RNA concentration is about 0.5 μg/μl**

A volume of 29.5 μl is used. If concentrations are much higher than 0.5 μg/μl samples have to be diluted to the correct concentration with RNase free water. 1 μl d(T) are added to the sample for 10 minutes at 70°C and incubated on ice for 3 minutes. Centrifugation is performed for 30 seconds at 13000 rpm and RT-Mix is added for 2 minutes at 42°C. 1 μl Revert Aid Reverse Transcriptase is added and incubated for 50 minutes at 42°C followed by incubation at 70°C for 15 minutes. Before centrifugation at 13000 rpm for 2 minutes samples are kept on ice for 5 minutes. Storage at -20°C.

Table 7.4: RT-mix

Ad 1. RT-Mix	*Ad 2. RT-Mix*
14 μl 5x Buffer	10 μl 5x Buffer
7μl 0.1M DTT	5μl 0.1M DTT
2.1μl RNase Inhibitor	1.5μl RNase Inhibitor
2.8μl 10mM dNTPs	2μl 10mM dNTPs
End-Volume: 25.9μl	End-Volume: 18.5μl

For further RT-PCR analysis concentrations of samples has to be balanced for equal amounts of cDNA. Therefore, it is necessary to balance the concentration of the mRNA product of the house keeping gene GAPDH.

7.7 PCR

38.75 μl dH2O

5 μl 10x buffer (Fermentas EP0402)

3 μl 25mM MgCl (Fermentas EP0402)

1 μl 10mM dNTPs (Fermentas R0192)

0.5 μl Forward primer (Vienna Bio Tec)

0.5 μl Reverse primer (Vienna Bio Tec)

0.25 μl Taq Polymerase (Fermentas EP0402)

Dependent on the number of samples applied for PCR a multiple of the mastermix is made. Aliquots of 49μl are added to each PCR sample and 1μl of sample DNA is added. PCR tubes (Klösch) are gently mixed and spinned followed by placing the tubes in a Biometra T-Personal PCR machine.

PCR - Program:

94°C for 60 seconds

94°C for 45 seconds

x °C for 45 seconds (usually 50°C < x < 66°C depending on primers)

72°C for 60 seconds

Repeating step 2-4 for 28-39 cycles (depending on TM of primers)

72°C for 240 seconds

4°C

7.8 FACS

7.8.1 Fixation

Embryoid body-like aggregates are grown onto gelatin-coated culture plates. Before staining with adequate antibodies aggregates have to be separated into single cell suspension and fixed. Therefore aggregates are washed twice with 1xPBS and a mixture of Trypsin, Collagenase and Pancreatin is added (1.5 ml) for 20 minutes at 37°C. 8 ml M10Gi is added to inactivate trypsin and cells are pooled in a 50 ml Falcon. This Falcon is then centrifuged at 1200 rpm for 2 minutes and the supernatant is collected in a fresh Falcon. The pellet is then resuspended in Trypsin/Collagenase/Pancreatin (2 ml) and incubated for 10 minutes at 37°C. 8 ml of M10Gi are added and the Falcon is centrifuged at 1200 rpm for 1 minutes. The supernatant is pooled with the previous collected supernatant. The pellet is resuspended in 1 ml Trypsin/Collagenase/Pancreatin for 7 minutes at 37°C. The cells are resuspended in 5 ml M10Gi and are centrifuged for 1 minute at 1200 rpm. The supernatant is pooled again followed by centrifugation for 5 minutes at 1200 rpm.

The pellet is once washed with 1x PBS and centrifuged again. Finally, the cells are fixed in 4% paraformaldehyde and the cell number is determined. Therefore Falcon is rotated for 20 minutes at room temperature and stored at 4°C.

Trypsin/Collagenase/Pancreatin mix:

40 ml Trypsin

20 mg Collagenase

24 mg Pancreatin

4% Paraformaldehyde:

8.648 ml 37% Formaldehyde

71.348 ml 1x PBS

7.8.2 Staining procedure

$6x\ 10^6$ cells per cell line are transferred into an eppendorf tube and are centrifuged for 5 minutes at 1200 rpm. Cells are washed with 1 ml 1x PBS and are centrifuged for 5 minutes at 1200 rpm. This washing step is repeated twice followed by resuspending the cell pellet in 0.15% Saponin in PBS (500μl) and incubating the pellet for 20 minutes at room temperature under pivoting. After 20 minutes cells are centrifuged for 5 minutes at 1200 rpm. To block unspecific bindings cells were incubated in 500μl 2% BSA in PBS for 10 minutes at room temperature under pivoting. A supplemental volume of 1xPBS is added to split whole volume into tubes with aliquots of 100μl (for example: addition of 300μl 1xPBS results in splitting the volume into 8 tubes with 100μl). Tubes are centrifuged for 5 minutes at 1000 rpm and primary antibody in 2%BSA/PBS (100μl) is added for 1 hour under pivoting or over night at 4°C, respectively. For control we used samples that are not stained with primary, but with secondary antibodies to determine background staining. Next, tubes are centrifuges for 8 minutes at 1200 rpm and supernatant is aspirated. Cells are washed with 1x

PBS and centrifuged for 5 minutes at 1200 rpm for three times. Secondary antibody diluted in 2%BSA/PBS is added for 30 to 45 minutes in the dark or overnight under pivoting, respectively. Centrifugation of 8 minutes at 1200 rpm is followed. Again the pellet was washed for three times (5' 1200rpm). Finally, the pellet is resuspended in 300 to 500μl 1xPBS and FACS analysis is performed.

For staining we used following primary and secondary antibodies in concentrations mentioned below:

Table 7.5: Antibody Dilutions

Antibody	Dilution
Anti-rabbit FOXA2	1:200
Anti-rabbit GFAP	1:200
Anti-rabbit vWF	1:200
Anti-mouse Beta3-tubulin	1:200
Anti-mouse SMA	1:200
Anti-mouse cTnT	1:200
2nd: anti-mouse Alexa Fluor 488	1:500
2nd: anti rabbit Alexa Fluor 647	1:500

7.9 TRANSIENTE TRANSFECTION

7.9.1 Plasmid preparation

E.coli transformed with distinct plasmids are embedded in glycerol and shock-frozen in liquid nitrogen for long-term storage at -80°C. E.coli carrying the plasmid of interest are transferred to an antibiotic-selective LB-agar plate with a toothpick. For isolation and expansion of pGl3b-Basic (AmpR), NKE 24 (Nkx-luc, AmpR) and TOPFLASH (AmpR) plasmids LB Amp plates are used and E.coli carrying these plasmids are incubated overnight at 37°C. The next day plates can be stored for several weeks at 4°C by sealing it with parafilm. For plasmid preparation the Endofree Plasmid Maxi Kit is used. A single E. coli colony is picked with a toothpick and transferred into a cuvette tube containing 3ml Amp-selective LB medium (50mg/ml Ampicillin).

E.coli are incubated for 4 hours at 37°C under shaking. After 4 hours the content is transferred into an Erlenmayer flask and 150 ml Amp LB medium is added and incubation proceeds overnight at 37°C under shaking.

The overnight-culture is transferred into a 50 ml Falcon the next day and is centrifuged for 15 minutes at 4000 rpm at 4°C. The pellet is then resuspended well in ice cold 10 ml buffer P1. 10 ml buffer P2 is added and Falcon is inverted three times followed by incubation of 5 minutes at room temperature to shear genomic DNA. Further 10 ml ice cold buffer P3 is added and Falcon is inverted eight times. The suspension is transferred in a Qiagen Cartridge and kept for 10 minutes at room temperature. The supernatant is pushed through the cartridge into a fresh Falcon and 2.5 ml ER buffer is added. Falcon is inverted ten times and kept on ice for 30 minutes. A Qiagen tip 500 is equilibrated with 10 ml QBT. The filtered lysate is transferred into the Qiagen tip 500 and the column is emptied by gravity flow. The Qiagen tip 500 is washed twice with 30 ml buffer QC. DNA is eluated into a new flask by adding 15 ml buffer QN and 10.5 ml Isopropanol is added to the eluate. The eluate is mixed well and centrifuged at 13000 rpm for 30 minutes at 4°C. The supernatant is discarded and the pellet is resuspended in 5 ml 70% EtOH and is centrifuged for 10 minutes at 13000 rpm at 4°C. Again the supernatant is discarded and the pellet is dried for 15 minutes. Next, the pellet is resuspended in TE-buffer and stored at -20°C. DNA concentration is measured by using a NanoDrop machine. Plasmids are ready to use for transfection.

Ampicillin Stock 1000x

250 mg Ampicillin
5 ml destilled water

steril filtered and storage at -20°C

7.9.2 Transfection of CVPCs

Lipofectamine Transfection on undifferentiated CVPCs

One day before transfection, cells grown on 24 well with feeders are trypsinized for 20 minutes at 37°C. This is followed by preabsorption of cells for 1 hour at 37°C to get rid of feeder cells. Feeder cells attach faster to the surface compared to CVPCs, therefore we are able to separate these cells easily from each other. 6 x 104 cardiovascular progenitor cells are seeded onto gelatin-coated 48 wells in M15Hy medium. The next day transient transfection is performed using lipofectamine 2000. Therefore cells are washed once with 1x PBS and 300 μl transfection medium is added for 2 hours at 37°C. During this incubation time Mastermixes and Lipofectamine Mixes are generated. Lipofectamine is added in a ratio of 1:50 to a DMEM and Glutamine solution followed by an incubation of 5 minutes at room temperature. Mastermix 1 and Lipofectamine Mix 1 as well as Mastermix 2 and Lipofectamine 2 are pooled and incubated for 20 minutes at room temperature to allow the generation of Lipofectamine-DNA complexes. After the two hours 60μl of these complexes are added to the cells for 3 hours at 37°C. During this incubation time complexes are able to enter the cells and deliver the DNA. Then the medium is aspirated completely and 300 μl fresh M15Hy medium is added to each well.

Transfection medium:

83 % DMEM

15 % HyClone

1 % Glutamine

1 % Beta-Mercaptoethanol

Mastermix 1	Mastermix 2
1μg pGL3b DNA	1μg NKE24 DNA
10ng Renilla DNA	10ng Renilla DNA

| DMEM (99%) + Glutamine (1%) | DMEM (99%) + Glutamine (1%) |

Lipofectamine Mix 1	*Lipofectamine Mix 2*
Lipofectamine	Lipofectamine
DMEM (99%) + Glutamine (1%)	DMEM (99%) + Glutamine (1%)

Lipofectamine Transfection on differentiated embryoid body-like CVPCs aggregates

Embryoid body -like aggregates of CVPCs are generated by using the hanging drop procedure (4.5 x 10^4 cells/ml). Five days after hanging drop cultivation aggregates were rinsed onto gelatin-coated culture plates with M15Si medium. On day 9 of cultivation cells are washed with 1x PBS and 2 ml trypsin is added for 20 minutes at 37°C. 6 x 10^4 cells are seeded onto gelatin-coated 48 well plate and after 24 hours transient transfection using lipofectamine 2000 is performed (see undifferentiated CVPCs).

Luciferase assay

Here we use the Promega Dual-Luciferase Reporter assay System Kit. Cells grown on culture plates are washed once with 1xPBS and supernatant is aspirated. 1x Passive Lysis Buffer (48 well: 120μl PLB) is added and with a pipette we scrape twice on the bottom of the well. PLB is incubated for about 40 minutes at room temperature and cells are resuspended and transferred into a Kloesch tube. The well is rewashed once with 60 μl PLB and collected in the same tube. At this point it is possible to freeze the sample at -20°C for one month. The sample is diluted 1:10 with 1x PLB and 20 μl are transferred onto a 96 well plate. For the measurement of Renilla and Firefly values we use the luminometer Berthold Centro LB960. LARII and Stop and Glo solutions are prepared and 1200 μl for priming the machine and 100 μl per well are transferred into the correct tubes that are connected with the injectors. Luciferase activity is measured using the software Microwin2000. Firefly substrate: LARII: One tablet is dissolved in Luciferase assay Buffer II and aliquoted in 2 ml tubes and stored at -80°C. Stop and Glo solution: Stop and Glo substrate is diluted 1:50 with Stop and Glo Buffer.

8 APPENDIX

Table 8.1: Percental distribution of cell types emerging in AB2.2, A5, H3, He2P11K13/5 (He2), and Hi2P11K15/6 (Hi2) aggregates measured by FACS analysis (Figure 4.7; Figure 4.13). Anti-cTnT, anti-SMA, anti-beta3-tubulin, anti-FOXA2, anti-GFAP, anti-vWF antibodies were used in concentration 1:200, while secondary anti-mouse Alexa Fluor488 and anti-rabbit Alexa647 antibodies 1:500. For each cell line and used antibody the same gate was set.

	AB2.2	*A5*	*H3*	*He2*	*Hi2*
cTnT	0.25 %	0.49 %	0.065 %	0.135 %	0.465 %
SM-actin	64.29 %	88.77 %	48.99 %	82.35 %	92.77 %
beta3-tubulin	0.15 %	0	0.05 %	0.055 %	7.14 %
FOXA2	1.83 %	2.51 %	0.97 %	15.89 %	10.29 %
GFAP	63.62 %	87.47 %	51.79 %	82.10 %	70.18 %
vWF	98.96 %	95.99 %	98.9 %	84.60 %	98.63 %

Table 8.2: Expression relation of indicated markers between differentiated CVPC (A5, H3) and SSC (He2P11K13/5, Hi2P11K15/6) to AB2.2 cell population (Figure 4.8; Figure 4.14). Data were obtained from table 8.1 and were divided through AB2.2 data (CVPC,SSC/AB2.2).

	A5	*H3*	*He2*	*Hi2*
cTnT	1.96	0.26	0.54	1.86
SM-actin	1.38	0.76	1.28	1.44
beta3-tubulin	0	0.33	0.37	47.60
FOXA2	1.37	0.53	8.69	5.62
GFAP	1.37	0.81	1.29	1.10
vWF	0.97	1.00	0.85	1.00

Table 8.3: Percental distribution of cell types emerging in undifferentiated AB2.2, A5, H3, He2P11K13/5 (He2), and Hi2P11K15/6 (Hi2). Anti-cTnT, anti-SMA, anti-beta3-tubulin, anti-FOXA2, anti-GFAP, anti-vWF antibodies were used in concentration 1:200, while secondary anti-mouse Alexa Fluor488 and anti-rabbit Alexa647 antibodies 1:500. For each cell line and used antibody the same gate was set.

	AB2.2	*A5*	*H3*	*He2*	*Hi2*
cTnT	0.93 %	0	0.35 %	0.24 %	1.15 %
SM-actin	99.88 %	99.46 %	99.63 %	99.42 %	98.31 %
beta3-tubulin	98.83 %	58.63 %	61.66 %	90.09 %	96.40 %
FOXA2	76.26 %	2.09 %	1.76 %	3.42 %	58.29 %
GFAP	99.07 %	96.32 %	97.17 %	97.54 %	98.47 %
vWF	89.13 %	99.15 %	99.09 %	99.22 %	91.28 %

Table 8.4: Expression relation of indicated markers between differentiated and undifferentiated CVPC (A5, H3) and SSC (He2P11K13/5, Hi2P11K15/6), respectively (Figure 4.9; Figure 4.15). Data were obtained from table 8.1 and table 8.3. Data of differentiated cells were divided through data of undifferentiated cells (differentiated/undifferentiated). Values for cTnT (A5) are missing due to the fact that a division through 0 is not possible.

	A5	*H3*	*He2*	*Hi2*
cTnT	/	0.19	0.56	0.40
SM-actin	0.89	0.49	0.83	0.94
beta3-tubulin	0	0	0	0.07
FOXA2	1.20	0.55	4.65	0.18
GFAP	0.91	0.53	0.84	0.71
vWF	0.97	1.00	0.85	1.08

Table 8.5: Cardiomyogenesis in CVPC (A5 and H3), SSC (He2P11K13/5 and Hi2P11K15/6) and AB2.2 ESC aggregates (Figure 4.10; Figure 4.16). Percentage of beating aggregates.

	AB2.2	*A5*	*H3*	*He2*	*Hi2*
7	0	0	0	0	0
8	0	0	0	0	0
9	85.00 %	0	0	0	0
10	87.50 %	2.50 %	0	0	0
11	85.00 %	30.00 %	0	0	0

12	82.50 %	77.50 %	0	0	0
13	92.50 %	80.00 %	7.50 %	0	0
14	95.00 %	92.50 %	0	0	0

Table 8.6: Influence of retinoic acid (RA) on beating aggregates, (Figure 4.18; Figure 4.19). Retinoic acid ($5x10^{-7}$ M) is added from day 5 on to aggregates of He2P11K13/5 (He2), A5 and AB2.2. Percentage of beating aggregates. Data are indicated as percentage.

day	AB2.2	AB2.2(RA)	A5	A5(RA)	He2	He2(RA)
7	0	2.86	0	0	0	0
8	0	18.10	0	0	0	0
9	71.04	47.14	0	0	2.50	3.64
10	82.92	44.29	5.63	0	0	2.42
11	87.92	47.14	31.46	4.76	0.83	1.82
12	87.71	50.90	82.92	5.24	7.08	0.91
13	92.50	51.90	84.38	5.71	23.33	1.21
14	91.25	8.89	96.25	8.89	25.21	2.22
15	91.25	4.44	93.33	10	28.13	2.22
16	90.42	2.22	96.67	4.44	64.44	6.67
17	89.58	1.11	96.67	2.22	60.00	6.67
18	89.59	1.11	96.67	0	22.22	6.67
19	74.17	1.67	90.00	0	8.89	6.67
20	65.83	5.00	85.00	0	0	13.33

Table 8.7: FACS analysis of undifferentiated CVPC clone A5-CSX treated with retinoic acid for 3h, 24h and 3d (Figure 4.21). Determination of EGFP expression of EGFP-Nkx2.5 reporter cell line (A5-CSX). Data are means of one experiment with duplicates. Data here presented are FACS values divided by mean value of control (+EGFP). SD..Standard deviation for indicated time intervals

time	CSX(-EGFP)	CSX(+EGFP)	CSX+RA
3 hours	0	1	0.99
SD 3h	0	0.01	0.01
24 hours	0	1	0.91
SD 24h	0	0.02	0.01

3 days	0	1	0.18
SD 3d	0	0.01	0.01

Table 8.8: FACS analysis of differentiated CVPC clone A5-CSX treated with retinoic acid for 3h and 24h (Figure 4.22). Determination of EGFP expression of aggregated EGFP-Nkx2.5 reporter cell line (A5-CSX). Data are means of one experiment with duplicates. Data here presented are FACS values divided by mean value of control (+EGFP). SD..Standard deviation for indicated time intervals

time	CSX(-EGFP)	CSX(+EGFP)	CSX+RA
3 hours	0	1	0.88
SD 3h	0	0.02	0.09
24 hours	0	1	0.39
SD 24h	0	0.09	0

Table 8.9: Percental incidence of neuron-like cells in retinoic-acid treated differentiated He2P11K13/5 (He2), Hi2P11K15/6 (Hi2) A5 and AB2.2 (Figure 4.26; Figure 4.27). Retinoic acid (5×10^{-7} M) is added from day 5 on to aggregates. Percentage of aggregates possessing neuron-like cells. Data are indicated as percentage.

day	AB2.2	A5	C3	H3	He2	Hi2
7	0	6.00	0	0	0	0
8	0	46.00	3.00	3.33	0	0
9	30	66.00	91.83	79.17	6.30	83.00
10	66.11	90.00	95.33	81.67	75.19	94.50
11	76.67	90.00	95.33	90.00	94.77	95.50
12	89.44	78.67	96.00	80.00	94.07	96.67
13	85.00	73.33	96.00	86.67	95.19	97.33
14	100	46.67	100	100	66.67	84.17
15	100	40.00	85.00	100	66.67	95.00
16	100	33.33	70.00	92.50	60.00	90.00
17	100	33.33	45.00	85.00	60.00	60.00
18	100	33.33	50.00	85.00	50.00	60.00
19	100		50.00	0	60.00	65.00
20	100				60.00	60.00
21	100					65.00

Continued on next page

| 22 | 100 | 60.00 |
| 23 | 100 | 50.00 |

Table 8.10: Percental incidence of neuron-like cells in untreated differentiated He2P11K13/5 (He2), Hi2P11K15/6 (Hi2) A5 and AB2.2 (Figure 4.28). Percentage of untreated aggregates possessing neuron-like cells. Data are indicated as percentage.

day	AB2.2	A5	C3	H3	He2	Hi2
7	0	0	0	0	0	0
8	0	0	0	0	0	0
9	1.67	0	0	0	0	0
10	1.67	0	0	0	0	0
11	3.89	0	0	0	0	1.43
12	13.33	0	0	0	2.38	1.43
13	10.56	0	0	0	0	1.43
14	25.00	0	0	0	8.89	0
15	20.00	0	0	0	8.89	5.00
16	30.00	0	0	0	8.33	15.00
17	33.33	0	0	0	8.89	15.00
18	40.00	0	0	0	10.00	20.00
19	26.67		0	0	0	25.00
20	26.67				3.33	15.00
21	26.67					15.00
22	26.67					20.00
23	23.33					10.00

Table 8.11: Percental frequency of neuron-like cells observed in retinoic acid(RA)-treated and untreated AB2.2, A5, He2P11K13/5 and Hi2P11K15/6 aggregates between days 14-17 (Figure 4.28, B). Data obtained from table 8.9 and table 8.10. Data represent mean value of neuron-like cell frequency between day 14 to 17. SD..Standard deviation.

	+RA	control
AB2.2	100 %	27.08 %
A5	38.3 %	0 %
He2	63.3 %	8.75 %

Hi2	82.3 %	11.25 %
AB2.2 SD	0	5.8
A5 SD	6.4	0
He2 SD	3.85	0.28
Hi2 SD	15.5	11.09

Table 8.12: Influence of PD98059 (20μM) on beating CVPC A5 aggregates (Figure 4.33). The inhibitor (PD98059) was added from days 0-5, 5-7, 7-10, 10-13. Percentage of beating aggregates. Dara are indicated as percentage.

day	d 0-5	d 5-7	d 7-10	d 10-13	control
6	0	0	0	0	0
7	0	0	0	0	0
8	0	0	0	0	0
9	0	0	0	0	0
10	2.94	6.52	0	0	20
11	2.94	15.22	59.26	70.59	95
12	41.18	29.79	82.760	93.75	100
13	57.58	42.22	96.43	100	100
14	64.86	52.08	93.33	100	95
15	56.25	52.17	85.29	100	100
16	57.07	53.45	82.65	94.12	100
17	57.89	54.72	80	88.24	100
18	65.12	45.65	70.59	84.21	100
19	66.93	48.47	61.76	74.46	87.50
20	68.75	51.28	52.94	64.71	75
21	54	41.18	28.13	61.90	20
22	52	31.70	29.58	43.02	15
23	50	22.22	31.03	24.14	10
24	26.47	10	0	3.33	0

Table 8.13: Influence of PD98059 (5μM) on beating aggregates (Figure 4.32).on beating CVPC A5 aggregates (Figure 4.32). The inhibitor (PD98059) was added from days 0-5. Percentage of beating aggregates. Dara are indicated as percentage.

day	d 0-5	control
6	0	0
7	0	0
8	0	0
9	0	0
10	0	20
11	3.57	95
12	17.86	100
13	36.67	100
14	41.94	95
15	52.17	100
16	49.84	100
17	47.50	100
18	42.86	100
19	45.70	87.50
20	48.72	75
21	37.14	20

Table 8.14: Effect of PD98059 when added for longer time periods, (Figure 4.34). The inhibitor (5μM) was added from days 0-13 and 5-13. Percentage of beating aggregates. Dara are indicated as percentage.

day	d 5-13	d 0-13	control
6	0	0	0
7	0	0	0
8	0	0	0
9	0	0	0
10	0	0	0
11	5	0	5
12	30	0	15
13	35	0	25
14	60	13	65

15	80	13	95
16	90	20	100
17	100	27	100
18	100	33	100
19	100	33	100
20	100	47	100
21	100	67	100
22	100	67	100
23	100	73	100
24	80	85	100
25	70	80	85
26	55	75	80
27	50	75	80
28	40	70	65
29	25	60	50
30	15	45	45

Table 8.15: Effect of PD98059 on Nkx2.5 gene expression (Figure 4.36). The inhibitor (5μM) was added from days 0-5. FACS analysis was performed by measuring the EGFP expression. Data are indicated as percentage.PD...PD98059, CSX...A5-CSX2, M...mean, Sd...standard deviation.

day	A5	CSX	CSX	+PD	+PD	M(CSX)	M(PD)	Sd(CSX)	Sd(PD)
0	0.24	94.16	94.49			94.32		0.233	
7	0.13	48.62	44.25	13.05	28.20	46.43	20.62	3.09	10.71
13	0	6.64	6.79	5.46	5.51	6.71	5.48	0.10	0.03
20	0.33	6.62	9.83	8.27	6.27	8.225	7.27	2.27	11.41

Table 8.16: The Nkx2.5 expression during aggregate development (Figure 4.37). A5-CSX2 aggregates were made and FACS analysis was performed by measuring the EGFP expression. Data are mean of EGFP positive cells in a gated population and indicated as percentage.

day	A5	CSX
0	0.03	88.70

5	0	63.27
7	0.08	58.02
10	0.1	38.65
13	0.03	14.06

Table 8.17: Effect of indicated factors on Nkx2.5 expression in undifferentiated and differentiated A5-CSX2 cells (Figure 4.39; Figure 4.40; Figure 4.41). EGFP expression was determined by FACS analysis. Data are mean of EGFP positive cells in a gated population. BMP2/4 (0.1μg/ml), anti-BMP2/4 (1.5μg/ml), SPARC (3 μg/ml), anti-SPARC (1:100). FACS values were divided by mean value of CSX control to obtain a constant basis line that make it able to compare the effect of these factors on Nkx2.5 gene expression. SD..standard deviation for indicated time points.

	A5	CSX	+SPARC	+ anti-SPARC	+ BMP2	+ anti-BMP2
Undifferentiated						
3 h	0.01	1.00	1.00	0.99	0.99	1.00
24 h	0.00	1.00	0.98	1.00	0.99	0.99
3 d	0.00	1.00	1.00	0.98	0.99	1.00
SD 3 h		0.01	0.01	0.01	0.01	0.01
SD 24 h		0.02	0.03	0.00	0.04	0.03
SD 3 d		0.01	0.03	0.01	0.00	0.01
Differentiated						
3 h	0.00	1.00	1.47	1.07	1.14	2.19
24 h	0.00	1.00	0.42	0.46	0.23	0.47
SD 3 h		0.12	0.10	0.09	0.19	0.21
SD 24 h		0.09	0.01	0.01	0.03	0.00

Bibliography

Aouadi, M., Bost, F., Caron, L., Laurent, K., LeMarchandBrustel, Y., and Binetruy, B. (2006). P38 mitogen-activated protein kinase activity commits embryonic stem cells to either neurogenesis or cardiomyogenesis. *Stem cells*, 24:1399–1406.

Bain, G., Kitchens, D., Yao, M., Huettner, J., and Gottlieb, D. (1995). Embryonic stem cells express neuronal properties in vitro. *Developmental Biology*, 168:342–357.

Bain, G., Ray, W., Yao, M., and Gottlieb, D. (1996). Retinoic acid promotes neural and represses mesodermal gene expression in mouse embryonic stem cells in culture. *Developmental Biology*, 223:691–694.

Brand, T. (2003). Heart development: molecular insights into cardiac specification and early morphogenesis. *Developmental Biology*, 258:1–19.

Burtscher, I. and Lickert, H. (2009). Foxa2 regulates polarity and epithelialization in the endoderm germ layer of the mouse embryo. *Development*, 136:1029–1038.

Callis, T., D.Cao, and Wang, D. (2005). Bone morphogenetic protein signaling modulates myocardin transactivation of cardiac genes. *Circulation Research*, 97:992–1000.

Cartwright, P., McLean, C., Sheppard, A., Rivett, D., Jones, K., and Dalton, S. (2005). Lif/stat3 controls es cell self-renewal and pluripotency by a myc-dependent mechanism. *Development*, 132:885–896.

Chambers, I., D.Colby, Robertson, M., Nichols, J., Lee, S., Tweedie, S., and Smith, A. (2003). Functional expression cloning of nanog, a pluripotency sustaining factor in embryonic stem cells. *Cell*, 113:643–655.

Cheshier, S., Morrison, S., Liao, X., and Weissman, I. (1998). In vivo proliferation and cell cycle kinetics of long-term self-renewing hematopoietic stem cells. *Proc. Natl. Acad. Sci.*, 96:3120–3125.

Christoffels, V. M., Habets, P., Franco, D., Campione, M., de Jong, F., Lamers,

W., Bao, Z., Palmer, S., Biben, C., Harvey, R. P., and Moorman, A. F. M. (2000). Chamber formation and morphogenesis in the developing mammalian heart. *Developmental Biology*, 223:266–278.

Davidson, S. and Morange, M. (2000). Hsp25 and the p38 mapk pathway are involved in differentiation of cardiomyocytes. *Developmental Biology*, 218:146–160.

Deb, A., Wang, S., Skelding, K., Miller, D., Simper, D., and Caplice, N. (2003). Bone marrow-derived cardiomyocytes are present in adult human heart: A study of gender-mismatched bone marrow transplantation patients. *Circulation*, 107:1247–1249.

Desbaillets, I., Ziegler, U., Groscurth, P., and Gassmann, M. (2000). Embryoid bodies: an in vitro model of mouse embryogenesis. *Experimental Physology*, 85(6):645–651.

Dudley, D., Pang, L., Decker, S., Bridges, A., and Saltiel, A. (1995). A synthetic inhibitor of the mitogen-activated protein kinase cascade. *Pro. Natl. Acad. Sci*, 92:7686–7689.

Edwards, M. and McBurney, M. (1983). The concentration of retinoic acid determines the differentiated cell type formed by a teratocarcinoma cell line. *Developmental Biology*, 98(1):187–191.

Eriksson, M. and Leppä, S. (2002). Mitogen-activated protein kinases and activator protein 1 are required for proliferation and cardiomyocyte differentiation of p19 embryonal carcinoma cells. *Journal of biological chemistry*, 227(18):15992–16001.

Fishman, M. and Chien, K. (1997). Fashioning the vertebrate heart: earliest embryonic decisions. *Development*, 124:1099–2117.

Gottschamel, T. (2010). The effect of desmin and sparc on early cardiomyogenesis. *Diploma thesis.*

He, S., Nakada, D., and Morrison, S. (2009). Mechanisms of stem cell self-renewal. *Annu. Rev. Cell Dev. Biol.*, 25:377–406.

Hoebaus, J. (2009). Self-renewal and differentiation of cardiovascular progenitor cells. *Diploma thesis.*

Hrabchak, C., Ringuette, M., and Woodhouse, K. (2008). Recombinant mouse sparc promotes parietal endoderm differentiation and cardiomyogenesis in embryoid bodies. *Biochemistry and cell biology*, 86:487–499.

Jamali, M., Rogerson, P., Wilton, S., and Skerjanc, I. (2001). Nkx2-5 activity is

essential for cardiomyogenesis. *The Journal of biological chemistry*, 276:42252–42258.

Kinder, S., Tsang, T., Quinlan, G., Hadjantonakis, A., Nagy, A., and Tam, P. (1999). The orderly allocation of mesodermal cells to the extraembryonic structures and the anteropoterior axis during gastrulation of the mouse embryo. *Development*, 126:4691–4701.

Kinder, S., Tsang, T., Wakamiya, M., Sasaki, H., Behringer, R., Nagy, A., and Tam, P. (2001). The organizer of the mouse gastrula is composed of a dynamic population of progenitor cells for the axial mesoderm. *Development*, 128:3623–3634.

Kispert, A. and Hermann, B. (1994). Immunohistochemical analysis oft he brachyury protein in wild-type and mutant mouse embryos. *Developmental Biology*, 161:179–193.

Kubo, A., Shinozaki, K., Shannon, J., Kouskoff, V., Kennedy, M., Woo, S., Fehling, H., and Keller, G. (2003). Development of definitive endoderm from embryonic stem cells in culture. *Development*, 131:1651–1662.

Leor, J., Patterson, M., Quinones, M., Kedes, L., and Kloner, R. (1996). Tranplantation of fetal myocardial tissue into the infracted myocardium of rat. a potential method for repair of infracted myocardium? *Circulation*, 94:II332–II336.

Liberatore, C., Searcy-Schrick, R., and Yutzey, K. (2000). Ventricular expression of tbx5 inhibits normal heart chamber development. *Developmental biology*, 223:169–180.

Lien, C., Wu, C., Mercer, B., Webb, R., Richardson, J., and Olson, E. (1998). Control of early cardiac-specific transcription of nkx2-5 by a gata-dependent enhancer. *Development*, 126:75–84.

Lough, J., Barron, M., Brogley, M., Sugi, Y., Bolender, D., and Zhu, X. (1996). Combined bmp-2 and fgf-4, but neither factor alone, induces cardiogenesis in non-precardiac embryonic mesoderm. *Developmental biology*, 178:198–202.

Lyons, I., Parsons, L., Hartley, L., Li, R., Andrews, J., Robb, L., and Harvey, R. (1995). Myogenic and morphogenetic defects in the heart tubes of murine embryos lacking the homeo box gene nkx2.5. *Genes and Development*, 9:1654–1666.

Manasek, F. (1969). Embryonic development of the heart. *J. Embryol. exp. Morph.*, 22:334–348.

Martin, G. (1981). Isolation of pluripotent cell line from early mouse embryos cultured in medium conditioned by teratocarcinoma stem cells. *PNAS*, 78(12):7634–7638.

Masui, S., Nakatake, Y., Toyooka, Y., Shimosato, D., Yagi, R., Takahashi, K., Okochi, H., Okuda, A., Matoba, R., Sharov, A., Ko, M., and Niwa, H. (2007). Pluripotency governed by sox2 via regulation of oct3/4 expression in mouse embryonic stem cells. *Nature cell biology*, 9(6).

Mitsui, K., Tokuzawa, Y., Itoh, H., Segawa, K., Murakami, M., Takahashi, K., Maruyama, M., Maeda, M., and Yamanaka, S. (2003). The homeoprotein nanog is required for maintenance of pluripotency in mouse epiblast and es cells. *Cell*, 113:631–642.

Murry, C. and Keller, G. (2008). Differentiation of embryonic stem cells to clinically relevant populations: Lessons from embryonic development. *Cell*, 132:661–680.

Narula, J., Haider, N., Virmani, R., DiSalvo, T., Kolodgie, F., Hajjar, R., Schmidt, U., Semigran, M., Dec, G., and Khaw, B. (1996). Apoptosis in myocytes in end-stage heart failure. *N Engl J Med.*, 335:1182–1189.

Niwa, H., Miyazaki, J., and Smith, A. (2000). Quantitative expression of oct-3/4 defines differentiation, dedifferentiation or self-renewal of es cells. *Nature genetics*, 24.

Orlic, D., Hill, J., and Arai, A. (2002). Stem cells for myocardial regeneration. *Circulation Research*, 91:1092–1102.

Pfendler, K., Yoon, J., Taborn, G., Kuehn, M., and Iannaccone, P. (2000). Nodal and bone morphogenetic protein 5 interact in murine mesoderm formation and implantation. *Genesis*, 28:1–14.

Saga, Y., Kitajima, S., and Miyagawa-Tomita, S. (2000). Mesp1 expression is the earliest sign of cardiovascular development. *Trends Cardiovasc Med*, 10:345–352.

Schlange, T., Andree, B., Arnold, H., and Brand, T. (2000). Bmp2 is required for early heart development during a distinct time period. *mechanisms of development*, 91:259–270.

Schofield, R. (1978). The relationship between the spleen colony-forming cell and the haemopoietic stem cell. *Blood cells*, 4:7–25.

Schott, J., Benson, D., Basson, C., Pease, W., Silberbach, G., J.P.Moak, Maron, B., Seidman, C., and Seidman, J. (1998). Congenital heart disease caused by

mutations in the transcription factor nkx2-5. *Science*, 281:108–111.

Searcy, R., Vincent, E., Liberatore, C., and Yutzey, K. (1998). A gata-dependent nkx-2.5 regulatory element activates early cardiac gene expression in transgenic mice. *Developmental*, 125:4461–4470.

Seger, R. and Krebs, E. (1995). The mapk signaling cascade. *FASEB J*, 9:726–735.

Smith, J., Gesteland, K., and Schoenwolf, G. (1994). Prospective fate map of the mouse primitive streak at 7.5 days of gestation. *Developmental Dynamics*, 201:279–289.

Spadling, A., Drummond-Barbosa, D., and Kai, T. (2001). Stem cells find their niche. *Nature*, 414:98–104.

Takeuchi, J. and Bruneau, B. (2009). Directed transdifferentiation of mouse mesoderm to heart tissue by defined factors. *Nature*, 459:708–711.

Tallini, Y., Greene, K., Craven, M., Spealman, A., Breitbach, M., Smith, J., Fisher, P., Steffey, M., Hesse, M., Doran, R., Woods, A., Singh, B., Yen, A., Fleischmann, B., and Kotlikoff, M. (2009). C-kit expression identifies cardiovascular precursors in the neonatal heart. *PNAS*, 106(6).

Taylor, D., Atkins, B., Hungspreugs, P., Jones, T., Reedy, M., Hutcheson, K., Glower, D., and Kraus, W. (1998). Regenerating functional myocardium: improved performance after skeletal myoblast transplantation. *Nat Med.*, 4:929–933.

Waldo, K., Kumiski, D., Wallis, K., Stadt, H., Hutson, M., Platt, D., and M.L.Kirby (2001). 3188 conotruncal myocardium arises from a secondary heart field. *Developmental*, 128:3179–3188.

Wang, X., Hu, Q., Nakamura, Y., Lee, J., Zhang, G., From, A., and Zhang, J. (2006). The role of the sca-1+/cd31- cardiac progenitor cell population in postinfarction left ventricular remodeling. *Stem Cell*, 24:1779–1788.

Wilkinson, D., Bhatt, S., and Herrmann, B. (1990). Expression pattern of the mouse t gene and its role in mesoderm formation. *Nature*, 343:657–659.

Wilson, A., Laurenti, E., Oser, G., vanDerWath, R., Blanco-Bose, W., Jaworski, M., Offner, S., Dunant, C., Eshkind, L., Bockamp, E., Lio, P., MacDonald, H., and Trumpp, A. (2008). Hematopoietic stem cells reversibly switch from dormancy to self-renewal during homeostasis and repair. *Cell*, 135:1118–1129.

Wu, S., Chien, K., and Mummery, C. (2008). Origins and fates of cardiovascular

progenitor cells. *Cell*, 132:537–543.

Yamashita, J., Takano, M., Hiraoka-Kanie, M., Shimazu, C., Peishi, Y., Yanagi, K., Nakano, A., Inoue, E., Kita, F., and Nishikawa, S. (2005). Prospective identification of cardiac progenitors by a novel single cell-based cardiomyocyte induction. *FASEB Journal*, 19:1534–1536.

Ying, Q., Stavridis, M., Griffiths, D., Li, M., and Smith, A. (2003). Conversion of embryonic stem cells into neuroectodermal precursors in adherent monoculture. *Nature Biotechnology*, 21:183–186.

Yuasa, S. and Fukuda, K. (2008). Multiple roles for bmp signaling in cardiac development. *Elsevier*, 5:209–214.

Zhang, H. and Bradley, A. (1996). Multiple roles for bmp signaling in cardiac development. *Development*, 122:2977–2986.

Zusammenfassung

Ein Herzinfarkt führt zum Verlust an Kardiomyozyten und beeinträchtigt die Herz-funktion. Neben den konventionellen Therapiemöglichkeiten hat sich eine neue eröffnet, die Zelltherapie. Hierbei wird der Verlust an Kardiomyozyten durch externe Stammzellen abgedeckt um die Herzfunktion zu verbessern. Extensive Forschung wird in diese Richtung betrieben um ein Verständnis über das regenerierende Potential dieser Zellen zu erhalten, sowie geeignete Kulturbedingungen und Isolierungsmetho-den zu etablieren. Diese Diplomarbeit befasst sich mit der Charakterisierung und der Kardiomyogenese von Vorläuferzellen (CVPC und SSC) isoliert vom Herzen und Hirn der Maus. Wir vermuteten dass die Zellen ein unterschiedliches Differenzierungspo-tential aufweisen und nur zu bestimmten Zelltypen differenzieren können. Zusätzlich wurde der Einfluss von positiven kardialen Regulatoren (BMP2 und SPARC), Retinol-säure sowie der Effekt von MAPK Signalweg auf die Kardiomyogenese von CVPC beschrieben. Mittels FACS Analyse und Immunfluoreszenz Färbungen konnten wir zeigen dass CVPCs ein limitiertes Differenzierungspotential besitzen, anders als SSCs, die multipotent sind. Um den Effekt von Faktoren auf die Nkx2.5 Genexpression in CVPCs zu untersuchen verwendeten wir eine Nkx2.5-EGFP Reporterzelllinie. Retinol-säure bewirkte eine Schwächung der Kardiomyogenese sowie eine verminderte Nkx2.5 Genexpression während es zu einer verstärkten neuronalen Differenzierung kam. Dage-gen konnte SPARC die Nkx2.5 Genexpression stimulieren und der MAPK Signalweg scheint eine wichtige Rolle in der frühen Herzentwicklung zu spielen. Diese Resultate zeigen, dass CVPCs eine geeignete Zelllinie darstellt um molekulare Mechanismen der Kardiomyogenese zu studieren. Die Optimierung von Kulturbedienungen und Anreicherung von bestimmten Herzzelltypen sind unerlässliche Schritte in Richtung Stammzelltherapie.

Abstract

A heart failure leads to a loss of cardiomyocytes and impairs heart function. Beside conventional therapeutic options a new therapy is established, the cell therapy. Here, the loss of cardiomyocytes is replaced by exogenous cells to improve heart function. Extensive research is carried on this field to gain understanding of the regenerative potential of stem cells as well as to establish adequate culture conditions and isolation methods. This diploma thesis deals with the characterization and cardiomyogenesis of progenitor cells (CVPCs and SSCs) isolated from the murine heart and brain. We assumed that the cells possess a diverse differentiation potential and were able to differentiate only to distinct cell types. We determined the influence of cardiac regulators (BMP2 and SPARC), retinoic acid and the effect of MAPK signaling on cardiomyogenesis of CVPCs. FACS analysis and immunofluorescence staining showed that CVPCs possess a limited differentiation potential, while SSCs seemed to be multipotent. To investigate the effect of factors on the Nkx2.5 expression in CVPCs we made use of the Nkx2.5-EGFP reporter cell line. Retinoic acid caused a weakening in cardiomyogenesis and a decrease in Nkx2.5 expression, while simultaneously enhancing neuronal differentiation. In contrast, SPARC stimulated Nkx2.5 expression and MAPK signaling seemed to play a critical role in early heart development. These results demonstrate that CVPCs represent an adequate cell line to study molecular mechanism of cardiomyogenesis. The optimization of culture conditions and the enrichment of distinct cell types are essential steps toward stem cell therapy.

Curriculum Vitae

Personal Information

Surname:	Walder
Given Name:	Diana
Address:	1230 Vienna, Perfektastraße 25/6/12
Telephone:	0650/7419574
E-mail:	d.walder@gmx.at
Date of Birth:	May, 11, 1985
Place of Birth:	Vienna
Nationality:	Austria

Education

1991 - 1992	Vorschule
1992 - 1996	Volksschule
1996 - 2000	Mittelschule
2000 - 2004	Oberstufe Bundesrealgymnasium
2004	General qualification for university entrance (Matura)
2004 - 2005	FH Campus Vienna - Molecular Biotechnology (University of applied Science)
2005 - present	University of Vienna - Molecular Biology
2009-2010	Medcial University of Vienna - Diploma student in the group of Ao. Univ. Prof. Dr. Georg Weitzer (Max F. Perutz Laboratories, Department of Biochemistry)

Eexperience

Zoo Schönbrunn	Participation in a project about rays and their behavior leaded by PhD Michael J.Kuba

```
Internship            AGES GmbH

Scientific Symposia   Poster
                      D. Walder,T. Gottschame, J. Höbaus, N. Vidovic,
                      M. Scheinast, T. Sauer:
                      CARDIOVASCULAR PROGENITOR CELLS SPONTANEOUSLY
                      DIFFERENTIATE TO CELLS OF THE CARDIAC LINEAGE,
                      BUT CAN BE INDUCED TO NEURONAL DIFFERENTIATION.
                      Annual Meeting of the Austrian Association of
                      Molecular Life Sciences and Biotechnology, in
                      Vienna 27 to 29 September, 2010
```